PROCESS DESIGN AND ECONOMIC EVALUATION OF AN ETHANOL PRODUCTION PROCESS BY BIOMASS GASIFICATION

By

SOLOMON GEBREYOHANNES

Bachelor of Engineering

Bahir Dar University

Bahir Dar, Ethiopia

2007

Submitted to the Faculty of the
Graduate College of the
Oklahoma State University
in partial fulfillment of
the requirements for
the Degree of
MASTER OF SCIENCE
December, 2010

PROCESS DESIGN AND ECONOMIC EVALUATION

OF AN ETHANOL PRODUCTION PROCESS BY

BIOMASS GASIFICATION

Thesis Approved:

Thesis Adviser – Dr. A. Johannes

Committee Member – Dr. N. Maness

Committee Member – Dr. R. Rhinehart

Dr. Mark E. Payton

Dean of the Graduate College

ACKNOWLEDGMENTS

First and foremost I would like to thank my advisor Dr. A. Johannes. It is an honor to be his Master's student. Without Dr. AJ's advice and guidance this thesis would not have been possible. I deeply appreciate all his contributions of time, encouragement, supervision and support from the initial to the final level of this research.

I would like to express the deepest appreciation to my committee members, Dr. N. Maness, Dr. K. High, and Dr. R. Rhinehart for their interest in the research. I am heartily thankful for their constructive comments.

I would like to thank the Biosystems and Agricultural Engineering department for providing the experimental data on the bioreactor and the gasifier units. I thank Dr. K. Patil for showing me the gasification units and providing me with important information about the experimental procedures.

A special thank to all my friends who were important to the successful realization of my thesis. It is a pleasure to thank my lab mate and friend Anirudh Patrachari for his interest and valuable comments in my research.

Finally, I owe my deepest gratitude to my family for all their love and encouragement. I am thankful for my parents support in all my pursuits. And, I am grateful to my sisters and their families from whom I received constant support, encouragement and love throughout my master's study.

Table of Contents

LIST OF TABLES

LIST OF FIGURES

NOMENCLATURE

Å	angstrom
atm	atmosphere
bar	bars
Btu	British thermal units
C	Carbon
°C	degree centigrade
C_2H_2	acetylene
C_2H_4	ethylene
C_2H_5OH	ethanol
$C_5H_{12}O$	methyl tertiary butyl ether
CH_4	methane
CO	carbon monoxide
CO_2	carbon dioxide
CBO	congressional Budget Office
C_{EI}	cost index at a specific time
cp	heat capacity
C_{ss}	molecular sieve capacity correction
D	diameter
D_i	internal diameter

DOE	department of energy
E10	gasohol (10% ethanol)
E85	85% ethanol
EIA	Energy information administration
EOS	equation of state
EPA	environmental protection agency
F_{BM}	Bare-Module factor (4.16 for vertical vessels
F_M	material factor
H_2	hydrogen
H_2O	water
HNO_3	nitric acid
K	kelvin
kg/hr	kilogram per hour
kg/sec	kilogram per second
kJ/mol	kilo joule per mole
kmol	kilo mole
L	height of the vessel
L_{MTZ}	length of the mass transfer zone
L_s	length of the saturation zone
mol	mole
mole %	percentage by mole
MTBE	methyl tertiary butyl ether
MTBE	methyl tertiary butyl ether

N_2O	nitrous oxide
NH_3	ammonia
NO_x	nitrogen oxide (x is 1, 2 or 3)
NRTL	Non random two liquid
O_2	oxygen
P7	strain identification of *C.* carboxidivorans species
psi	pounds per square inch
Q	heat
$\dot{q}$	volume flow rate
RFA	renewable Fuels Association
RFG	clean air act reformulated gasoline
RFS	renewable Fuel Standard
S_s	mass of desiccant
V	superficial velocity
vol %	percentage by volume
W	weight of the vessel
wt %	percentage by weight

Chapter 1

Introduction

1.1 Background Information

The demand of energy is increasing due to the growing population of the world and the rising standards of living in many developing countries. The world energy consumption is projected to increase by 44% from 2006 to 2030 (Energy information administration (EIA), 2009). Non-renewable energy source like petroleum, natural gas, coal and nuclear energy will continue to dominate the global energy supply. The world consumption of liquid fuels including petroleum is expected to increase from 85 million barrels per day in 2006 to 107 million barrels per day in 2030 (EIA, 2009). The current EIA report also shows that the consumption of natural gas will rise from 104 trillion cubic feet in 2006 to 153 trillion cubic feet in 2030.

Producing energy from non-renewable energy sources has a significant adverse impact on the environment. Combustion of petroleum based fuels release large quantities of toxic emissions (CO_2, CO, NO_x) which lead to environmental pollution. A combination of energy conservation and alternative energy source is necessary to stabilize the concentration of carbon dioxide (CO_2) in the atmosphere (Jay, *et. al.*, 2007). Many countries have made a commitment to reduce the emission of green house gase.

The United States has recently promised to reduce the emissions of green house gases to 42% below the 2005 levels by 2030 (Environmental Protection Agency (EPA), 2008).

The depletion of resources is the other problem of using non-renewable energy sources. The existing supplies are declining and finding new oil supplies is continuously becoming harder and more expensive (Renewable Fuels Association (RFA), 2009). It has been projected that the global demand will increase by 1.7% every year, reaching about 15.3 billion tons of oil equivalent (btoe) by 2030 (International energy agency (IEA), 2000). Because of the fast depletion of petroleum deposits, the world needs an alternative source of energy to meet the steady increase in the demand of energy.

A large number of studies are being conducted on finding eco-friendly substitutes for petroleum-based fuels. Renewable energy sources are environmentally friendly and can be replenished naturally in a short period of time. They could be the answer for the problem that the world is facing in meeting the growing global energy demand. According to the 2009 EIA report, renewable energy sources are the fastest-growing energy source, with a projected consumption increasing by 2.9 percent annually from 2006 to 2030.

Figure 1.1 shows the U.S energy consumption by different energy source. The figure shows, about 7% of the United States energy supply is from renewable energy sources. In 2009, about 53% (nearly 3.87 quadrillion btu) of the total renewable energy consumption was obtained from biomass. The amount of energy from biomass has surpassed hydropower as the largest domestic source of renewable energy in the United States (EIA, 2009). The United States has a potential of producing 1.3 billion tons of

biomass per year. This is enough to meet more than one third of the country's current demand for a transportation fuel. (EIA, 2009)

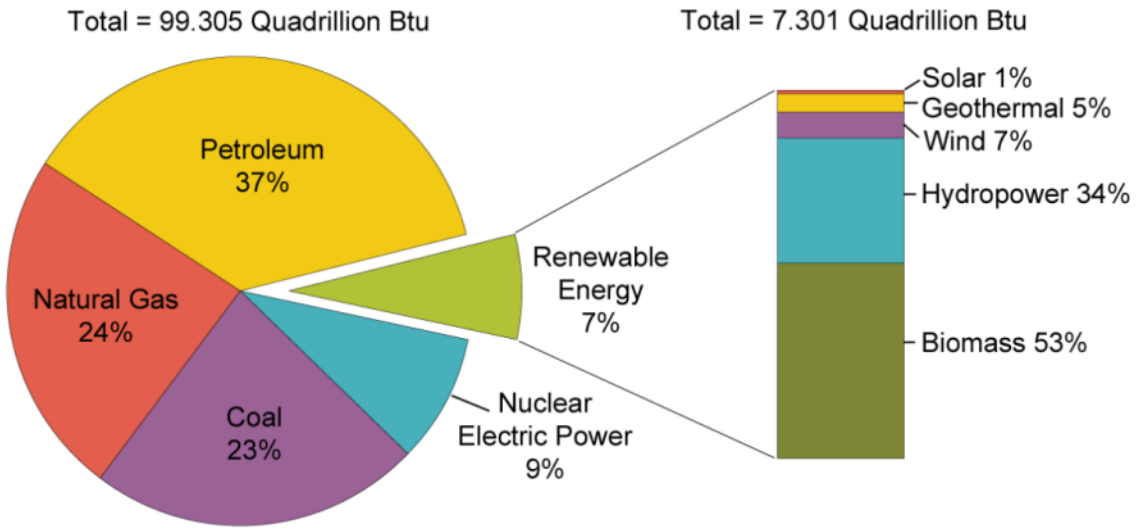

Figure 1.1 U.S energy consumption by energy source July 2009 (U.S Energy information administration)

Utilizing biomass as an energy source can significantly reduce the dependency on petroleum, and the emission of green house gases. It is estimated that the amount of energy from biomass currently contributes 10-14% of the world's energy supply (Peter, 2002). At present, biomass is being used to produce liquid transportation fuel (ethanol) which can be mixed with the conventional fuels or can be used independently.

1.2 Ethanol as a Renewable Energy Source

The interest in ethanol as an alternative fuel rose when the US was more concerned for the environment and the need to reduce energy dependence on foreign supplies (Morrison, 2004). Due to this reason production of ethanol has increased steadily since 1980 in the United States (RFA, 2009). Figure 1.2 shows the U.S annual ethanol production. From 1980 to 2008, Fuel ethanol production had increased from 175

million gallons per year to 9 billion gallons per year. More than 10.5 billion gallons of ethanol was expected to be produced in the United States in 2009 (RFA, 2009).

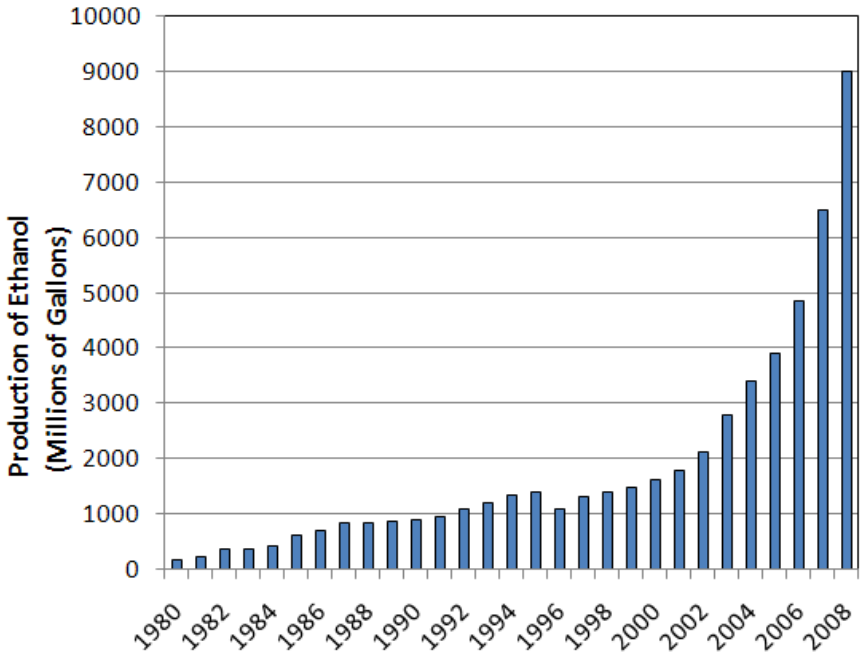

Figure 1.2 U.S Annual Ethanol Production (RFA, 2009)

1.3 Ethanol as Fuel Additive

Ethanol is used as an additive in gasoline to increase the fuel efficiency and reduce green house gas emissions. The use of ethanol as an additive has increased because of the Clean Air Act Reformulated Gasoline (RFG) program which requires oxygenating gasoline (Yacobucci, 2006). Gasohol or E10 (10% ethanol) is a typical mixed fuel which can be used without need for any modification on the engine. Major U.S. auto manufacturers have begun producing flexible-fueled vehicle models which are capable of working with E85 (85% ethanol) (EIA, 2009).

Ethanol has a high octane rating which increases the fuel's tendency to burn in a controlled manner. Due to the presence of oxygen in its chemical structure, it burns cleanly which consequently reduces the emission of green house gases to the atmosphere.

1.3.1Advantages of Ethanol Additive

The other commonly oxygenated fuel additives that have been used with gasoline are methanol and methyl tertiary butyl ether (MTBE). Natural gas or petroleum can be used to produce MTBE ($C_5H_{12}O$). There are several advantages of MTBE over ethanol. In many states MTBE was preferred to ethanol because it is available in greater supply, less costly and easier to transport and distribute (Yacobucci, 2006).

According to some studies MTBE has been found out to be a potential carcinogen compound at high concentrations (Yacobucci, 2006). MTBE have adverse health effects if it is inhaled at high concentrations. A contamination of ground water is also the other disadvantage of using MTBE as an additive. Compared to other gasoline compounds MTBE seeps more rapidly through the ground and contaminates drinking water (Rao, 2004). Due to the environmental and health concerns the Clean Air Act Amendments of 1990 list MTBE as a hazardous air pollutant (EPA, 1994). About 19 states in the United States have either a partial or complete ban on the use of MTBE in gasoline (EPA, 2004). On the other hand ethanol is readily biodegradable; this eliminates the risk of contamination. Ethanol also contains more oxygen so only about half as much ethanol (by volume) is needed for RFG (reformulated gasoline) (EIA, 2009).

1.3.2 Environmental Benefits of Ethanol

The use of ethanol as a transportation fuel has a positive effect to the environment. Although the combustion of ethanol releases carbon dioxide, the produced CO_2 will be recaptured as a nutrient by plants that are used to produce ethanol. As it is shown in figure 1.3, unlike fossil fuels, ethanol combustion doesn't have a net increase in

the atmospheric carbon dioxide. The carbon dioxide released from the combustion of ethanol is used by plants during the photosynthesis process.

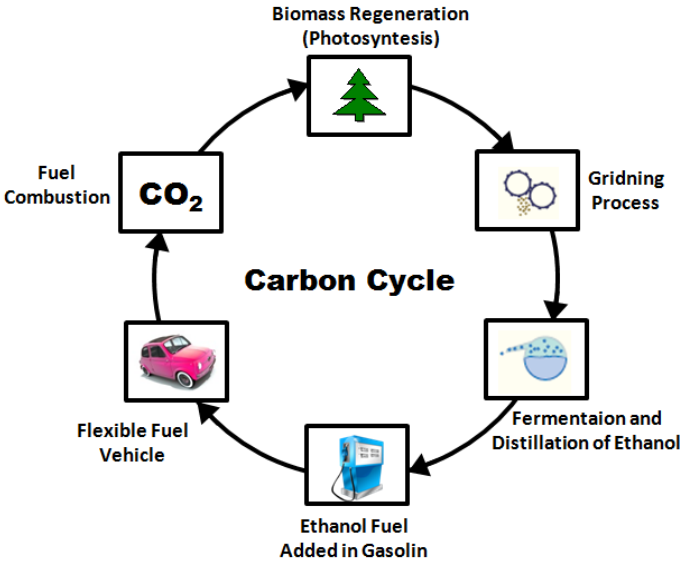

Figure 1.3 Carbon dioxide cycle

The use of ethanol can reduce the green house gas emissions by as much as 48 - 59 %, when compared to gasoline (EPA, 2009). In 2008, the use of 9 billion gallons of ethanol in the United States reduced approximately 14 million tons of CO_2-equivalent greenhouse gas emissions. This is equivalent to removing 2.1 million cars from the roads. (EPA, 2009).

1.3.3 Economic Benefits of Ethanol

Ethanol production is a new industry which is showing a positive impact on the economy of the countries like United States and Brazil. This new industry has quickly become a major contributor to the U.S economy. It has reduced America's dependency on foreign oil which consequently strengthens the economy of the country. In 2008 the ethanol industry has displaced the need for 321.4 million barrels of oil in the U.S. which saved the government from spending about $32 billion. (RFA, 2009)

The 2009 ethanol industry outlook report shows that in 2008 the ethanol industry has added more than $65 billion to gross domestic product through capital spending for new plants under construction. It has also supported the creation of more than 494,000 jobs (RFA, 2009). In United States there are about 170 biorefineries in production and 20 are under construction. It has been estimated that the ethanol industry has generated $12 billion in federal tax revenue and $9 billion in state and local government tax revenue (RFA, 2009).

1.3.4 Challenges Facing the Ethanol Industry

One of the major challenges facing in the ethanol industry today is the relatively high production cost of ethanol compared to gasoline and other additives. The U.S. government has established a tax incentive program to encourage ethanol production. Prior to 2004, the primary federal incentive was, 5.2 cents per gallon exemption that blenders of gasohol (E10) received from the 18.4¢ federal excise tax on motor fuels (Yacobucci, 2006). Since the exemption was applied to a 10% ethanol blended fuel, the exemption offered a subsidy of 52 cents per gallon of pure ethanol. The energy content of a gallon of ethanol is about one third lower than a gallon of gasoline. Even with the tax credit, ethanol is more expensive than gasoline when their prices are compared on an equivalent energy basis (Yacobucci, 2006).

The other concern in the ethanol industry is the rapid increase in the prices of corn and other farm commodities. Due to the rising demand of corn for production of ethanol, its price rose by more than 50% from April 2007 to April 2008 (CBO, 2009). The price of many agricultural commodities (soybeans, meat, poultry, and dairy products) also rose

in the same year. The CBO report shows the food prices rose by almost 2.5 %, 4%, 5% in 2006, 2007 and 2008 respectively.

1.4 Overview of Ethanol Production Methods

Ethanol has been used as source of energy for centuries. Ethanol can be produced from different types of feedstock. The commonly used raw material is sugar cane which is mainly a fermentable sugar. Raw materials which are polysaccharides can also be used to produce ethanol. Polysaccharides like corn require hydrolysis of carbohydrates into soluble sugar before the fermentation process takes over.

The cost of ethanol production processes mainly depend on the type of feedstock being used as the raw material. Lignocellulosic biomass which is composed of several polysaccharides can also be used for the production of ethanol. The following section describes the different ethanol production processes using sugar, starch and lignocellulosic feedstock.

1.4.1 Using Sugar Containing Feedstock

The ethanol production process begins with washing, crushing and milling the sugarcane. The cane juice (molasses) is then used to produce ethanol, whereas the baggase (solid waste of the juice extraction process) can be used to generate electricity by producing steam. Unlike other feed stocks, conversion of simple sugars (sucrose) into ethanol doesn't require enzymatic hydrolysis of the feed stock. After removing impurities and adjusting the PH, the cane juice is then fed to a fermentation unit where yeasts are used to ferment the molasses into ethanol. The yeast (S. cerevisiae) is continuously separated by centrifugation and recycled to the fermenter (Cardon and Sánchez , 2006).

Finally, the sugarcane ethanol from the fermentation unit is distilled to increase its purity level to approximately 95 weight% of ethanol.

1.4.2 Using Starch Based Feedstock

The production of ethanol from corn requires scarification or breakdown of polysaccharides into fermentable sugar. Initially, the corn grains are washed and crushed into small particles to expose the corn starch which is then milled into a fine power which is used in the fermentation process. The powder is mixed with water to dissolve the enzymes (*alpha - amylase*) that will break it partially into smaller particles (Cardon and Sánchez , 2006). To liquefy the starch, the mesh is cooked at 120 to 150 degrees. The temperature is then increased to 225 degrees to break down the starch further. Before adding the second enzyme *glucoamylase* (which converts starch to glucose) the mesh is cooled (Ahmed and Cateni, 2006). Then the glucose is fed to the fermentation unit. The fermentation process takes about 48 hours and it converts sugar to ethanol and carbon dioxide. Ethanol is then purified to remove the remaining water and is denaturized by adding 2 to 5% gasoline to make it unfit for human consumption.

1.4.3 Using Lignocellulosic Biomass by Enzymatic Hydrolysis and Fermentation

Lignocellulosic biomass is the most abundant and inexpensive raw material for the production of ethanol. The sources of Lignocellulosic biomass include woods, agricultural residues and paper wastes (Guffey and Wingerson, 2002). They have a complex structure which is composed of cellulose (~45% of dry weight), hemicelluloses (~30% of dry weight), and lignin (~25% of dry weight) (Wiselogel et al. 1996).

Biomass can be converted to ethanol in different ways. Enzymatic hydrolysis followed by fermentation can be used to produce ethanol from biomass. The main challenge of this process is the pretreatment step where an enzyme is used to convert the cellulose to glucose (Cardon and Sánchez , 2006). Chemicals like dilute sulphuric, hydrochloric or nitric acids can also be used in this step to hydrolyze the cellulose (Rao, 2004). However, the complexity of this process leads to higher production costs compared to processes that use sugar and starch as raw materials (Cardon and Sánchez, 2006).

1.4.4 Using Lignocellulosic Biomass by Gasification and Fermentation

Ethanol can be produced by gasification of biomass and then subsequent fermentation of the syngas. In this process, a gasifier is used to convert the lignocellulosic material into a synthesis gas at high temperature. The syngas is then cooled and fed to a bioreactor where the fermentation process takes place. The conversion of syngas to ethanol takes place in the bioreactor by using special strains of bacteria under anaerobic conditions. Finally, the ethanol produced from the bioreactor is separated from water using a distillation column and a molecular sieve column. The summary of the ethanol production process from syngas fermentation is shown in the following figure.

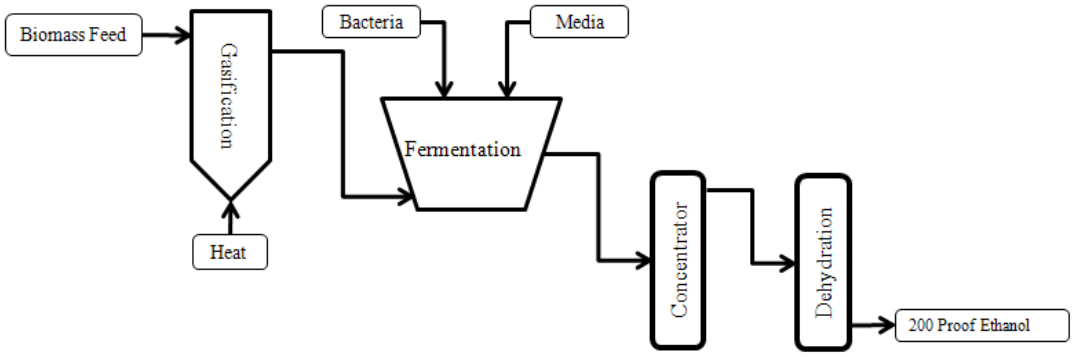

Figure 1.4 Production of ethanol from Lignocellulosic biomass

1.5 Problem Statement and Research Objective

A large number of studies are being conducted to find cost effective ways of producing ethanol. Lignocellulosic materials seem to be the most promising raw materials due to their ease of availability with low cost. Production of ethanol from biomass by gasification and then subsequent fermentation is relatively a new process. In many universities including Oklahoma State University investigations are being carried out on understanding the gasification and fermentation processes in laboratory scale units. Since this process has not yet been demonstrated at a commercial scale, a detailed process design and costing analysis is required.

Process design plays a big role in developing cost effective method of production by analyzing different process configurations and parameters. The process design and integration of ethanol production by syngas fermentation has not been studied in great detail. Overall process design is necessary to evaluate the feasibility of the ethanol production process. The objectives of this research include:

1. Develop full scale steady-state process models for ethanol production from syngas using a computer aided simulation (ASPEN^{TM} Plus software).
2. Determine the optimum operating conditions and equipment sizes to maximize ethanol production.
3. Validate simulation results with experimental data.
4. Perform a sensitivity analysis to explore the effects of temperature, pressure, feed ratio on major units using the developed process model.
5. Develop a molecular sieve model for dehydration of ethanol process
6. Perform an economic comparison between the two commonly used dehydration processes (Azeotropic distillation and molecular sieves).

Chapter 2

Literature Review of Ethanol Production Process Modeling

There are several studies available in the literature, that discuss the different processes for ethanol production. Many of these articles are focused on the use of sugar cane or corn as a raw material. However, there are only a few who have investigated process modeling and design of the ethanol production by gasification and fermentation process.

Although gasification has been studied widely for many years, its integration with the fermentation and ethanol dehydration process has not been studied in detail. The main focus of this chapter is discussing previously published information about the gasification, fermentation and dehydration processes. A brief discussion of each of the processes for producing ethanol is presented below.

2.1 Gasification

Gasification can be defined as a process of changing carbon containing materials such as biomass or coal into gases by a partial oxidation process at high temperature. The product gas mixture (syngas) is composed of CO, CO_2, CH_4, H_2, N_2, water, ethane,

ethene and various contaminants such as small char particles, ash and tar (Bridgwater, 1994). The partial oxidation is carried out by using air, oxygen or steam as the oxidation agent. Gasification of biomass using oxygen produces a higher heating value gas compared to air gasification. However, air is used more widely than oxygen due to the higher costs and hazards associated with oxygen production and usage (Bridgwater, 1995).

The three steps in a gasification processes are drying, pyrolysis and gasification. In the first zone all the moisture from the biomass is evaporated by up flowing hot product gas. Then the pyrolysis process occurs at a temperature of 400-600 ^{o}C. This region is where a thermochemical decomposition of biomass takes place and produces char, tar, gas and volatile compounds (Maschio, *et al.*, 1994). Finally, a gasification process occurs at a temperature of 700-900 ^{o}C. The char reacts with the oxidizing agent (air or oxygen) to produce syngas primarily composed of CO, CO_2, CH_4, H_2, and N_2 (Bettagi, *et al.*, 1995).

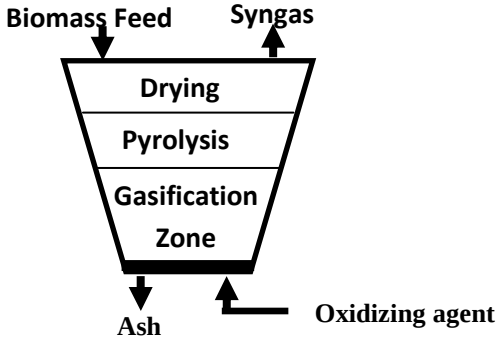

Figure 2.1Different zones in a downdraft gasifier

Datar, Shenkman and Cateni (2004) conducted a research at Oklahoma State University on fermentation of syngas to produce ethanol. They generated syngas by gasification of switchgrass using a fluidized-bed gasifier. They found out that the optimum temperature of the gasification zone was between 750 to 800 ^{o}C. When the

temperature was increased above 850 ^{o}C, there was a loss of fluidization due to the melting of alkali compounds in the switchgrass leading agglomeration of the sand.

2.1.1 Types of Gasifiers

Gasifier designs can generally be classified depending upon the type of flow conditions inside the unit. A ***Fixed bed*** gasifier consists of a fixed bed of biomass through which the oxidation agent flow in different flow configurations. Figure 2.1 shows the different zones of a downward gasifier. The other gasifier design is a ***Fluidized bed*** in which the oxidizing agent flows upwards through the bed while the biomass remains suspended. Silica sand is usually used as a fluidizing material and catalysts are used to reduce the formation of tar and modify product gas composition (Bridgwater, 1995).

2.1.2 Chemical Reaction Mechanisms in a Gasifier

The chemical reactions which occur in a gasification process are shown in the following reactions (McKendry, 2001).

Partial oxidation	$C + 0.5O_2 \leftrightarrow CO$	(2.1)
Complete oxidation	$C + O_2 \leftrightarrow CO_2$	(2.2)
Water gas reaction	$C + H_2O \leftrightarrow CO + H_2$	(2.3)
Water gas shift reaction	$CO + H_2O \leftrightarrow CO_2 + H_2$	(2.4)
Methane formation	$CO + 3H_2 \leftrightarrow CH_4 + H_2O$	(2.5)

The above reactions are at equilibrium. Thus depending on the temperature, pressure and concentration the reaction can proceed in either direction.

2.2 Syngas Fermentation

Syngas from the gasification process can be converted to alcohol by fermentation. The fermentation process takes place at a low temperature and pressure in the presence of microorganisms (Morrison, 2004). Anaerobic bacteria like *Clostridium ljungdahlii* and *Clostridium autoethanogenum* are capable of converting syngas to ethanol and acetic acid (Abrini, *et al.*, 1994). The stochiomety of synthesis gas fermentation to ethanol and acetate is as follows (Klasson, *et al.*, 1992a):

$$6CO + 3H_2O \rightarrow C_2H_5OH + 4CO_2 \quad (2.6)$$

$$6H_2 + 2CO_2 \rightarrow C_2H_5OH + 4H_2O \quad (2.7)$$

$$4CO + 2H_2O \rightarrow CH_3COOH + 2CO_2 \quad (2.8)$$

$$2CO_2 + 4H_2 \rightarrow CH_3COOH + 2H_2O \quad (2.9)$$

Datar, Shenkman and Cateni (2004) demonstrated the production of ethanol from syngas. They conducted experiments using a 4 liter bioreactor for 20 days. They observed that when they introduce the producer gas (syngas) the microorganisms stopped growing and ethanol was produced. Microorganisms began growing again when clean gases are introduced following exposure to the producer gas.

2.3 Dehydration Processes for Ethanol Water Mixture

The product from the bioreactor contains a substantial amount of water which needs to be dehydrated in order to be used as a transportation fuel. The mixture of ethanol and water form an azeotrope (a mixture which has the same vapor and liquid composition at a constant temperature). At atmospheric pressure the azeotrope occurs at 351 K (77.85 ^{O}C) where the purity of ethanol does not exceed to more than 90 mole% (Luyben, 2006). Due to the formation of azeotrope, the separation of Ethanol-water mixture cannot be performed by using a single distillation column. The two most commonly applied processes for the dehydration of ethanol are azeotropic distillation and molecular sieve (Jacques, 2003).

2.3.1 Azeotropic Distillation Using Benzene as Entrainer

Azeotropic distillation uses a third component, typically benzene or cyclohexane, to break the azeotrope. When an azeotropic agent is added to a mixture of water and ethanol, it forms two liquid phases which are partially miscible (Jacques, 2003). Benzene, ethanol and water form a ternary azeotrope with a boiling point of 64.9 ^{O}C (Luyben, 2006). Since this azeotrope is more volatile than the ethanol-water azeotrope, it can be distilled out of the ethanol-water mixture, extracting all of the water in the process. The overhead product is then separated in a decanter into a water-rich layer and organic (benzene)-rich layer (Jacques, 2003).

2.3.2 Dehydration of Ethanol Using Molecular Sieve

Most new ethanol plants use molecular sieve columns for dehydration of ethanol (Jacques, 2003). A molecular sieve column uses an adsorbent with a strong affinity for

water and little affinity for ethanol and other impurities. When wet ethanol vapor passes through the bed, the desiccant adsorbs the water molecules. Synthetic zeolites (aluminosilicates minerals) are the most commonly used desiccants. They have a crystalline lattice structure that contains very precise openings (pores) of a certain pore size, measured in angstroms (Å). The pore size of synthetic zeolite is 3 Å of in diameter, whereas water and ethanol molecules are 2.8 Å and 4.4 Å respectively. Therefore, water molecules are strongly attracted into the pores but ethanol molecules are excluded. (Jacques, 2003) The heat of adsorption of water in a type 3 Å molecular sieve is 1800 BTUs (heat is released) for each pound adsorbed. The same amount of energy is required to regenerate the bed by using a regeneration gas (Gas processors suppliers association (GPSA), 1998).

A continuous process requires two (or more) vessels with one removing water while the other is being regenerated. The ethanol-water mixture flows downward during the adsorption process typically for 8-24 hrs. When the bed is taken off-line, the water is removed by heating the bed up to 600 ^{o}F. The regeneration gas used to heat the bed is usually preheated air. After the regeneration process the gas is then returned to the process after it has been cooled and the free water removed (Jacques, 2003).

2.4 Experimental Setup of Gasification Process Unit

At present, a fluidized bed and down draft gasifiers are being investigated on a laboratory scale at Oklahoma State University. The fluidized bed gasifier was designed by Carbon Energy Technology, Inc. and the Center for Coal and the Environment at Iowa State University (Cateni, 2007). In 2003, the down draft gasifier was designed and constructed in the Biosystems and Agricultural Engineering fabrication shop at Oklahoma State University. Due to the generation of high amount of char residue, the initial design was modified in 2005 (Patil, *et. al.*, 2008).

The two gasifier designs are shown in Figure 2.2 and 2.3. The fluidized bed gasifier is made of mild steel and has an internal diameter of 25–cm with a 5-cm refectory. This reactor is filled with sand particles as the fluidizing medium. (Cateni, 2007)

The pilot scale gasifiers consist of a biomass feeding unit, gasification reactor, cyclone separator and ignition system (producer gas burner). The biomass feeding unit includes a hopper, an air lock valve and two screw feeders. The biomass from the cylindrical fuel hopper is fed using an injection auger which pushes the material into the reactor. Air is fed through the bottom of the bed using a distribution plate. Once the temperature of the bed reaches 800 ^{O}C, the flow of the air feed is reduced to minimize combustion (full oxidation) and maximize H_2 and CO production. The syngas that exits from the gasifier is then sent to a purification process. Both gasification reactors use the same cyclone separator to remove impurities from the syngas. The final clean syngas is then fed to a compressor where it is compressed to a pressure of 120 psia. Two storage tanks with a capacity of 650 Liters are used to store the product gas. (Patil, *et. al.*, 2008)

Figure 2.2 Fluidized bed gasifier system at Oklahoma State University

Figure 2.3 Downdraft gasifier system at Oklahoma State University

2.5 Experimental Setup of Fermentation Units

A syngas fermentation process is presently under study at Oklahoma State University. The use of Colstridium Carboxidivorans (type of bacteria that changes syngas to alcohol) is being investigated. Experiments are carried out using a BioFlo 110 Benchtop Fermentor. This bioreactor has a volume of 3 liters and works with a continuous liquid feed and product removal. The main units in the reactor are agitator, sparger, pH probe, dissolved oxygen probe, ports for liquid inlet and outlet, jacket for temperature control and pumps for feed, product removal and pH control (Ahmed and Lewis, 2005).

As it is shown in Figure 2.4, gases from the four storage tanks are mixed up to obtain the feed gas. The mixture gas is composed of CO, CO_2, and H_2 (balance N_2) and has a same composition as the syngas from a gasification process. The 4-way valve is used to change the feed from pure bottled gases to syngas (produced from the gasification process). The feed gas is introduced to the reactor using a sparger which bubbles the gases through the rector. A sterile media, from the two liquid tanks, is also fed into the bioreactor during the continuous fermentation process. The final product and unreacted gases from the reactor are then sampled and analyzed (Ahmed and Lewis, 2005).

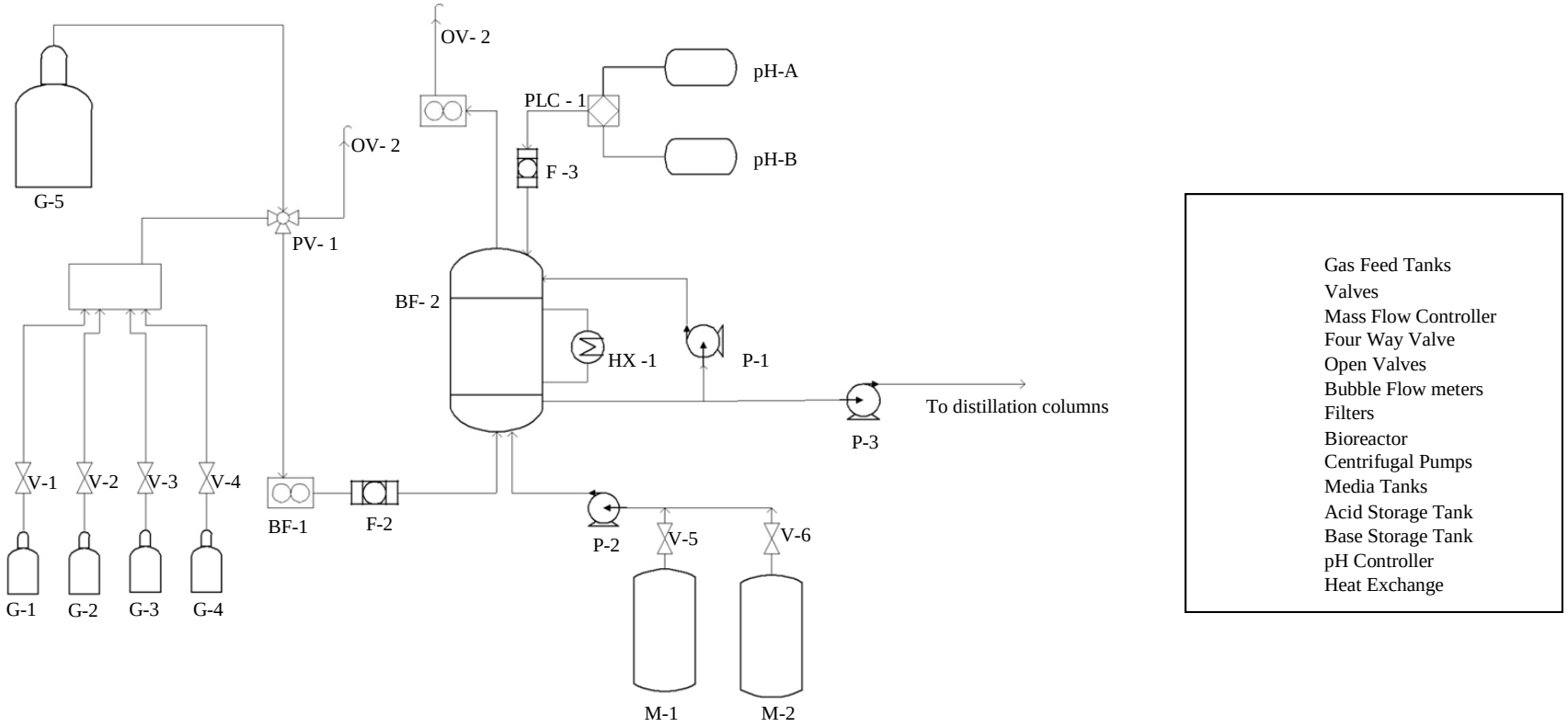

Figure 2.4 Schematic of the fermentation unit at Oklahoma State University (Rao, 2004)

2.5 Process Modeling and Simulation

In order to evaluate the feasibility of the ethanol production process, it is important to assess the efficiencies of the gasification, fermentation and the dehydration processes. Evaluating these processes by performing experiment requires a substantial investment of money and time and effort. Due to this reason, it is necessary to come up with a better technique to evaluate the performance of a process with out conducting full scale experiments. Process models are a convenient way to accomplish this.

The two approaches in developing a process model are theoretical and empirical models. Empirical models are based on experiment or experience with out theoretical basis. It is used when there is no well known process mechanism or when developing a theoretical model is very complicated (Latwik, 1999). Empirical models can be derived from experimental data using statistical regression techniques.

Theoretical models are developed from theoretical considerations. They are used when the phenomena governing the process are well known (Latwik, 1999). Theoretical models are used to understand the relationship of input parameters, to answer "what-if" questions and to find optimal solutions for a given process.

The schematic representation of a process design procedure is shown in figure 2.5. Preliminary process synthesis is the first step in a developing a chemical process model. In this step, different unit operations are selected to convert raw materials to a desired product.

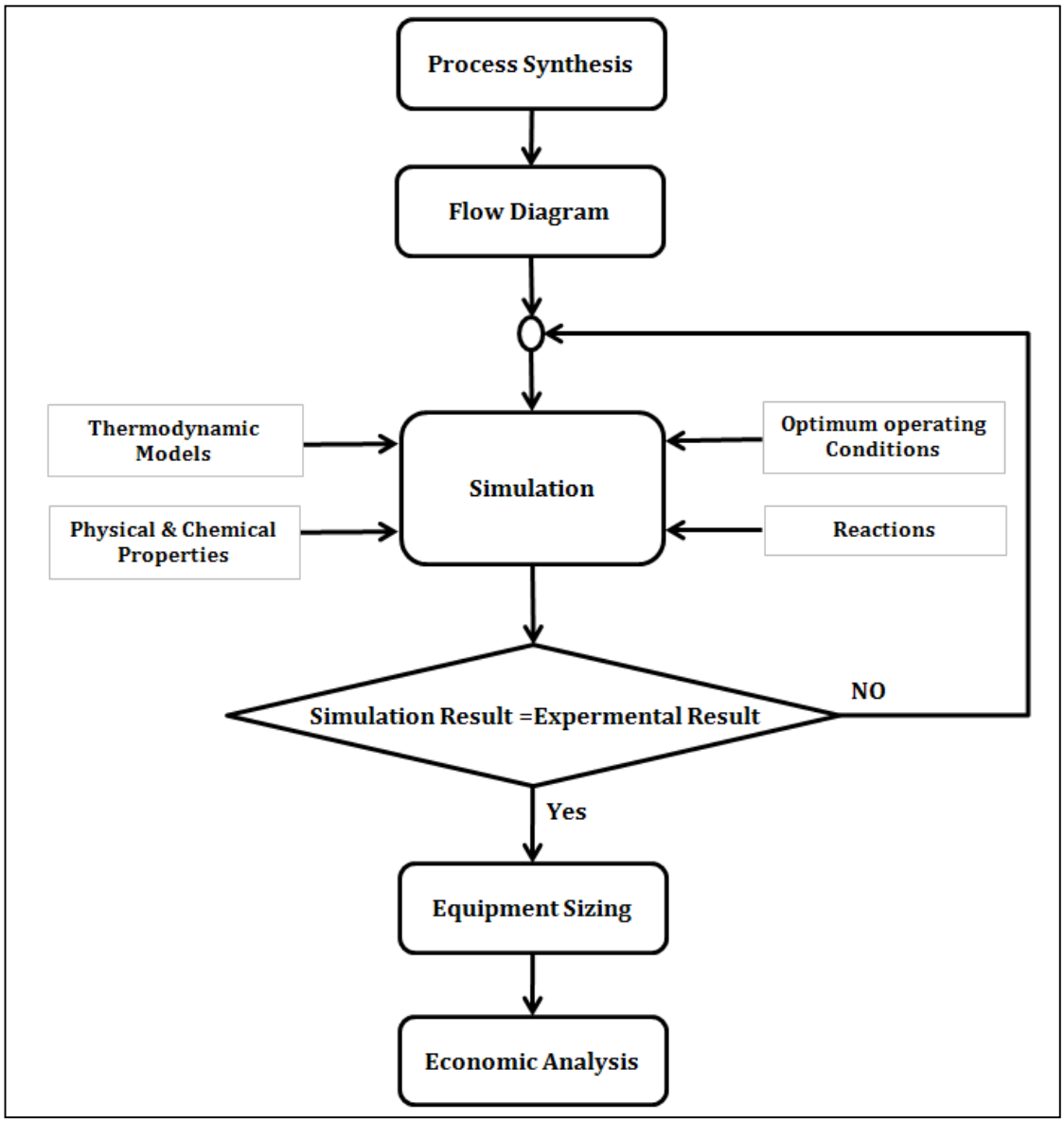

Figure 2.5 Schematic of process design

After the process synthesis step, a base case design is created by developing a process flow diagram. The process flow diagram provides a more detailed view of the production process. It displays all the major processing units and provides stream information (Seider, 2009).

The simulation step is used to replicate an actual system using mathematical equations, to relate the parameters that describe the system. Developing a chemical process model for simulation requires a large amount of data. These data include the physical and chemical properties of the various compounds involved in the process, thermodynamic models, reaction chemistry and process conditions (Figure 2.5). After feeding all the required data, the predicted simulation results are validated by comparing with experimental results. If the model is in good agreement with the experimental results, it can be used for future process analysis such as optimization, plant expansion, economic analysis, etc. However, if the model does not fit the experimental data, input parameters are changed until the model gives a reasonable fit (Patrachari, 2008).

Simulators play an important role in a chemical process modeling. They are a convenient tool for analyzing and understanding a process. There are various chemical process simulation software packages available on the market. These include ASPEN, ChemCAD, HYSYS, PRO-II, etc. The big advantage of these simulators is, they have built in thermodynamic data and equation of state (EOS) models. One of the most widely used commercial process simulation software for steady state and dynamics simulation is Aspen^{TM} (Luyben, 2006). Aspen Plus^{TM} has many advantages compared to other process simulation softwares. It has built in thermodynamic models and unit operations that includes reactors, distillation columns, separators, mixers, pressure changers, etc. Using Aspen Plus^{TM}, a process flowsheet diagram can be developed easily by interconnecting different unit operation models. Unlike other simulators, Aspen Plus^{TM} has a built in thermodynamic model for solids. Additionally, Aspen Plus^{TM} allows users to access predefined subroutines to develop a new user defined unit operation.

2.5.1 Modeling and Simulation of the Gasification Process

Developing a model for the gasification process is a complex task which requires knowledge of thermodynamics, fluid dynamics, and chemistry. A large amount of theoretical and experimental background is required to model the process. Most of the parameters needed for modeling biomass gasification are not available in the literature (Bettagli et al., 1995). Most of the biomass gasification models are developed for a fluidized-bed gasifier. Generally, these models can be categorized into kinetic or equilibrium models.

Kinetic models provide information about the reaction condition for all intermediate steps and also provide the product composition at different locations along the reactor. In developing such a model, kinetic data (pre-exponential and reaction rate constants) are required for each individual reaction. Equilibrium models predict the maximum achievable yield of a desired product from a gasification process. This model assumes that all the reactions which occur in the process are at thermodynamic equilibrium.

There are many kinetic and thermodynamic models for biomass gasification that are presented in the literature. (Lu, *et al.,* (2009), Corella and Sanz (2005), Mansaray, *et al.,* (2000), Schuster, *et al.,* (2001)). Lu, *et al.,* (2009) introduced a model for the gasification of biomass using a fluidized – bed gasifier. They considered eight chemical reactions and assumed steady-state, isothermal and one-dimensional flow. They came up with a mathematical model after solving simultaneous ordinary differential equations that describe the system. Corella and Sanz (2005) presented a one-dimensional model for a circulating fluidized bed biomass gasifier (CFBBG). Their model was based on kinetic

equations for a twelve reaction model. They developed a semi-empirical model by solving mass and energy balance differential equations along with experimental data. Schuster et al. (2001) developed a model for steam gasification of biomass by applying thermodynamic equilibrium calculations. They used an equation-oriented simulation tool IPSEpro^{TM} to develop the model.

Thermodynamic equilibrium models are more convenient to apply than kinetic models for designing a gasifier. Thermodynamic equilibrium calculations are independent of the gasifier type. Developing a kinetic model requires experimentation to determine the kinetic parameters of the reactions that take place in the gasification process. Due to this reason thermodynamic equilibrium models are easier to design a gasifier. In this research, a thermodynamic equilibrium model for biomass gasification of switch grass was developed using the Aspen Plus™ simulator. The following assumptions were made when modeling the gasification process.

1. Due to the high operating temperature, the reactions are assumed to be at thermodynamic equilibrium.
2. The process is at steady state
3. Perfect mixing occurs inside the reactor
4. Ash and tar are neglected from the gasifier product
5. The process is isothermal

2.5.2 Modeling and Simulation of the Fermentation Process

Biological, physical and chemical data are required to develop a model for biological reactors. Biological information such as cell growth rate, product concentrations and substrate consumption rate are needed to describe the fermentation process quantitatively. The major physical factors that need to be considered in the model are mass transfer rate and intensity of mixing (Dunn at el, 2003).

Many bioreactor models which are presented in the literature are kinetic models (Silva et al. (1999), Pascal et al. (1995), Kalil et al. (2000), Nihtila et al. (1997)). These mathematical models of biological systems are complex and highly non-linear. They are developed by solving sets of differential equations which are derived from mass and energy balance of the process.

Some of the simulation software packages that are usually used for a bioreactor modeling are BERKELEY, MODELMAKER, ACSL-OPTIMIZE, and MATLAB-SIMULINK (Dunn at el., 2003). Pascal et al. (1995) presented a simulation model for a fermentation process for a perfectly well-stirred, isothermal and isobaric biological reactor. Six independent chemical reactions were considered in the model. The model predicts the amount of ethanol and other compounds by solving the governing differential equations using Prosim^{TM} simulation software. The main limitations of this model are that it does not consider all of the metabolic reactions and it does not take into account the effect of product inhibition.

The syngas fermentation process involves mass transfer of gasses (substrate) into the liquid media. In order to have a rigorous model, equilibrium properties must be considered as boundary conditions (Pascal et al, 1995). In this work, the fermenter model

was developed using a thermodynamic equilibrium approach. A Gibbs energy minimization technique was applied to find out the maximum possible amount of ethanol produced in the process. The key assumptions that are taken in modeling the bioreactor are as follows.

1. The reactions are at thermodynamic equilibrium
2. The process is at steady state
3. The bioreactor is perfectly well-stirred
4. The process is isothermal and isobaric
5. Microorganisms are neglected.
6. Negligible mass transfer resistance

2.5.2 Modeling and Simulation of the Dehydration Process

Ethanol separation from a water-ethanol mixture can be performed using azeotropic distillation, extractive distillation, supercritical fluid extraction, or molecular sieve. Several models for azeotropic and extractive distillation separation processes have been proposed in the literature. (Cho et al. (2006), Piccolo et al., (2008), Llano-Restrepo et al. (2003)). Many of these models were developed using process simulation software such as Aspen Plus™, PRO II™ and CHEMICAD™. Several compounds like benzene, cyclohexane, acetone and pentane have been used as an entrainer to achieve separation in these models.

Not many sources discuss the dehydration process using molecular sieve. Therefore, preparing a mathematical model is necessary to investigate this process. Standard Aspen Plus™ simulation software does not have a built-in model for a

molecular sieve. Therefore, this process is modeled with a new user defined unit operation using a FORTRAN program code and Microsoft Excel.

In this work, azeotropic distillation and molecular sieve models were developed for dehydration of ethanol. In the azeotropic separation model benzene was used as an azeotrope breaking agent. Different flowsheet configurations were analyzed to minimize the energy consumption of the process. In the second model (using molecular sieve), a new “user model” has been created and implemented.

Chapter 3

Process Model development

Aspen Plus™ is a powerful process simulation tool that is extensively used to predict the behavior of chemical processes and analyze their results. Applications range from a single process model to profitability analysis of a chemical plant. The specific capabilities of Aspen Plus include, solving mass and energy balances, predicting phase and chemical equilibrium, data fitting, meeting design specifications, sensitivity analysis, enabling user to create process flowsheets and charts, etc. In this chapter, steps of developing steady state process model for ethanol production using Aspen plus are discussed in detail.

3.1 Chemical Components

Aspen Plus™ has a large database of chemical compounds that are commonly used in the industry. The built-in database contains more than 8,500 components, covering organic, inorganic, aqueous, and salt species. It also includes more than 3,000 organic and inorganic electrolytic species (Aspen Plus™ User Manuals, 2003). In developing the process model of ethanol production, all the chemical compounds involve in the process were selected from the built-in database.

3.1.2 Thermodynamic Model Selection

Thermodynamic models are generalized mathematical correlations that describe the physical and chemical behavior of a substance. They are used to predict system properties such as density, entropy, K-values, Gibbs free energy, enthalpy, VLE properties, etc.

Aspen Plus™ has built-in thermodynamic property models, data and estimation methods which cover a wide range of processes from simple ideal behavior to strongly non-ideal mixtures and electrolytes. There are about 80 EOS based thermodynamic models in Aspen Plus™. The built-in database also contains more than 37,000 sets of binary interaction parameters which were determined using data obtained from the DECHEMA (Aspen Plus™ User Manuals, 2003). The most commonly used thermodynamic models in Aspen Plus™ are listed in Table 3.1.

Table 3.1Thermodynamic property models

Equation of State Models	Activity Coefficient Models
Ideal gas law	NRTL
Peng-Robinson (PR)	UNIQUAC
Redlich-Kwong(RK)	UNIFAK
Redlich-Kwong-Soave(RSK)	Van Laar
Lee-Kesler(LK)	Wilson
Predictive SRK	**Special Models**
Sanchez-Lacombe	Steam Tables
Lee-Kesler-Plocker	Chao-Seader

The accuracy of a simulation model strongly depends on the choice of property models used to predict the properties of the components. Hence, a proper selection of thermodynamic models is necessary while using process simulation softwares. The four main factors to consider in selecting property methods are (Carlson, 1996):

1. Nature of the properties of interest
2. Operating conditions (temperature and pressure)
3. Composition of the mixtures
4. Data availability

The process simulation of ethanol production was carried out by selecting proper thermodynamic models for each unit operation. In the gasification process, biomass at ambient pressure and temperature is in solid phase. Therefore, the SOLIDS EOS property model was used to predict the physical and thermodynamic properties of biomass.

For mixtures containing polar components like water and ethanol, activity coefficient models are used to accurately predict non-ideal liquid behaviors. The recommended thermodynamic property methods for mixture with polar compounds are WILSON, NRTL, UNIQUAC and UNIFAC (Carlson, 1996).

The activity coefficients for the water-ethanol mixture were calculated using NRTL property model. Vapor liquid equilibrium (VLE) experimental data from the literature was used to validate the simulation predictions of vapor and liquid compositions of water-ethanol mixture. Figure 3.1 shows the comparison made between the VLE values predicted by the simulation using NRTL (Eqation 3-1 and 3-2) and experimental data reported by Lei (2002). A good agreement between the experimental data and the simulation result can be observed from the figure. The simulation accurately predicted the formation of azeotrope when the liquid composition is around 0.94. The average percentage deviation from the experimental result was around 1%.

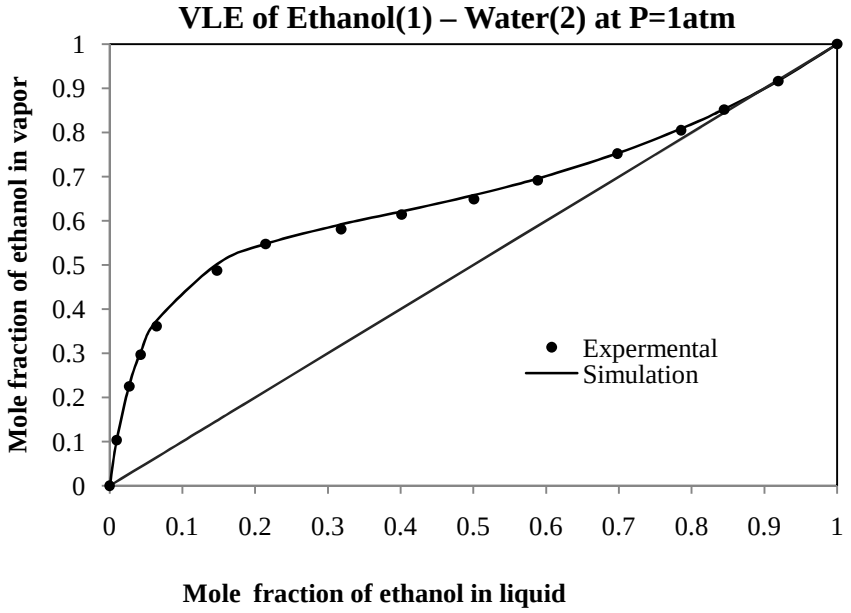

Figure 3.1 Experimental and simulation Binary equilibrium data of ethanol-water mixture

NRTL model (Non-Random Two Liquids Model) was used to simulate the ethanol dehydration process. The activity coefficient expression is shown as follows.

$$\ln \gamma_i = \frac{\sum_j x_j \tau_{ji} G_{ji}}{\sum_k x_k G_{ki}} + \sum_j \frac{x_j G_{jj}}{\sum_k x_k G_{kj}} \left(\tau_{ij} - \frac{\sum_m x_m \tau_{mj} G_{mj}}{\sum_k x_k G_{kj}} \right) \tag{3.1}$$

$$\begin{aligned} &where: \\ &G_{ij} = \exp(-\alpha_{ij} \tau_{ij}) \\ &\tau_{ij} = a_{ij} + {b_{ij}}/{T} + e_{ij} \ln T + f_{ij} T \\ &a_{ij} = c_{ij} + d_{ij}(T - 273.15K) \\ &\tau_{ii} = 0 \\ &G_{ij} = 1 \end{aligned} \tag{3.2}$$

Table 3.2 NRTL parameters of Ethanol (1)-Water (2) Mixture

NRTL Parameters	Values
a_{12}	3.4578
a_{21}	-0.8009
b_{12}	-1054.94
b_{21}	443.124
c_{12}	0.3
d_{12}, e_{12}, e_{21}, f_{12}, f_{21}	0

The thermodynamic property models used in the process simulations are listed in the following table.

Table 3.3 Physical property methods for different unit operations

Unit Operation	Property Method
Gasifier	SOLIDS EOS
Bioreactor	NRTL
Cooler	NRTL
Gas Separator	NRTL
Decanter	NRTL
Distillation Column(1,2,3)	NRTL
Pump and Heat exchanger	NRTL

3.1.3 Unit Operation Selection

The built-in model library of Aspen Plus™ has several process units. Process units operations that are used in the simulations are reactors, heat exchangers, distillation columns, flash drums, pumps, valves and mixers.

The gasification and the fermentation processes were modeled using a Gibbs reactor model. The separation process of unreacted gases from the fermentation unit was designed as a flash drum unit. The final process (dehydration of ethanol) was designed by using distillation columns followed by a user defined unit for the molecular sieve column. The customized unit was created by writing a program code in Excel worksheet and importing the unit into Aspen Plus™ model library.

3.1.4 Stream Input and Equipment Specification

The simulation was carried out by entering all the required input data for each unit operations. Temperature, pressure, flow rate and composition were specified in the input specification sheet of each stream. Using the defined input information, other parameters were calculated by the selected thermodynamic models. Figure 3.2 shows an input specification snapshot of the biomass feed stream. The input data is an experimental result from the gasifier pilot plant at OSU.

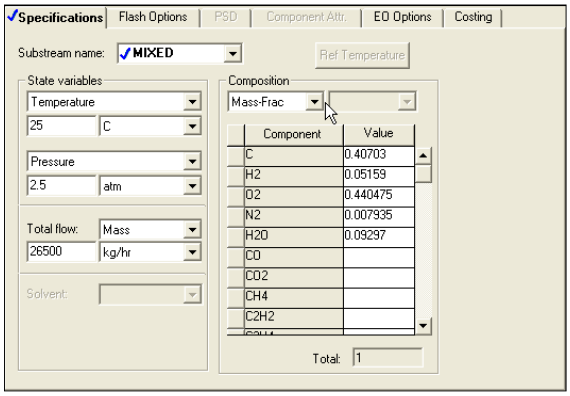

Figure 3.2 Input specification sheet in Aspen Plus™ of a stream

The process units that are defined in the simulation have different specification parameters. Figure 3-2 shows a block specification snapshot of a distillation column. The required specification are type of column (equilibrium or rate-based), Number of stages, distillate rate, reflux ratio, etc.

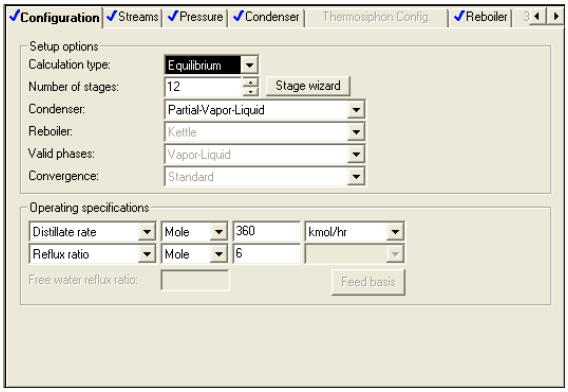

Figure 3.2 Input specification sheet in Aspen Plus™ of a distillation column

3.1.5 Simulation Output

Once the feed to each unit operation is defined, the outputs of each process are calculated by performing mass and energy balances. The results are displayed in the form of tables or graphs. Figure 3.3 shows the block result summary of syngas cooler. All the calculated values from the simulation (outlet temperature, pressure, heat duty and pressure drop) are listed in the output sheet. Figure 3.4 shows the temperature profile of the distillation column which is used the dehydration process.

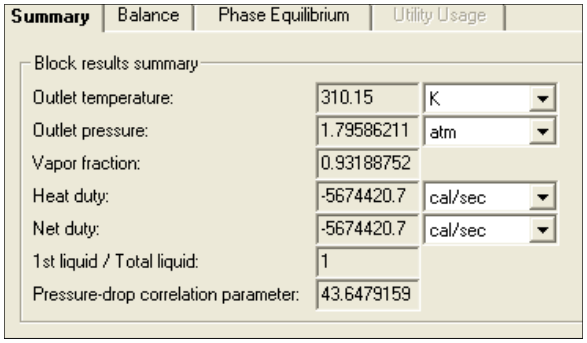

Figure 3.3. Syngas cooler Result summary

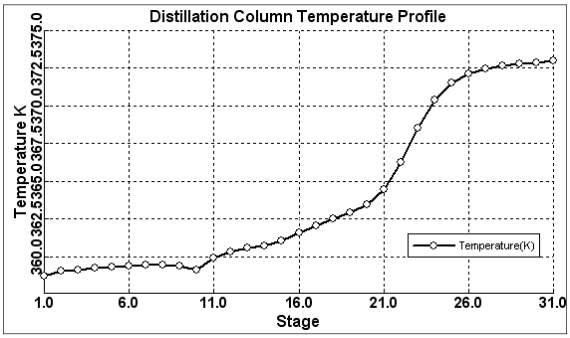

Figure 3.4. Distillation Column Temperature profile

3.1.6 Sensitivity Analysis

Sensitivity analysis are performed to study the effect of changes in input variables (temperature, pressure, vapor fraction, etc) on process outputs. Results from the sensitivity analysis give us an idea of how a process behaves when they are carried out at different operating conditions. They are very important in determining feasible and optimum operating conditions of chemical processes.

Sensitivity analyses were performed on major units to obtain the minimum ethanol production cost. Input variables that were investigated are as follows.

Gasification process	• The effect of operating temperature and pressure • The effect of Air to biomass ratio.
Fermentation process	• The effect of operating pressure, • The effect of media to syngas ratio
Flash Drum (Separation)	• The effect of operating temperature and pressure
Dehydration process	• The effect of operating temperature and pressure • The effect of distillate flow rate, reflux ratio, etc…

3.1.8 Process Flowsheet

The process flowsheet indicates the general flow of materials and the arrangement of unit operations in the process. The flowsheets of ethanol production process were constructed by connecting inlet and outlet material streams with each unit operation. The major units in the process are gasifier, bioreactor, flash drum, distillation column, decanter, pump and molecular sieve. Flow sheets of the two alternative ways of ethanol production by syngas gasification are shown in Figures 4.1 and 4.2

Chapter 4

Process models

In this chapter, two alternative process models for the production of 99.5% ethanol are briefly discussed. These process models use different dehydration techniques to separate the azeotropic mixture of Ethanol-Water (95wt % ethanol) which comes from the distillation column. In the first model, the dehydration process is carried out using azeotropic separation. The second method is use of a molecular sieve column.

Flowsheets of the two process models are shown in Figures 4.1 and 4.2. A number of design specifications and assumptions were made while developing the process models of ethanol production through syngas gasification.

1. The annual production rate is about 20 million gallons per year. The number of working days in a year is assumed to be 300.
2. Experimental gasification and fermentation data obtained from the Biosystems and Agricultural Department experiments are the basis for the process design.
3. Complete biomass to syngas conversion was assumed. Since tar and char are not considered in the product, the syngas purification process was not included in the simulations.

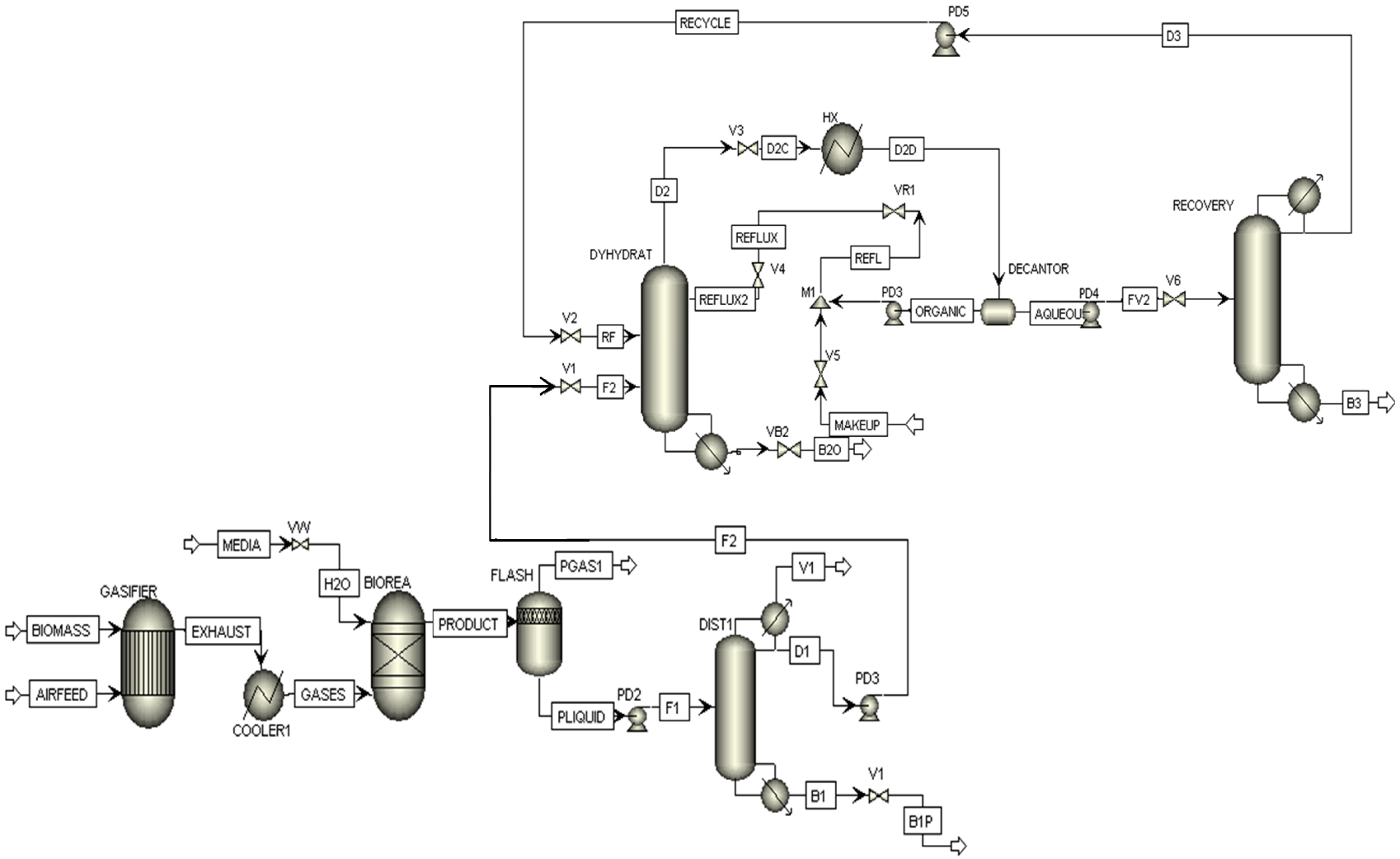

Figure 4.1. Process flow sheet diagram of ethanol production by syngas fermentation followed by azeotropic separation

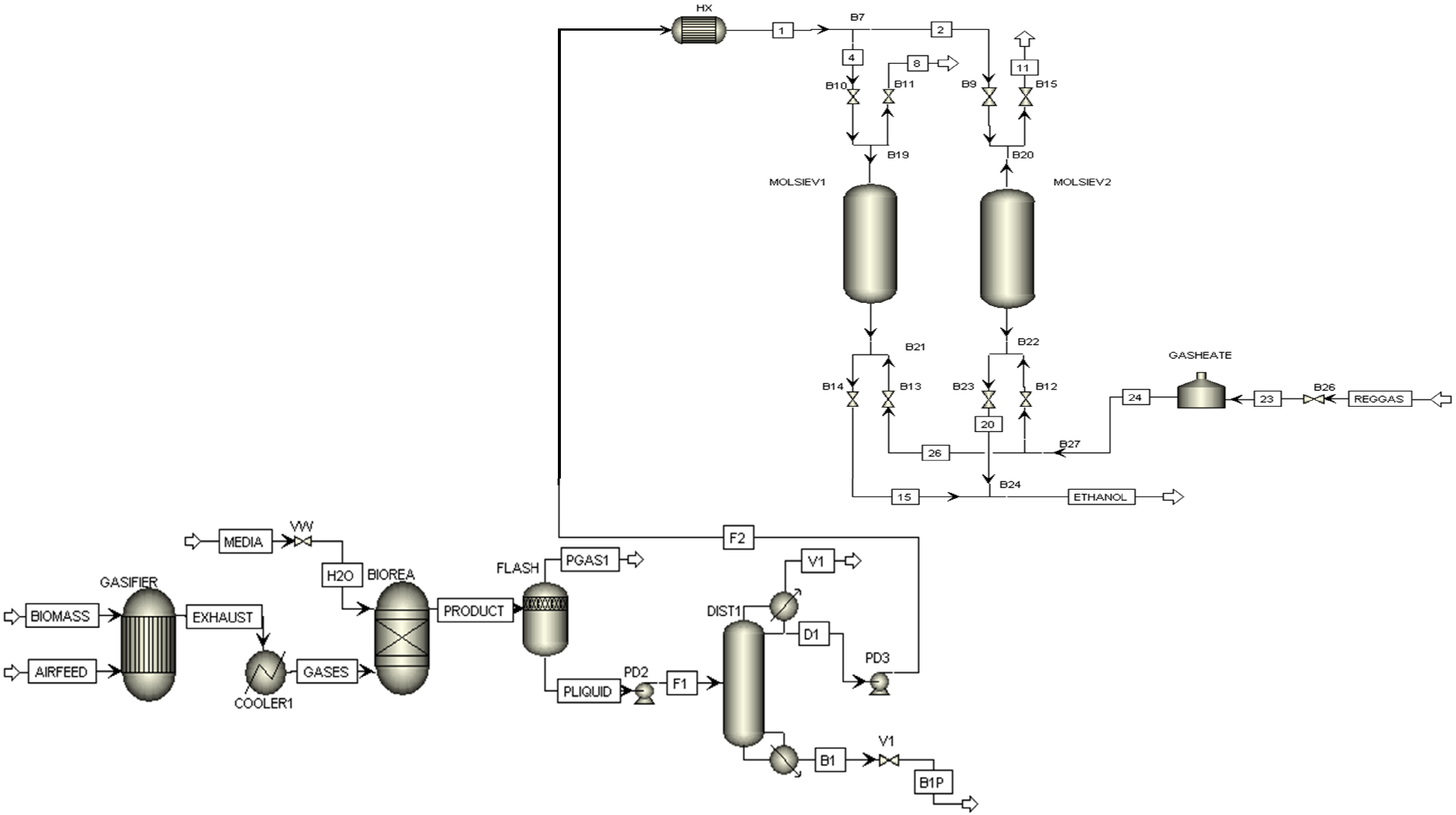

Figure 4.2 Process flow sheet diagram of ethanol production by syngas fermentation followed molecular sieve dehydration process

4.1 Gasification Model

The gasifier was modeled as a Gibbs reactor. In this model all reactions are assumed to be at chemical equilibrium in which the forward and reverse reaction rates are the same. The chemical equilibrium compositions are determined by minimizing the Gibbs free energy at the system conditions.

The RGIBBS model is the only unit in Aspen Plus^{TM} that can compute a solid-liquid-vapor phase equilibrium (Rao, 2004). All reactants and possible products that are involved in the gasification process are defined in the RGIBBS model. According to the experimental result the major products from the gasification process are H_2, N_2, O_2, CO, CH_4, CO_2, C_2H_2, C_2H_4, C_2H_6, and H_2O.

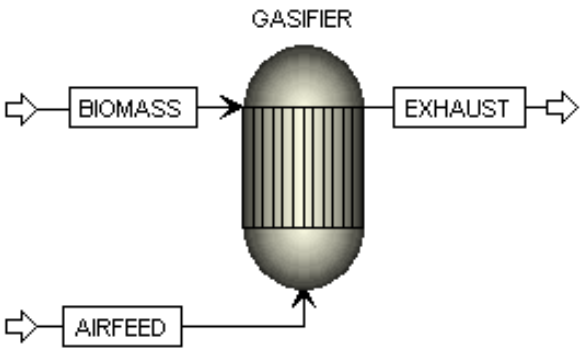

Figure 4.3. Process diagram of gasifier

Figure 4.3 shows a schematic representation of the gasification process. The basis for the simulation is experimental data obtained from an earlier research project conducted at Oklahoma State University. The base case simulation was performed using the same 1.7:1 air to biomass feed ratio as the experimental result (Table 5.1). The gasification process is operated at a temperature of 815 ^{o}C (1500 ^{o}F) and a pressure of 2

atm (37 psia). Switch grass (composed of carbon, hydrogen, oxygen, nitrogen and water) and air are feed to the gasifier unit. Air and biomass enter to the gasifier at 25 ^{o}C (77 ^{o}F) with a mass flow rate of 26500 kg/hr and 45,200 kg/hr respectively. Air is considered to be composed of only oxygen and nitrogen with a 21 mole % and 79 mole % respectively. Input compositions are shown in Table 5.1.

4.4 Bioreactor Model

The Gibbs reactor model (RGIBBS) was also used to model the fermentation process. This model gives the maximum possible amount of ethanol that can be produced at the specified operating temperature and pressure. The Gibbs energy minimization technique is applied to predict the product distribution resulting from fermentation unit.

The possible products from the bioreactor are ethanol, water and trace amount of unreacted gases (CO, CO_2, H_2 and N_2). The experimental results show the production of butanol and acetic acid in the reactor (Rao, 2004). These compounds were not considered in the simulation because the main purpose of this work is to investigate the ethanol production.

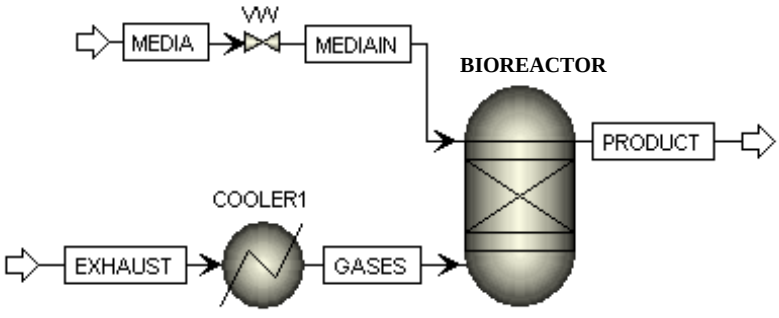

Figure 4.4. Process diagram of cooler and bioreactor

A schematic representation of the fermentation process is shown in Figure 4.4. The syngas (mainly composed of CO, CO_2, H_2 and N_2) from the gasifier is cooled from 815^{o}C to 37^{o}C before it is sent to the fermentation unit. The cooled syngas and media are then fed to the bioreactor. The simulation was carried out by assuming that the media is 100% water. The operating pressure and temperature of the fermentation unit are 1.5atm and 37 ^{o}C respectively.

4.5 Flash Drum Model

The product from the bioreactor consists of water, ethanol and significant amounts of unreacted gases mainly (CO, CO_2, H_2 and N_2). The unreacted gases will result in accumulation or build-up of non-condensable gases in the distillation columns. Therefore, all the unreacted gases need to be separated from the mixture before entering the distillation column.

In order to remove the unreacted gases a flash drum model was used in the simulation. A flash separation is basically a one stage separation process in which gases are separated from a saturated liquid stream at reduced pressures. The flash model in Aspen Plus^{TM} performs vapor-liquid or vapor-liquid-liquid equilibrium calculations for specified outlet conditions.

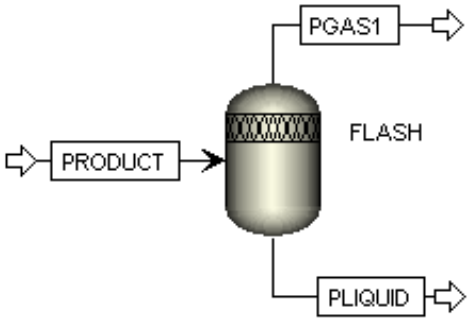

Figure 4.5. Process diagram of cooler and bioreactor

Figure 4.5 shows a schematic representation of the flash separation process. The flash drum is designed to operate at a pressure of 19.33 psia and temperature of 298 K (37^{o}C). These operating temperature and pressure were selected by performing various sensitivity analyses on the flash drum.

Although most of the unreacted gases are separated in the flash drum, a small amount of these gases still remain in the liquid mixture. The rest of the unreacted gases are separated in the distillation column condenser using a pressure relief valve.

4.6 Ethanol Concentrator Model

The product from the fermentation process has low ethanol concentration. This mixture has to be concentrated in order to be used as a transportation fuel. Typically, distillation columns are used to separate liquid mixtures of significantly different boiling temperatures. At atmospheric pressure the boiling point of ethanol and water is 78 ^{o}C and 100 °C respectively. This difference in boiling temperature makes the distillation separation process possible.

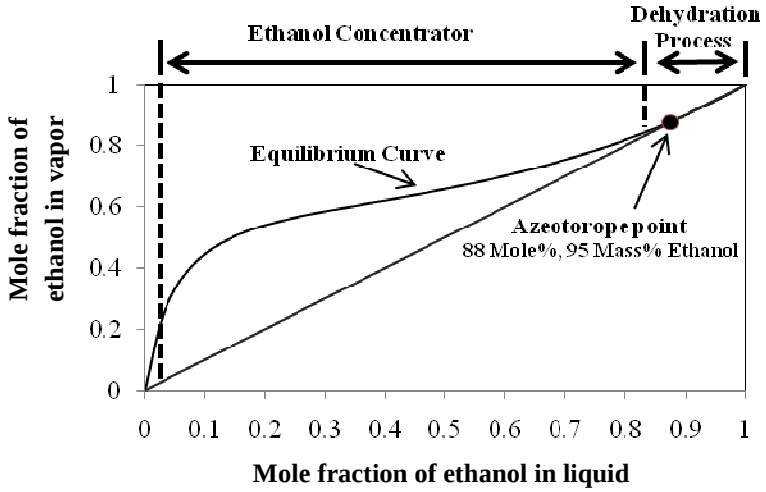

Figure 4.6. VLE of ethanol-water mixture and separation processes

Figure 4.6 shows the VLE plot for an ethanol and water mixture. The mixture forms an azeotrope when the composition of ethanol is 95 wt%. This is a mixture with

identical vapor and liquid composition. Therefore the maximum purity of ethanol using a single distillation column is 95 wt% which is an azeotropic ethanol-water mixture. Hence, a different technique must be used to further purify ethanol beyond 95 wt%.

The separation process in the simulation is divided into two sections (Ethanol concentrator and dehydrator). The ethanol concentrator process was designed using a RadFrac distillation model. The number of distillation columns, minimum number of trays and reflux ratio were determined by performing several optimization analyses.

Initially, a DSTWU (shortcut distillation) model was used to predict the column operating conditions. Then the results are used to design the RadFrac distillation column in the process. DSTWU model calculates the minimum number of trays and reflux ratio using built-in correlations. After comparing the energy and cost of different column configurations, the two-column arrangement (Figure 4.7 B) was selected to be used in the base-case simulation. The optimization analyses results are shown in the chapter 5.

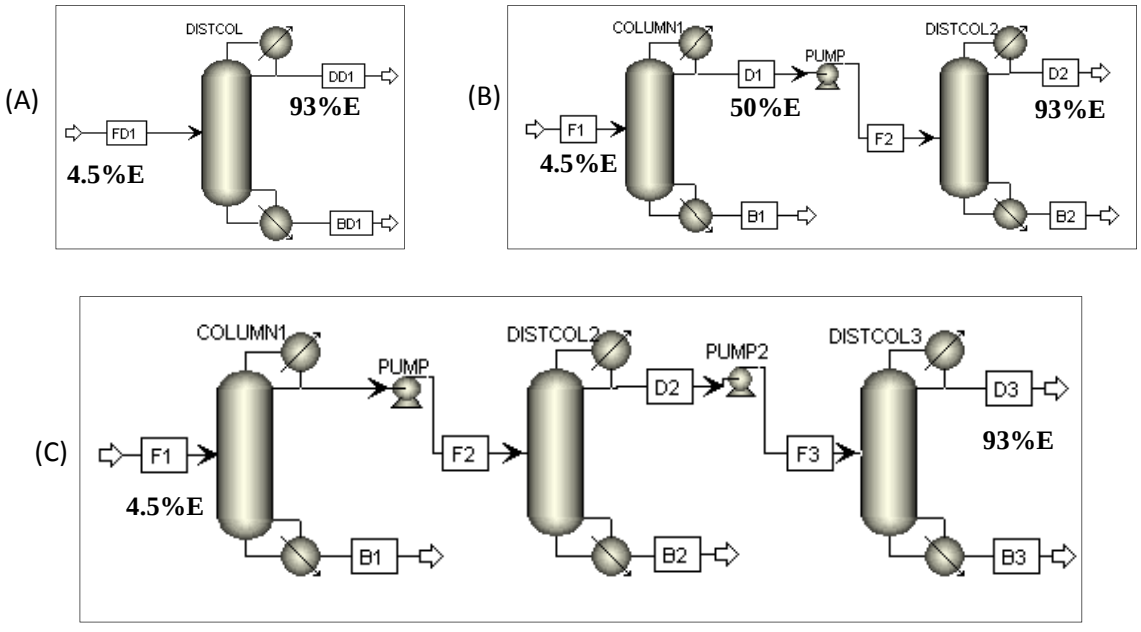

Figure 4.7, (A) one, (B) two, and (C) three – column configuration of ethanol concentration process

The ethanol mixture enters the first column at 1.4 atm and 27 ^{o}C. This column is operates at a condenser pressure of 1.1 atm and at a reboiler pressure of 1.5 atm. The distillate of the first column has a purity of 50 wt% ethanol and is sent to the second distillation column. The second distillation column further separates water from the mixture and produces a distillate with 93 wt% ethanol.

4.7 Azeotropic Separation Model

The azeotropic separation process was carried out by adding benzene as an entrainer to break the azeotrope. Benzene forms a ternary azeotrope mixture with ethanol and water. The mixture has a lower boiling point (64.9°C) than pure ethanol (78°C). Since this azeotrope mixture is more volatile, it can be distilled out by extracting water from the ethanol-water mixture. The desired product (pure ethanol) is finally obtained in the bottoms of the distillation column.

Figure 4.8 shows the flowsheet for the azeotropic separation process. This process was designed using two distillation columns, decanter, heat exchanger and pumps. The first distillation column is a dehydration unit which produces high purity ethanol product as the bottoms of the column. The overhead is then condensed and fed into the decanter where it forms two liquids layers which are partially miscible. The organic-rich layer is recycled back to the first column and the water-rich layer is sent to the second distillation column. The recovery column is used to separate all the benzene and recycle it back to the first column.

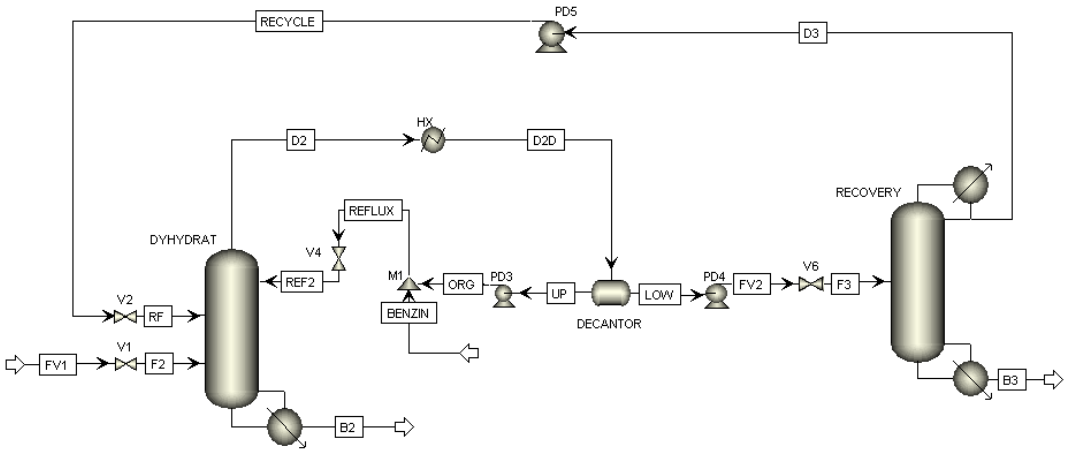

Figure 4.8. Flow diagram of azeotropic separation processes

The base case simulation is carried out using the following stream and block specifications. The product from the previous process (ethanol concentrator) that contains 93wt% ethanol is fed to the dehydration unit at 80°C and 2.2 atm. The recycle stream containing mainly benzene is also fed to the column at 67°C and 2.2 atm. The overhead product is passed through a heat exchanger where the temperature is lowered to 30°C. Upon condensing, the mixture separates in the decanter into an organic-rich layer and a water-rich layer. A small amount of make up benzene (0.9 kmol/hr) is added to the organic-rich stream from the decanter before it is fed to the dehydration column as reflux. The water-rich layer is then pumped to the recovery distillation column, in which benzene and ethanol are separated and recycled back to the first distillation column. The stripped water emerges from the base of the recovery tower.

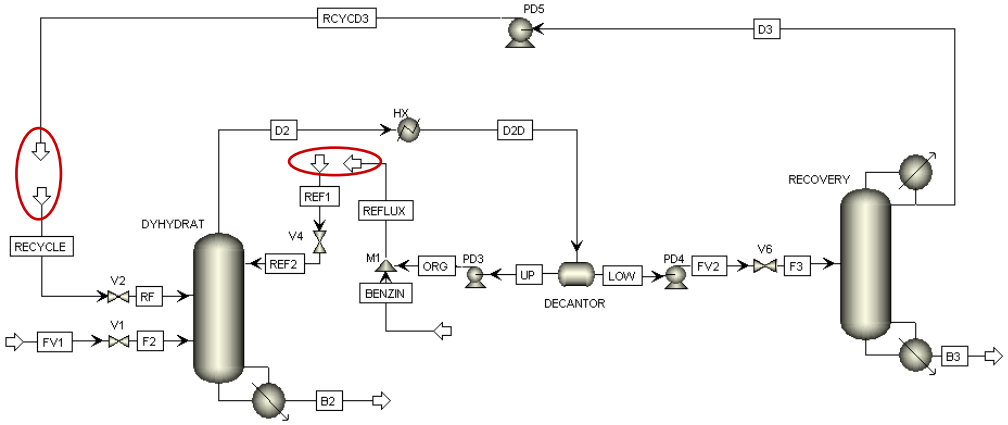

Figure 4.9. Flow diagram of azeotropic separation processes

As it is shown in Figure 4.9, the simulation was first performed by opening the recycle and reflux streams. To get pure ethanol in the dehydration tower, the bottoms flow rate was specified at 161 kmol/hr which is all the ethanol in the feed (192 kmol/hr). Likewise, the recovery unit bottoms flow rate was specified at 30 kmol/hr.

In order to close the loop, the flow rate and composition of the recycle and reflux inputs have be determined. The convergence process was performed by guessing the input flow rates (reflux and recycle) and comparing them with the corresponding simulation result (Luyben, 2006). After several iterations, Reflux and recycle flow rate and composition values that gave very close flow rate and composition with the simulation result were used in the final simulation.

4.8 Molecular Sieve Model

A separation process using molecular sieves was carried out by integrating a "user model" into the simulation. The "user model" was designed using FORTRAN and Visual Basic subroutines. Initially, all the process variables (flow rate, pressure temperature and composition of inlet streams) are transferred to an Excel spreadsheet. These variables are then used to determine the parameters that describe the molecular sieve. Finally, the results are transferred to Aspen Plus™ and are displayed in the "user model" result.

Figure 4.10 shows the schematic representation of a continuous dehydration process using two molecular sieve columns. A 93 wt% of ethanol and water mixture is heated to a temperature of 363 K and fed to the user defined unit which represents the molecular sieve columns. The molecular sieve columns were designed by following the design procedures that are given in the "Gas Processors Suppliers Association" Hand Book. The "user model" calculates the bed diameter and height, mass and cost of the

desiccant, vessel thickness and regeneration gas flow rate. The design steps are as follows.

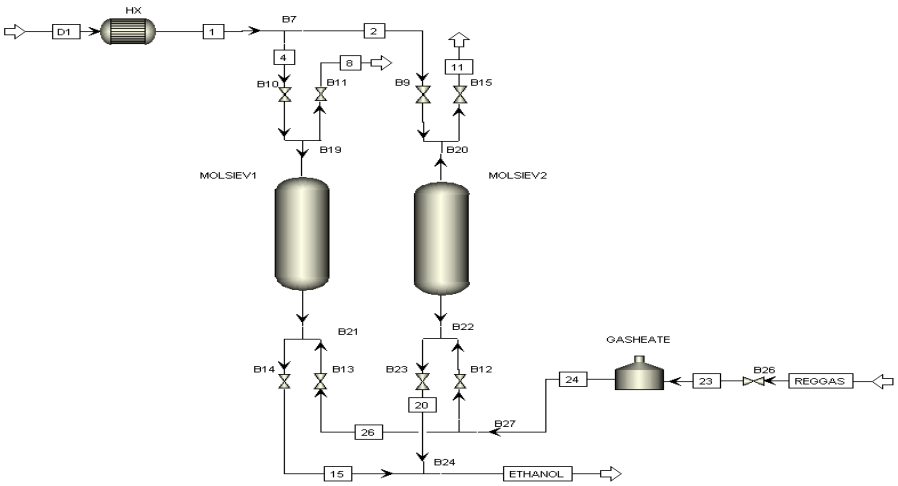

Figure 4.10. Flow diagram of continuous separation process using molecular sieves

Step one: Determining the bed diameter

The bed diameter depends on the superficial velocity of the fluid. The pressure drop along the bed is determined by a modified Ergun equation. This equation relates pressure drop to superficial velocity as follows.

$$\frac{\Delta P}{L} = B\mu V + C\rho V^2 \qquad (4.1)$$

Where ΔP : Pressure drop (psia)

V : Superficial velocity (ft/min)

μ : Viscosity (cp)

ρ : Density (lb/ft^3)

B and C: Constants supplied by the manufacturer

From the simulation result, the viscosity and density of the feed mixture (93 wt% ethanol and 7 wt% water) are 0.01405 cp and 0.10114 lb/ft^3 respectively. This desiccant material is assumed to be 1/8" bead (4x8 mesh). This desiccant material is used by major ethanol producers (GPSA, 1998). The B and C constants for this type of molecular sieve are as follows (GPSA, 1998).

Table 4.1. Physical parameters of 1/8" bead (4X8 mesh) desiccant (GPSA, 1998).

Particle type	B	C
1/8" bead (4x8 mesh)	0.056	0.0000889

The maximum allowable ΔP/L is 0.33 psia/ft and the total pressure drop through the bed should be 5-8 psia (GPSA, 1998). Plugging these values into Equation 4.1 the superficial velocity is calculated to be 95.62 ft/min. Once the superficial velocity is determined the bed minimum diameter can be calculated by using the following two equations (GPSA, 1998).

$$D_{\min} = \left(\frac{4q}{\Pi V_{\max}} \right)^{0.5} \qquad (4.2)$$

$$q = \frac{\dot{m}}{60\rho} \qquad (4.3)$$

Where D_{min} : Bed minimum diameter

q : Volumetric flow rate (ft^3/min)

V_{max} : Maximum superficial velocity (ft/min)

$\dot{m}$: Mass flow rate (lb/hr)

Step two: Determining the mass of desiccant needed

The second step is to choose the adsorption period and calculate the mass of desiccant required. Typically 8-12 hrs adsorption periods are used. Molecular sieves have the capacity to hold approximately 13 pounds of water per 100 pounds of sieve (GPSA, 1998). The mass of desiccant required in this process is calculated by dividing the amount of water to be removed during the cycle by the effective capacity.

$$Ss = \frac{W_r}{0.13\, C_{ss}\, C_T} \qquad (4.4)$$

Where Ss : Mass of desiccant (lbs)

W_r : Amount of water to be removed (lbs)

C_{SS} : Mol. Sieve capacity correction for % relative saturation

C_T : Mol. Sieve capacity correction for temperature

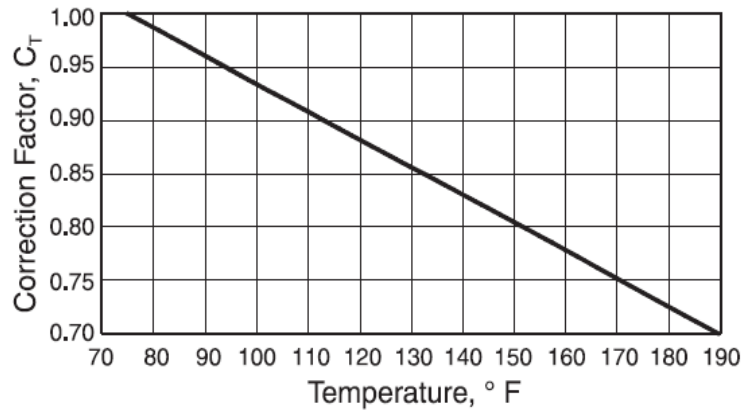

Figure 4.11. Molecular sieve capacity correction (C_T) for temperature (GPSA, 1998)

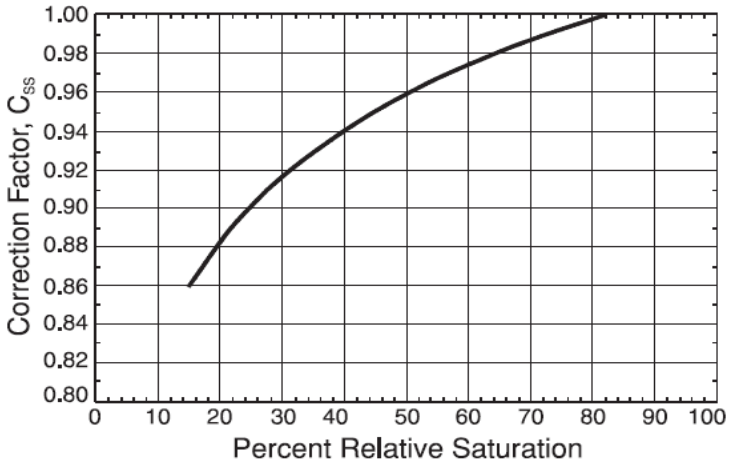

Figure 4.12. Molecular sieve capacity correction (C_{ss}) for % relative saturation (GPSA, 1998)

Using regression analysis the data in figures 4.11 and 4.12 were fitted using linear (Equation 4-5) and exponential models (Equation 4-6) respectively. C_T values of 0.7 and 1 were used for temperatures below 70 ^oF and above 190 ^oF respectively.

$$C_T = -0.0026T + 1.1974 \qquad (4.5)$$

$$C_{SS} = 0.084\ln(RS) + 0.6306 \qquad (4.6)$$

Where *T* : Temperature (^oF)

RS : Percent relative saturation

The effective desiccant capacity depends on the temperature and percentage relative saturation of the feed to the molecular sieve. Figure 4.11 and Figure 4.12 show the capacity correction factors as functions of temperature and relative saturation.

Step three: Determining the bed height

A molecular sieve column has a saturation zone and the mass transfer zone (Figure 4.13). The length of the saturation zone (L_s) can be calculated using the formula below.

$$Ls = \frac{S_s * 4}{\Pi * D^2 * bulkdensit\,y} \qquad (4.7)$$

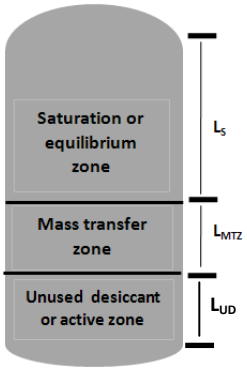

Figure 4-13. Different zones in a molecular sieve column

Where Ls : Length of the saturation zone

Molecular sieves have a bulk density of 42 to 46 lb/ft^3 for spherical particles and 40 to 44 lb/ft^3 for extruded cylinders (GPSA, 1998). The length of the mass transfer zone (L_{MTZ}) can be estimated using equation 4-8. The total bed height is the summation of the saturation zone and the mass transfer zone heights.

$$L_{MTZ} = (V / 35)^{0.3} Z \qquad (4.8)$$

Where Z : 1.7 ft for 1/8inch sieve

L_{MTZ} : Length of the mass transfer zone

Step four: Vessel thickness and total heat required

The thickness (t) and the weight of the vessel (Wst) are determined by using equation 4-9and 4-10. Equation (4-10) is based on the maximum allowable tensile stress of 18,800 psia.

$$W_{St}(lb) = 155(t + 0.125)(L_s + L_{MTZ} + 0.75D_{bed} + 3)D_{bed} \qquad (4.9)$$

$$t(in) = \frac{(12 D_{bed} P_{design})}{(2 * 18{,}800 - 1.2 P_{design})} \quad (4.10)$$

Where P_{design} : Vessel design pressure (110% of the operating pressure)

W_{st} : Weight of the vessel (lb)

t : Thickness (in)

Equations 4-11 to 4-13 are used to calculate the total heat required to desorb the water (Q_w) and heat the desiccant (Q_{si}) and vessel (Q_{st}). A 10% heat loss (Q_{hl}) to the environment is assumed.

$$Q_W = (1800 \frac{Btu}{lb}) * (lbs \cdot of \cdot water \cdot in \cdot bed) \quad (4.11)$$

$$Q_{Si} = (lbs \cdot of \cdot sieve)(\frac{0.24 Btu}{lb^o F}) * (T_{rg} - T_i) \quad (4.12)$$

$$Q_{St} = (lb \cdot of \cdot steel)(\frac{0.12 Btu}{lb^o F}) * (T_{rg} - T_i) \quad (4.13)$$

$$Q_{hl} = (Q_W + Q_{si} + Q_{st}) * 0.1 \quad (4.14)$$

Where Q_w : Total heat required to desorb the water (Btu)

Q_{si} : Total heat required to heat the desiccant (Btu)

Q_{st} : Total heat required to heat the vessel (Btu)

Q_{hl} : Total heat required to heat the desiccant (Btu)

T_{rg} : Regeneration temperature (^oF)

T_i : Adsorption temperature (^oF)

The total heat which is required from the regeneration gas is calculated from equation 4-15.

$$Q_{tr} = 2.5(Q_W + Q_{si} + Q_{st} + Q_{hl}) \quad (4.15)$$

Where Q_{tr} : Total regeneration load (Btu)

Step five: Flow rate of the regeneration gas

The regeneration gas flow rate (m_{rg}) is calculated from equation 4-16 where C_p is the average heat capacity of the gas.

$$m_{rg} = Q_{tr} /(Cp(T_{hot} - T_b)(heating.time) \qquad (4.16)$$

4.9 Equipment Pressure Drop

Pressure drop must be considered for all the equipment when developing process models. Acceptable pressure drop values were taken from Seider, *et. al.* reference.

The pressure drop of a process which involves liquids depends on the viscosity of the fluid. For liquids with low-viscosity, the typical pressure drop is 5 psia. In the case of liquids with high-viscosity, the typical pressure drop is 8 psia. If only gases are involved in the process, the typical pressure drop is 3 psia (Seider, 2009). The pressure drop across the molecular sieve is calculated by using Equation (4.1). The following table summarizes the pressure drops that were used for each unit operation.

Table 4.2. Pressure drop of different unit operations

Unit	Operating Pressure (psia)	ΔP(psia)
Gasifier	32.33	
Cooler	29.33	3
Bio Reactor	24.33	5
Flash Drum	19.33	5
Condenser		3
Tray		0.1
Molecular Sieve		6.4

Chapter 5

Results and Discussion

5.1 Gasification process

In this section, the base case simulation and sensitivity analysis results of the gasification process are discussed in detail. The results from the Gibbs reactor model are presented in different tables and charts below.

5.1.1 Base Case Simulation Results

The base case simulation was carried out using the same air to biomass ratio as the experimental run. Flow rates and compositions of the feed streams to the gasifier are shown in Table 5.1. Air was assumed to be composed of only oxygen and nitrogen while the other gases are ignored. Switch grass which is composed of C, H, N, O, S, ash and water is considered as an input in the gasifier. The final simulation results of the gasification process are presented in Table 5.2. The yields obtained for the Gibbs rector are compared with the results obtained from the experimental runs in Figure 5.1. A complete stream report is shown in Appendix A-1.

Table 5.1 Experimental input composition of feed streams to the gasifier (Rao, 2004)

	Element / Gas	Flow Rate kg/hr	Flow Rate kmol/hr
Air	N_2	23.11	0.83
	O_2	7.02	0.22
	Total	30.13	
Switchgrass	C	7.18	0.60
	H	0.91	0.91
	N	0.14	0.01
	O	7.77	0.49
	S	0	0
	Ash	0.55	
	H_2O	1.64	0.09
	Total	18.19	0.83

The simulation result shows that there was 10.55 kg/hr of carbon monoxide in the syngas stream. The simulation over-predicted the amount of carbon monoxide in comparison to the experimental result. This is because a Gibbs reactor model predicts the maximum CO amount that can be produced in a gasification process. The higher CO production indicates that there is a possibility to increase the experimental CO production from the process.

The amount of carbon dioxide from the simulation was 9.73 kg/hr. The experimental carbon dioxide result shows there was 10.48 kg/hr in the syngas stream. The simulation prediction of carbon dioxide is fairly close to the experimental result.

The simulation result shows all the oxygen from air and switchgrass was consumed in the gasification process. The experimental result also shows almost all of the oxygen was converted to products.

Table 5.2 Experimental and simulation results comparison

	Mass Flow Rate (Kg/hr)		Mole Flow Rate (Kmol/hr)	
Exhaust gas	**Simulation**	**Experimental**	**Simulation**	**Experimental**
H_2	0.695	0.16	0.348	0.080
N_2	23.25	23.11	0.830	0.825
O_2	1.92E-17	0	6.00E-19	0
CO	10.55	6.43	0.377	0.230
CO_2	9.728	10.48	0.221	0.238
CH_4	1.40E-03	0.96	8.75E-05	0.060
C_2H_2	1.19E-10	0.06	4.58E-12	2.31E-03
C_2H_4	1.94E-09	0.62	6.93E-11	0.022
C_2H_6	2.46E-10	0.05	8.20E-12	1.67E-03
H_2O	3.544	3.06	0.197	0.170
NO	1.47E-13	-	4.91E-15	-
NO_2	5.28E-24	-	1.15E-25	-
N_2O	6.98E-18	-	1.59E-19	-
NH_3	3.25E-05	-	1.91E-06	-

The predicted flow rate of nitrogen in the syngas was 23.25 kg/hr. Although nitrogen is inert, the simulation result predicts a small increase in the N_2 gas flow rate. The experimental result shows no increase in the amount of nitrogen. This is due to the fact that the amount of nitrogen in the output was not measured instead it was calculated by subtracting the input from the output total flow rate.

The simulation result indicates that the hydrogen flow rate in the exhaust gas was 0.695 kg/hr. However, the experimental result shows a much smaller production of hydrogen. The presence of higher amount of hydrocarbons is the reason for a lesser production of hydrogen gas. The simulation result shows that a higher production of hydrogen can be achieved in the gasification process.

Other products in the gasification process are hydrocarbons like methane, ethane, acetylene and ethylene. The simulation result shows there is 1.4E-03 kg/hr of methane and trace amount of other hydrocarbons in the syngas stream. The experimental results show a high amount of hydrocarbons which is a result of incomplete combustion in the fluidized bed gasifier. The presence of hydrocarbons in the exhaust gas also results in lower hydrogen gas production.

The predicted amount of water in the exhaust gas is 3.54 kg/hr. This result is higher than the experimental result which is 3.06 kg/hr. The higher production of hydrocarbons is the reason for a smaller amount of water in the experimental result. Figure 5.1 shows a graphical comparison of the experimental and Aspen simulation syngas composition result.

Rao (2004) did similar study of this biomass gasification process also using a Gibbs reactor. The gasifier product compositions from Rao's paper were nearly identical to the above simulation results.

5.1.2 Energy Requirement

The gasifier was operated at a temperature of 1,088 K and a pressure of 29.4 psia. The simulation result shows the heat duty of the gasifier was -199,037 kJ/sec. This shows the gasification process is an exothermic operation.

(a)

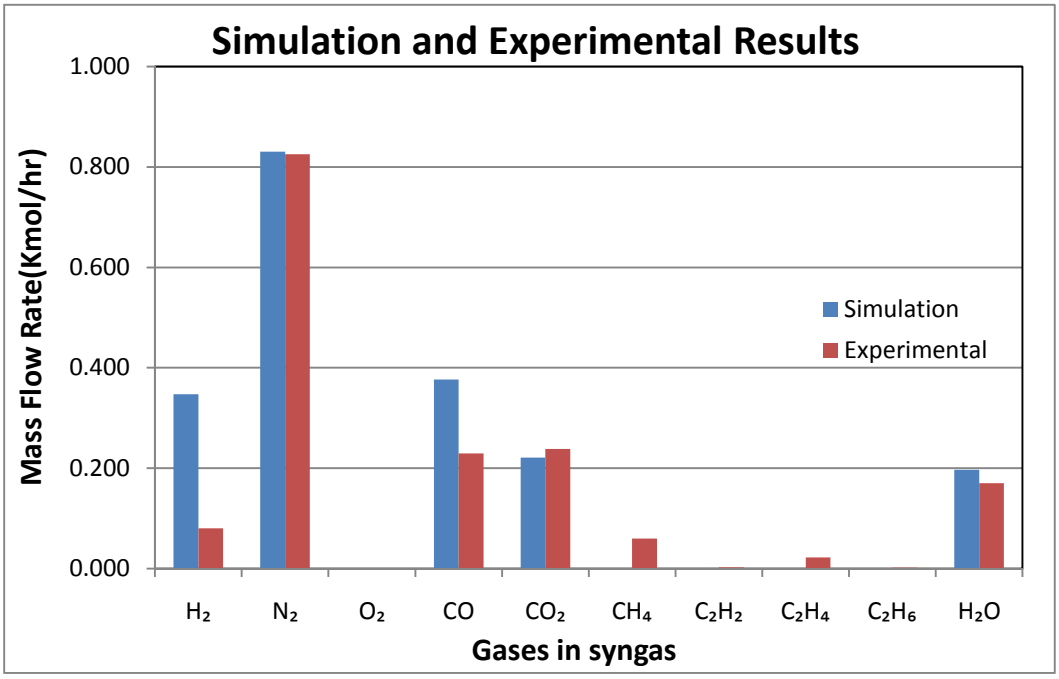

(b)

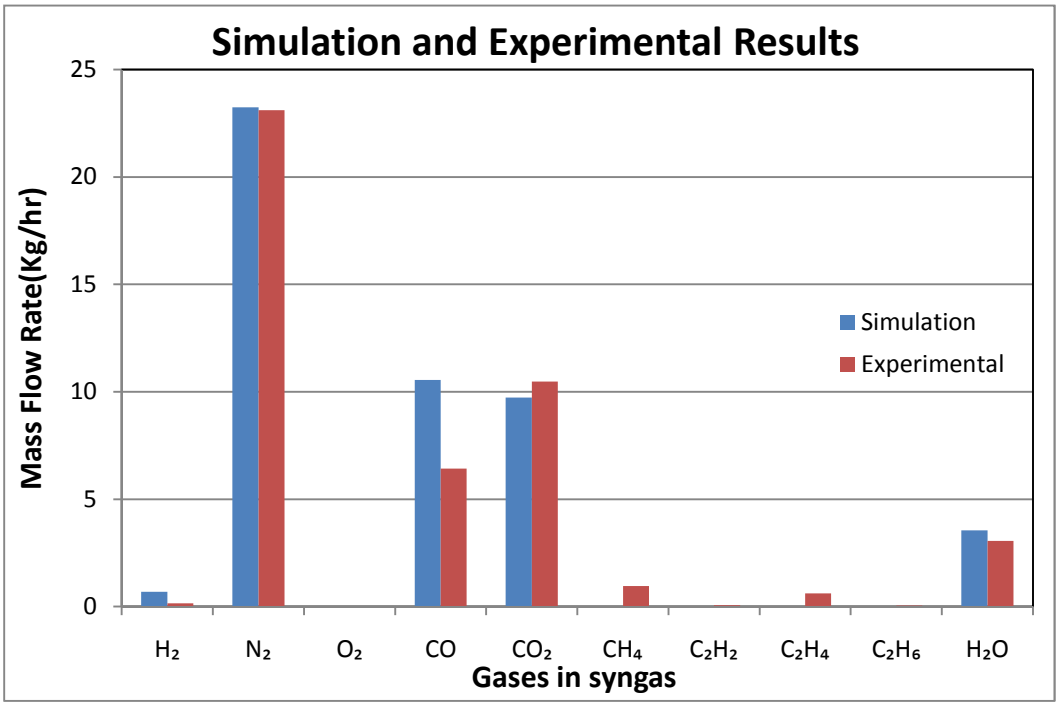

Figure 5.1 (a) Mole and (b) mass flow rate comparisons of the experimental and simulation syngas results

5.1.2 Temperature Sensitivity Analysis

A temperature sensitivity analysis was carried out to investigate the effect of operating temperature on the exhaust gas composition. The gasification temperature was varied from 800 K to 1200K. The result from temperature sensitivity analysis is shown in Appendix B-1.

Figure 5.2 shows the effect of variation of the operating temperature on the mole flow rate of CO, H_2, CO_2, N_2, and CH_4. The result indicates the production of CO increased as the operating temperature was increased. From 800 K to 890K, there was an exponential increase in CO production but further increase in temperature results in only a small increase in the production of CO. The graph also shows that the production of CO_2 and CH_4 decreased as the temperature was increased. The production of H_2 increased initially up to 0.38 Kmol/hr at 950 K. But when the temperature further increased H_2 production decreased slightly. This is due to the increase in the production of water when the operating temperature is above the pyrolysis temperature of 873 K. Since nitrogen is an inert gas there is no change in the production rate regardless the operating temperature change.

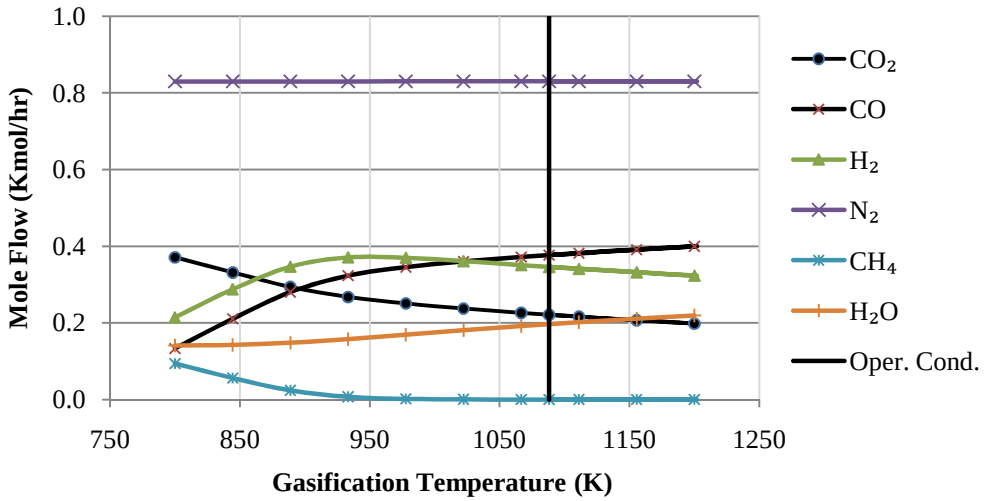

Figure 5.2 Effect of temperature on syngas composition

5.1.3 Feed Ratio Sensitivity Analysis

The air to biomass mass ratio in the feed stream is one of the key parameters in a gasification process. To better understand the effect of air to feed ratio on the composition of products, a sensitivity analysis was preformed. The air to biomass ratio was varied from 0.5 to 6.2. The results are shown in Appendix B-2.

Figure 5.3 shows the effect of air to biomass ratio on the mass flow rate of CO, H_2, H_2O, CO_2, N_2, and CH_4 in the syngas stream. The amount of oxygen in the air stream has a big influence on the syngas composition. When an excess amount of oxygen exists in the gasifier, complete oxidation (combustion) dominates other reactions. The sensitivity analysis result shows, the increase in the air to fuel ratio results a higher production of CO_2 and water. The production of CO, H_2, and CH_4 decreases as the air to fuel ratio increases.

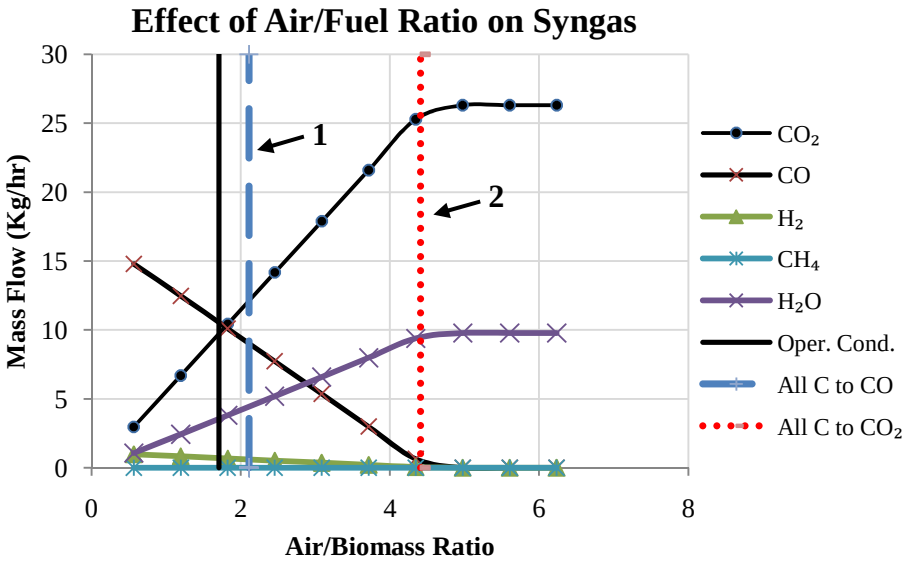

Figure 5.3 Effect of air to biomass ratio on syngas composition

Lines 1 and 2 indicate the air to biomass ratios for complete and partial combustions. The ratio for complete combustion of C to CO_2 and H to H_2O (line 2) was 4.41 and for complete conversion of all C to CO and H to H_2O (line 1) was 2.1. Since, the

experimental air to biomass ratio (1.71) is lower than the value at line 1, the calculated unburned carbon (ash and tar) in the syngas is about 20 wt%.

5.2 Fermentation Process

This section focuses on the base case simulation and sensitivity analysis results of the fermentation process. Simulation results are presented in different tables and charts below.

5.2.1 Base Case Simulation Results

The base case simulation was performed using the experimental input compositions. Table 5.2 shows the experimental and simulation input compositions of the syngas and media streams to the fermentation unit. The media was considered to be made up of only water. Syngas from gasifier enters the bioreactor at a temperature of 298 ^{O}C and pressure of 37 psia. The Table 5.3 summarizes the output composition of the bioreactor product. A complete stream report is included in Appendix A-2.

The maximum weight percentage of ethanol obtained from the experiment was 0.073 % of the total media weight (Rao, 2004), where the simulation predicted 3.69 wt % of ethanol in the product. The Gibbs reactor predicts the maximum possible amount of ethanol which can be produced at the operating conditions. This indicates it is theoretically possible to get a much higher conversion of biomass into ethanol.

The simulation result predicted higher exiting amount of CO_2. Production of CO_2 was 3.25E-08 kmol/s which is higher that the experimental result 2.16E-08 kmol/s. The amount of H_2 and CO from the simulation result is less than the experimental result. This is due to the conversion of H_2 and CO into ethanol.

Table 5.2 Experimental input composition of feed streams to the gasifier (Rao, 2004)

Bioreactor Input		Experimental Results	
		Flow Rate(kmol/sec)	% Mole Fraction
Gases	CO	2.16E-08	15.55
	CO_2	2.02E-08	16.53
	H_2	6.81E-08	4.89
	N_2	8.22E-08	63.03
Media	H_2O	3.31E-07	

Table 5.3 Experimental and simulation results comparison

Bioreactor Products		Flow Rate (kmol/sec)		% Mole Fraction	
		Simulation	Experimental	Simulation	Experimental
Gases	CO	3.28E-14	2.03E-08	0.00	15.58
	CO_2	3.25E-08	2.16E-08	28.23	16.56
	H_2	4.24E-10	6.40E-09	0.37	4.90
	N_2	8.22E-08	8.22E-08	71.40	62.95
Media	H_2O	3.23E-07	3.31E-07		
Ethanol	C_2H_5OH	4.67E-09	9.45E-11	3.69 wt. %	0.073 wt. %(max)

The amount of N_2 was basically the same as the feed in both the experiment and simulation results. The production of H_2O in the simulation was slightly smaller than the experimental result. The H_2O flow rate in the product stream was 3.23E-07 Kmol/s and 3.31E-07 Kmol/s in the simulation and experimental results respectively.

(a)

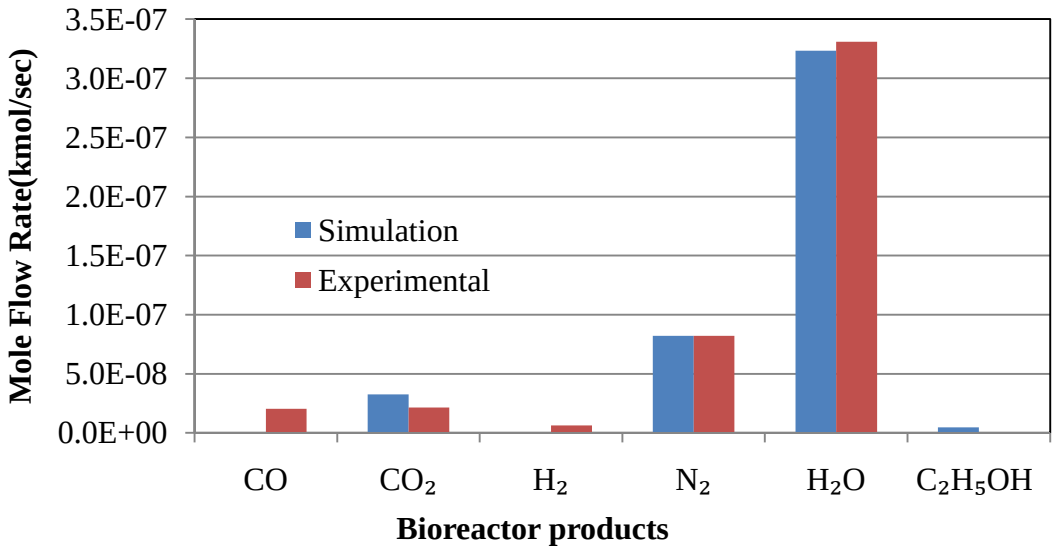

(b)

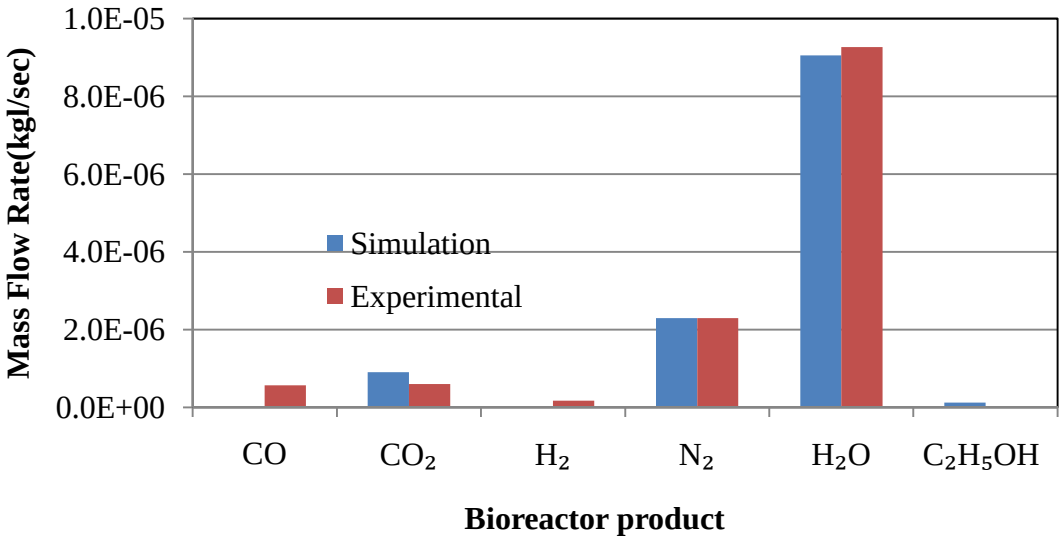

Figure 5.4 (a) Mole and (b) mass flow rate comparisons of experimental and simulation bioreactor product results

5.2.2 Media Flow Rate Sensitivity Analysis

A sensitivity analysis was carried out using a range of media flow rates to observe the change in the output flow rates of CO, H_2, CO_2, N_2, ethanol and water. Figure 5.5 shows the change in media flow rate against ethanol weight percentage for a fixed syngas flow rate. The flow rate of the media was varied from 1E-06 kg/sec to 1E-05 kg/sec. The syngas flow rate was kept constant at 3.81E-06 kg/sec. All the results from the media flow rate sensitivity analysis are shown in Appendix B-3.

The effect of variation of the media flow rate on the ethanol weight percentage is shown in Figure 5.5. The result shows an increase in the ethanol weight percentage as the media flow rate decreases. The increase in the percentage ethanol weight is mainly due to dilution. The weight ratio decreased gradually when the media flow rate was increased above 6E-06. There was an exponential increase in the % ethanol weight when the media flow rate decreased below 6E-06.

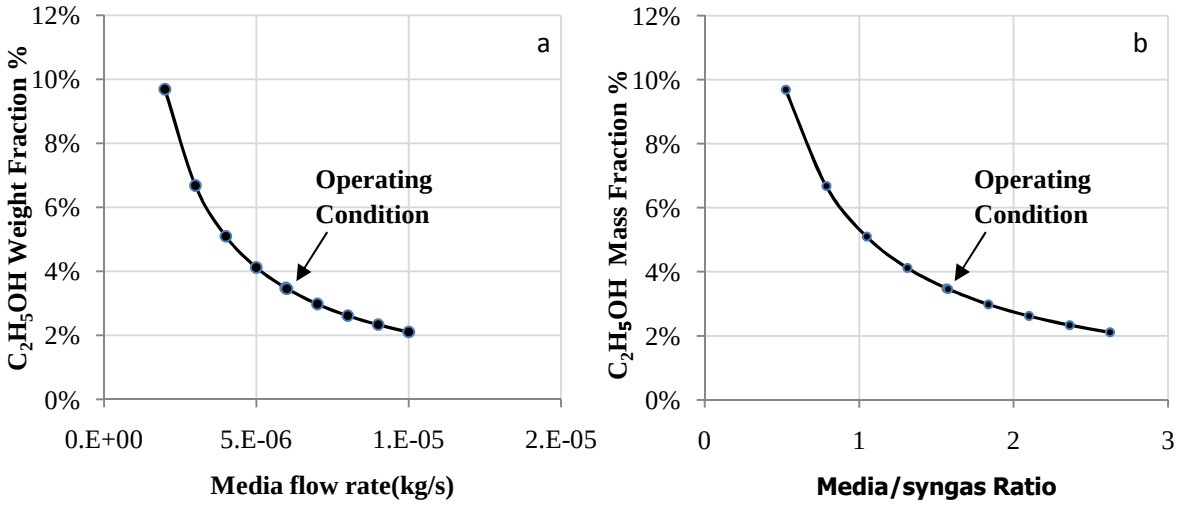

Figure 5.5 Media flow rate (a) and media to syngas ratio (b) versus ethanol weight percentage

5.3 Flash Drum Results

A flash drum simulation was used to separate the unreacted gases from the bioreactor. The base case simulation operating conditions were selected by performing a sensitivity analysis on the flash drum.

5.3.1 Base Case Simulation Results

A flash drum was designed to remove 90% of the CO_2 and more than 99% of the H_2 and N_2. The operating temperature and pressure were selected to be at 298K and 19.33 psia respectively. Table 5.4 shows the simulation results of the flash separation process. The result indicates that, at this operating condition, there is about 7.99 kmol/hr (4.4%) loss of ethanol. About 40.8 Kmol/hr of H_2O also leaves the flash drum with the product gas. The rest of the unreacted gases are separated in the distillation processes.

Table 5.4Flash separation simulation result

	Input (Kmol/hr)	Product (Kmol/hr)	
		Vapor	Liquid
H_2	4.03	4.03	0.00
N_2	1246.80	1237.67	9.13
H_2O	9091.97	40.80	9051.17
CO	0.00	0.00	0.00
CO_2	537.54	482.88	54.66
C_2H_5OH	180.25	7.99	172.26

5.3.2 Temperature and Pressure Sensitivity Analysis on the Flash Drum

A sensitivity analysis on the flash drum was performed to find out the best operating condition for the separation of unreacted gases from the Ethanol-Water mixture. Flash drum operating conditions were varied from a temperature of 290 K to 345 K and from a pressure of 14.7 psia to 44 psia.

Figure 5.9 shows the effect of temperature and pressure on ethanol loss in the flash drum. The plot indicates that when the temperature was increased the percentage ethanol loss also increased. At the same temperature when the pressure was decreased the percentage ethanol loss increased. The reason for this is that the volatility of a compound increases when the temperature is increased and pressure is decreased. The operating condition was selected to be at 298 K and 19.33 psia. The loss of ethanol is 4.4% when the flash drum is operated at this condition.

Figures 5.7 and 5.8 show the effect of temperature and pressure on removal of hydrogen and nitrogen gases from the liquid bioreactor product. Increasing the operating temperature results in a high percentage removal of H_2 and N_2. The same is true when the operating pressure is decreased. More than 99% of the H_2 and N_2 in the mixture can be removed when the flash drum is operated at a temperature of 298 K and a pressure of 19.33 psia

Figure 5.6 shows the effect of flash drum temperature and pressure on the percentage CO_2 removal. The graph reveals that when the operating pressure decreases the % CO_2 removal increases. Due to an increase in the volatility, the % CO_2 removal increases as the operating temperature increases. The flash drum was designed to remove

90% of the CO_2 by selecting the operating temperature and pressure at 298K and 19.33 psia respectively.

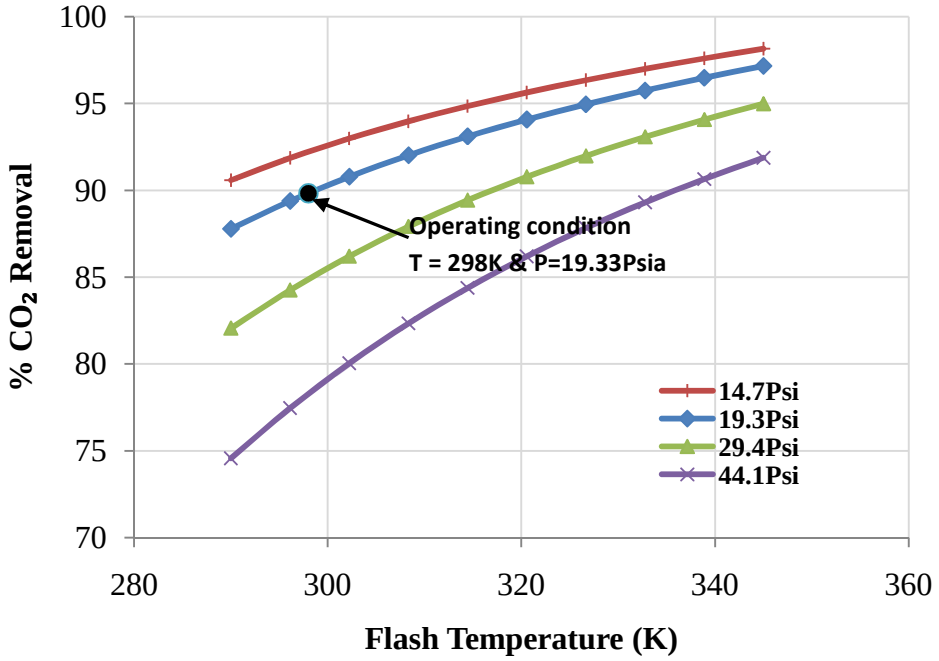

Figure 5.6 Effect of flash temperature and pressure on the percentage CO_2 removal

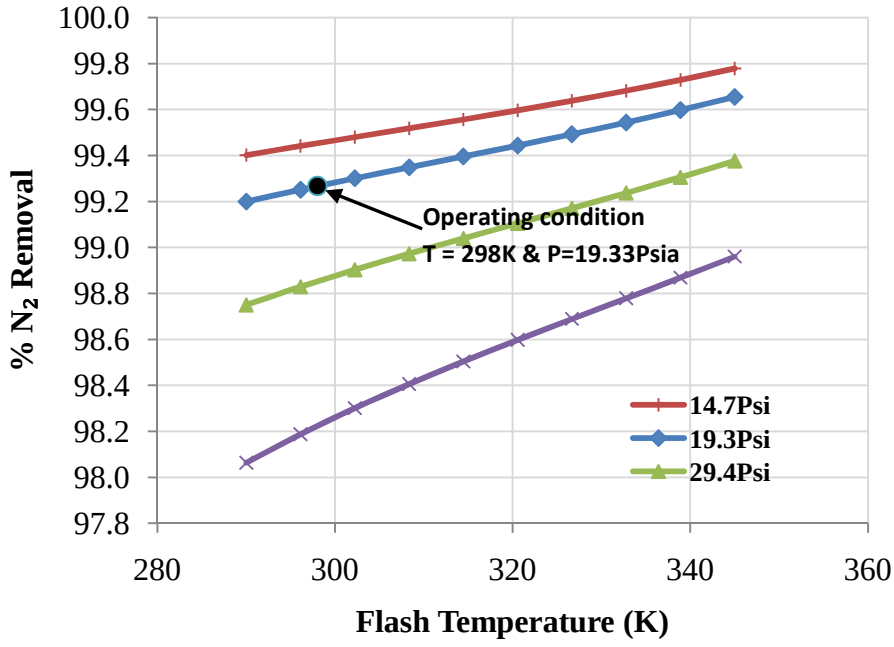

Figure 5.7 Effect of flash temperature and pressure on the percentage N_2 removal

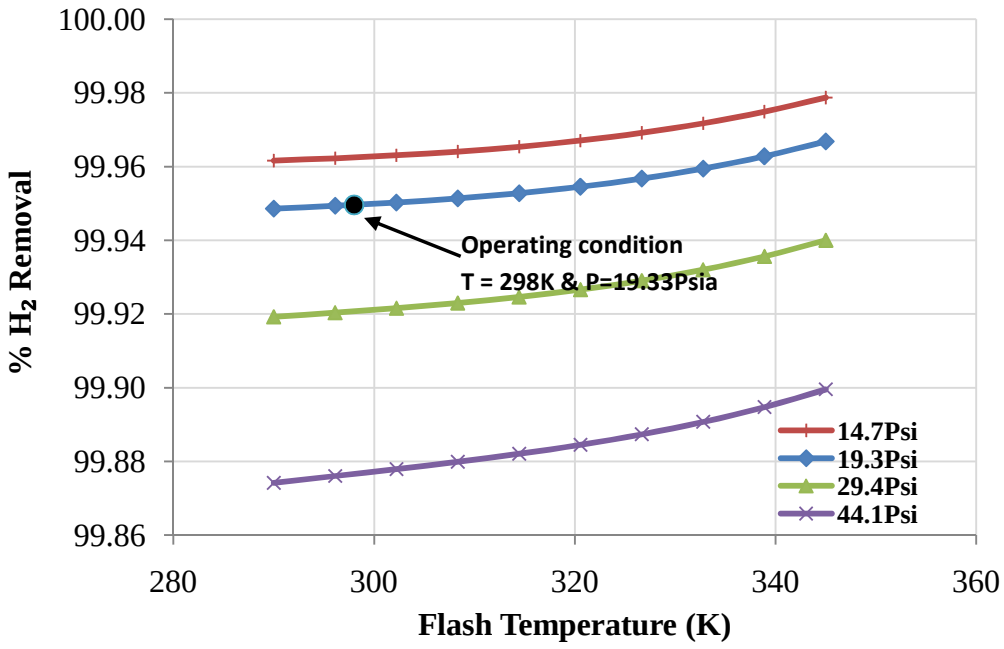

Figure 5.8 Effect of flash temperature and pressure on the percentage H_2 removal

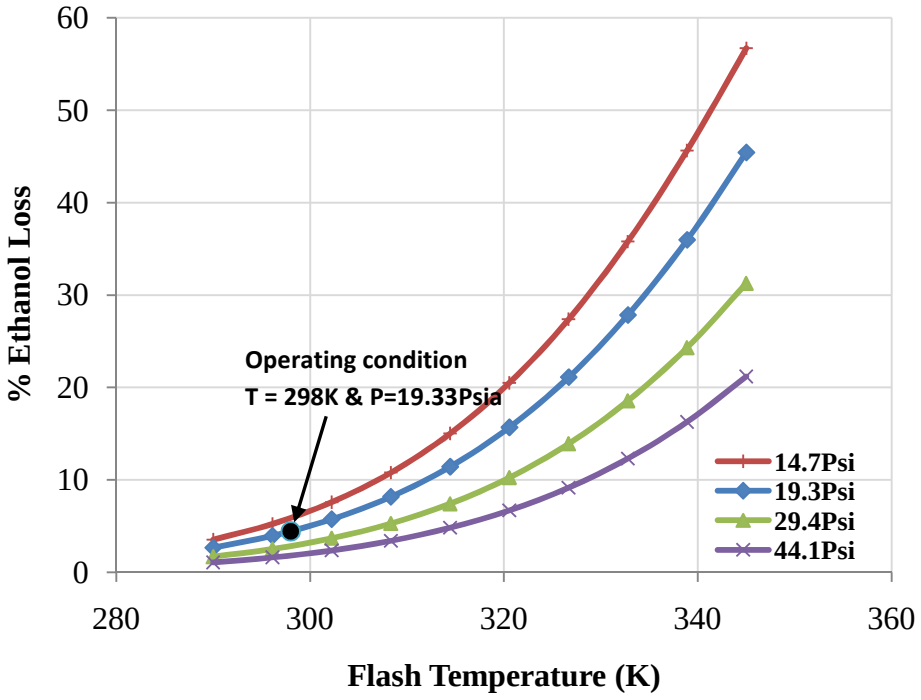

Figure 5.9 Effect of flash temperature and pressure on the percentage ethanol loss

5.4 Ethanol Concentrator Result

The number of distillation columns for ethanol separation was selected by performing energy and cost comparisons between one-column, two-column and three-column arrangements. The three different column arrangements are shown in Figure 4.7. The simulation results are presented in Appendix B - 4 to 11.

5.4.1 Effect of Number of Distillation Columns

The energy requirement and cost of a separation process highly depends on the number of distillation columns used. So, cost and energy consumption sensitivity analyses were carried out for different column arrangements. The cost analysis was performed using Aspen ICARUS simulation software.

Figure 5.10 shows reboiler and condenser heat duties for the one-column, two-column and three-column arrangements. As shown in the figure, the one-column arrangement consumes a higher amount of energy compared to other arrangements. The reboiler and condenser duty were about 1.8E+08 Btu/hr and 1.3E+08 Btu/hr respectively. But when two columns are used the energy consumption decreases significantly. The reboiler duty reduces to 9.6E+07 Btu/hr and the condenser duty comes down to 4.6E+07 Btu/hr respectively. When one more column is added (Three-column) the condenser duty and reboiler duty increases to 1.02E+08 Btu/hr and 5.2E+07 Btu/hr respectively.

Figure 5.11 shows the capital cost of the three different distillation column arrangements. The cost of two-column arrangement was $1.1E+6 which is lower than the other two arrangements. The two-column arrangement uses a lower energy with smaller cost, and hence it has been used in the process simulation.

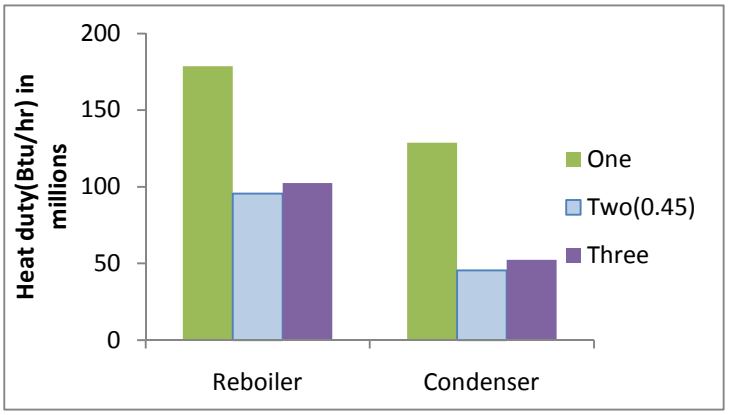

Figure 5.10 Energy consumptions of different distillation column arrangements

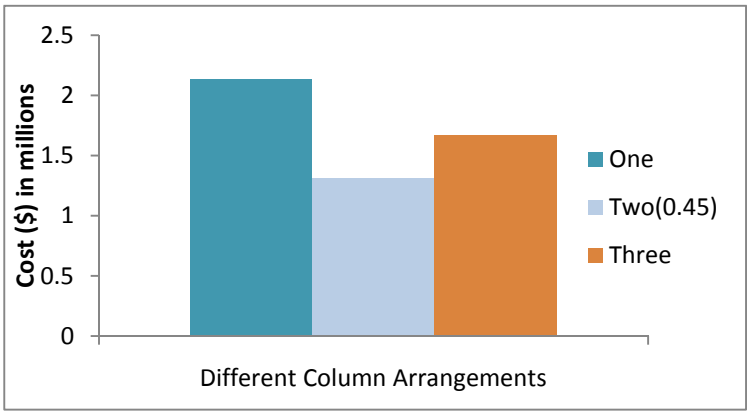

Figure 5.11 Total capital cost of different distillation column arrangements

5.4.2 Effect of First Column Product Purity on Energy Consumption and Cost

The two-column arrangement for the ethanol separation process requires less energy and capital cost as compared to one and two-column arrangements. The product purity of the first column has an effect on the energy consumption and capital cost of the process. To select the best operating product purity, several simulation runs were carried out with different product compositions.

Figure 5.12 shows the reboiler and condenser heat duty of four different product purities of the first distillation column. The figure indicates that, the energy requirement

increases as the product purity increases. Due to simulation convergence problem the purity was limited to the minimum value of 45 mole% Ethanol.

Figure 5.13 shows the capital cost of two-distillation arrangement with different product composition of the first column. The composition of the first column was varied from 45 mole% to 70 mole% ethanol. As shown in the figure, when the product purity is 45 mole% ethanol the capital cost becomes lower than others. Since 45 mole% ethanol has lower energy consumption and lesser capital cost, it is selected and used in the process simulation.

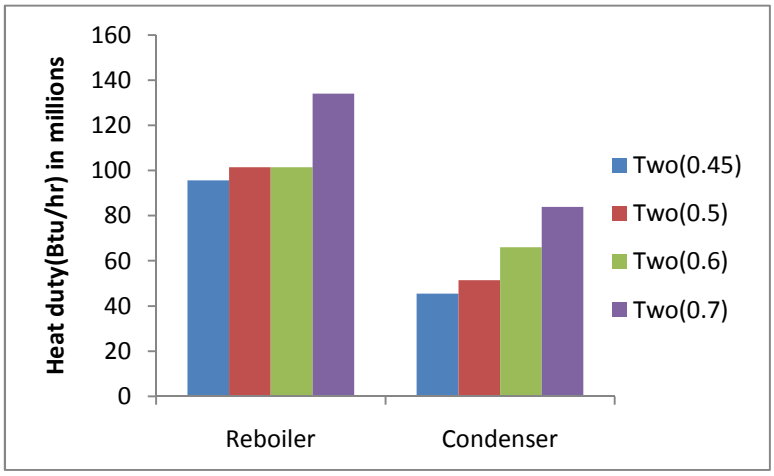

Figure 5.12 Effect of product purity on the reboiler and condenser heat duties

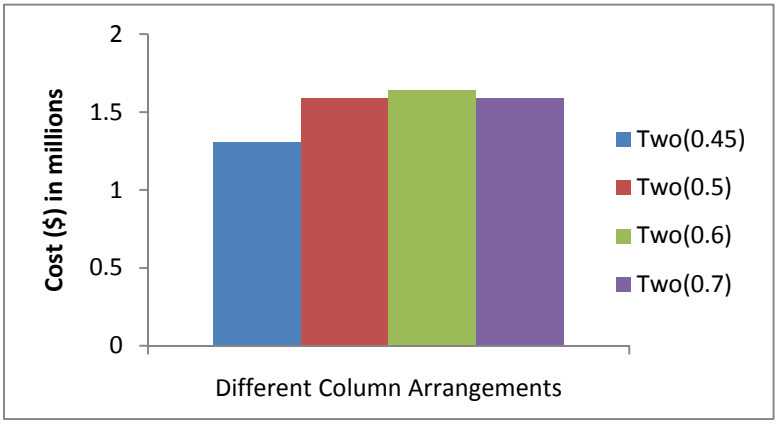

Figure 5.13 Total capital cost of different product purity of the first distillation column

5.4.3 Ethanol Concentrator Result at the Selected Conditions

Two distillation columns were used to separate the product of the bioreactor. Figure 4.7(b) shows the schematics representation of the separation process. The feed to the first distillation column was assumed to have a purity of 4.5wt% ethanol. Table 5.5 shows the input specification of the first distillation column. These values were estimated using the DSTWU (a shortcut distillation column model) which calculates the minimum number of stages, reflux ratio and feed stage of a distillation column. The design was performed by specifying the condenser and tray pressure drop of 3 psia and 1 psia. A 65% Murphree efficiency for the trays and 90% efficiency for the condenser and reboiler were assumed. The operating reflux ratio is two times the minimum reflux ratio.

Table 5.5 Input specifications of the first distillation column

Distillation Column I	
Number of stages	12
Reflux ratio	6
Distillate rate (kmol/hr)	360
Feed stage	7
Condenser pressure (psia)	16.2
Condenser pressure drop (psia)	3
Tray pressure drop (psia)	1
Tray efficiency	65%
Condenser and reboiler efficiency	90%

Tables 5.6 and 5.7 show the stream summary of the first distillation column. The result indicates there is 56 mole % ethanol in the distillate stream. The vapor stream contains about 85 mole % of CO_2 and 99 mole % of N_2 of the feed stream. The result also shows a 2.2 mole % loss of ethanol in the stream that leaves the distillation column in the vapor stream.

Table 5.6 Stream summary of the first distillation column

Compounds	Mole Flow (kmol/hr)			
	Feed	Bottoms	Distillate	Vapor
H_2	2.03E-03	7.84E-24	1.11E-06	2.03E-03
N_2	9.13	2.08E-14	0.08	9.05
H_2O	9051.17	8927.03	121.24	2.90
CO	3.80E-06	7.26E-21	3.73E-08	3.76E-06
CO_2	54.66	4.92E-09	8.13	46.53
C_2H_5OH	172.26	0.19	167.55	4.52

Table 5.7 Components mole fractions in feed and product streams

Compounds	Mole Fraction			
	Feed	Bottoms	Distillate	Vapor
H_2	2.19E-07	8.79E-28	3.73E-09	3.22E-05
N_2	9.84E-04	2.33E-18	2.78E-04	0.14
H_2O	0.97	1.00	0.41	0.05
CO	4.09E-10	8.14E-25	1.26E-10	5.98E-08
CO_2	5.89E-03	5.51E-13	0.03	0.74
C_2H_5OH	0.02	2.15E-05	0.56	0.07

The second distillation column was designed to increase the purity of mixture to 93 wt% ethanol. Table 5.8 shows block input values that are specified in the second distillation column. The same procedure as the first distillation column was followed to estimate the input specifications of the second column. Twenty four stages and a reflux ratio of 1.45 were used for the separation process. The feed enters the second distillation column at the 16^{th} stage.

Table 5.8 Input specifications of the second distillation column

Distillation Column II	
Number of stages	24
Reflux ratio	1.45
Distillate rate(kmol/hr)	205.5
Feed stage	16
Condenser pressure(psia)	16.2
Condenser pressure drop (psia)	3
Tray pressure drop (psia)	1
Tray efficiency	65%
Condenser and reboiler efficiency	90%

Table 5.9 and 5.10 show the summary of feed and product streams of the second distillation column. The distillate from this distillation column is an azeotropic mixture that has 93 wt% (84 mole%) ethanol. About 12 % of the unreacted CO_2 from the bioreactor leaves the distillation column in the vapor stream. The vapor stream also contains almost all of the unreacted nitrogen and hydrogen left in the mixture. The results show the ethanol loss in the second distillation column was about 3.5 mole %. All the simulation results are shown in Appendix A-4 and 5.

Table 5.9 Stream summary of the second distillation column

	Mole Flow (kmol/hr)			
Compounds	**Feed**	**Bottoms**	**Distillate**	**Vapor**
H_2	1.11E-06	3.33E-43	1.48E-09	1.10E-06
N_2	0.08	9.10E-29	1.24E-03	0.08
H_2O	121.24	90.04	30.72	0.49
CO	3.73E-08	2.60E-35	5.95E-10	3.67E-08
CO_2	8.13	3.90E-19	1.06	7.07
C_2H_5OH	167.55	1.46	161.40	4.69

Table 5.10 Components mole fractions in feed and product streams

	Mole Fraction			
Compounds	**Feed**	**Bottoms**	**Distillate**	**Vapor**
H_2	3.72E-09	7.67E-12	3.64E-45	8.95E-08
N_2	2.77E-04	6.42E-06	9.94E-31	6.58E-03
H_2O	0.41	0.16	0.98	3.96E-02
CO	1.25E-10	3.08E-12	2.84E-37	2.97E-09
CO_2	0.03	5.48E-03	4.26E-21	0.57
C_2H_5OH	0.56	0.84	0.02	0.38

5.4 Azeotropic Distillation Result

The product from the ethanol concentrator is further purified using an azeotropic separation process. The design of this process was performed using two distillation columns. Figure 5.14 shows a simplified flow-sheet of the azeotropic distillation process. Simulation results of the two distillation columns are presented in the following sections.

.

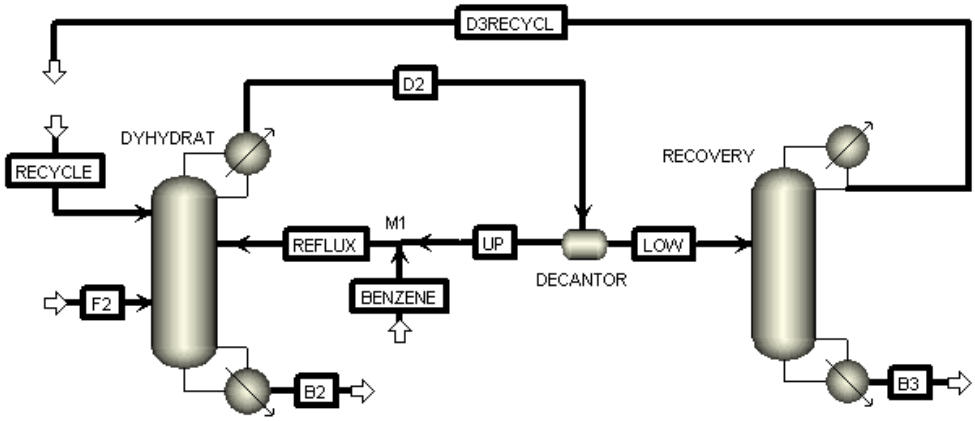

Figure 5.14 Simplified flow sheet of azeotropic distillation process

As it is shown in the figure 5.14, the recycle and reflux streams need to be closed to complete the process. However, the simulation encountered a convergence problem when the recycle and reflux streams were closed. Therefore, the recycle stream was left open while the reflux stream was closed. The convergence process was carried out by guessing the flow rate and composition of the recycle stream and comparing it with the simulation result (D3RECYLCE stream). Several guesses were taken until closer values for the recycle and D3RECYLCE streams were found (Luyben, 2006).

Table 5.11 shows the input specifications of the dehydrator column. There are 31 trays in the dehydration unit. The two feed streams enter the dehydration column at the

10^{th} and 15^{th} stages (numbered from the top). The bottoms rate (161.1 kmol/hr) was specified so as to obtain near 100% recovery of feed ethanol.

Table 5.11 Input specifications of the dehydrator distillation column

Dehydrator	
Number of stages	31
Bottoms rate(kmol/hr)	161.1
Feed stage	15
Recycle stage	10
Condenser pressure(psia)	29.4
Condenser pressure drop (psia)	3
Tray pressure drop (psia)	1
Tray efficiency	65%
Condenser and reboiler efficiency	90%

The dehydration simulation results are presented in Table 5.12. The result indicates the mixture in the B2 (bottoms) is 99.3 wt% of ethanol. The amount of benzene needed from the recycle stream was 2,456 kg/hr. The reflux stream which came from the decanter was mostly hydrocarbons (ethanol and benzene). This shows the organic-phase in the decanter has been separated and recycled back in the dehydration process.

Table 5.12 Stream summary of the dehydrator distillation column

Mass Flow kmol/hr					
	F2	**Recycle**	**Reflux**	**D2**	**B2**
H_2O	30.57	35.01	4.14	69.48	0.23
C_2H_5OH	161.70	120.74	44.38	166.51	160.31
C_6H_6	0.00	31.45	218.64	249.53	0.56
Mass Fraction					
H_2O	0.07	0.07	0.00	0.04	0.00
C_2H_5OH	0.93	0.64	0.11	0.27	0.99
C_6H_6	0.00	0.28	0.89	0.69	0.01

Table 5.13 Input specifications of the benzene recovery column

Benzene Recovery Column	
Number of stages	21
Bottoms rate(kmol/hr)	29.5
Reflux rate(kmol/hr)	2
Feed stage	11
Condenser pressure(psia)	16.2
Condenser pressure drop (psia)	3
Tray pressure drop (psia)	1
Tray efficiency	65%
Condenser and reboiler efficiency	90%

Table 5.13 shows the input specification of the benzene recovery column. Based on initial estimate of the short cut distillation column, Twenty one trays with a bottoms rate of 29.5 kmol/hr were used to recover benzene. The feed enters the distillation column at the 11^{th} stage.

Table 5.14 shows the simulation results of the recovery column. The distillate stream shows most of the benzene and ethanol were separated and recovered. The bottoms (b3) of the distillation column contains 99 wt% water.

Table 5.14 Stream summary of the benzene recovery column

Mass Flow kg/hr			
	F3	**B3**	**D3**
H_2O	1177.21	530.67	646.54
C_2H_5OH	5626.40	0.28	5626.13
C_6H_6	2483.69	2.94	2480.76
Mass Fraction			
H_2O	0.13	0.99	0.07
C_2H_5OH	0.61	5.20E-04	0.64
C_6H_6	0.27	5.50E-03	0.28

Table 5.15 shows the amount of energy that is required for each unit operations in the azeotropic separation process.

Table 5.15 Heat duty of different process units

	Heat Duty (MMBtu/hr)	
	Reboiler	**Condenser**
Dehydration Column	21.80	-20.91
Recovery Column	17.97	0
Heat Exchanger	-18.27	
Decantor	-0.002	

5.6 Molecular Sieve Columns Result

Molecular sieve columns were used to purify the azeotropic ethanol-water mixture from the ethanol concentrator process. A user defined unit operation was created to model the separation process using molecular sieves. Stream summary and design parameters of the molecular sieve columns are discussed in the following sections.

5.6.1 Molecular Sieve Columns Design Parameters

The design parameters for the molecular sieve columns were calculated by following the design procedure which is discussed in Chapter four. Table 5.16 shows the calculated design parameters of the molecular sieve columns.

Six molecular sieve columns were used to perform the separation process. The desiccant material type used was 1/8'' bead (4x8 mesh) sieve. After selecting the desiccant type, the bed diameter was calculated using equation 4-1. The adjusted bed diameter of each molecular sieve column was 6.5 ft.

The amount of water to be removed in each molecular sieve columns was 138 kg/hr. To remove the water in the feed, the mass of desiccant needed was about 220,228

lbs. The adsorption period, typically between eight to twelve hour (GPSA, 1998), was assumed to be ten hours and was used while calculating the mass of the desiccant.

Equations 4-5 and 4-6 were used to calculate the total height of the bed. The equilibrium and mass transfer zone heights were about 22.09 ft and 2.22 ft. As shown in Table 5.16 the total bed height was 24.31 ft. Once the diameter and height of the bed are determined, the pressure drop was checked to see whether it is in the acceptable range. It is found that the pressure drop was 0.26 psia/ft which is lower than the maximum allowable pressure drop of 0.33 psia/ft (GPSA, 1998). The vessel is assumed to be made of SA-516 Grade 70 steel. The mass of the vessel was calculated using Equation 4-7 and came out to be 5,800 lbs. The thickness of the vessel was about 0.25 in (Seader, 2009).

Table 5.16 Molecular sieve columns design parameters

Molecular Sieve Specifications	
Type of sieves	1/8'' bead (4x8 mesh) sieve
Number of vessels	6
Vessel height (ft)	24.31
Vessel diameter (ft)	6.5
ΔP/ft (psia/ft)	0.26
Total ΔP (psia)	6.39
Regeneration gas flow rate (ft^3/hr)	20,630
Thickness(in)	0.25
Weight of steel for one column(lb)	12,160
Desiccant weight(lb)	36,704
Total desiccant weight(lb)	220,228
Total price ($)	628,277

The adsorption process was carried out at a temperature of 193 ^oF and a pressure of 32 psia. Hot air at a temperature of 464 ^oF was used to regenerate the bed. The regeneration air flow rate was determined using equation 4-14. The calculated volume flow rate of the air was around 24,922 ft^3/hr. The total regeneration load (heat required to

regenerate the bed) was about 11 MMBtu/hr which is much lower than that of the azeotropic separation process.

Table 5.17 Molecular sieve columns operating conditions

Operating Conditions	
Regeneration temperature (^oF)	464
Vessel design pressure in psia	32
Vessel design temperature in ^oF	193.7
Adsorption cycle time(hr)	10
Regeneration cycle time(hr)	10

5.6.2 Molecular Sieve Columns Stream Summary

The simulation results for the dehydration process using molecular sieve columns are presented in Table 5.18. The feed stream consists of H_2O, C_2H_5OH, N_2, CO_2 and trace amounts of H_2O and CO. The molecular sieve columns were designed to produce 99.4 wt% of ethanol. The mass flow rate of the ethanol in the ethanol rich stream was 7447 kg/hr which is about 99 mole % of the ethanol in the feed stream. As it is shown in the simulation result, the amount of water removed in the molecular sieve columns was around 400 kg/hr.

Table 5.18 Stream summary of the dehydration process using molecular sieve columns

Mass Flow kg/hr			
	Feed	**Water**	**Ethanol Rich**
N_2	0.045	0.02	0.02
H_2O	413.1	400.7	12.4
CO_2	63.9	31.9	31.9
C_2H_5OH	7454.8	7.5	7447.4
Mass Frac			
N_2	5.64E-06	5.08E-05	2.98E-06
H_2O	0.05	0.91	0.002
CO_2	0.01	0.07	0.004
C_2H_5OH	0.94	0.02	0.994

5.7 Sizing and Cost Analysis

The sizing and cost analysis was performed using Aspen Plus and Aspen Icarus simulation software for azeotropic distillation and molecular sieves separation processes. In both of the processes, the production rate was about 175 liters/min of 99.5% ethanol. Assuming 300 working days of production, the annual production becomes 20,040,000 gallons/year. Sizing and costing analysis results are presented in Appendix D.

The chemical engineering plant cost index (CEPCI) values of Aspen Icarus 7.1 are for the 1st quarter of 2008. The CEPCI values for 1st quarter of 2008 are shown in Table 5.19.

Table 5.19 CEPCI cost index for 1st quarter of 2008 (Chemical engineering magazine, 2008)

CEPCI	**Feb.' 08**
CE INDEX	539.8
Equipment	645.8
Heat exchangers and Tanks	618.4
Process Machinery	610.3
Pipes, valves and fittings	768.2
Process Instruments	420.2
Pumps and Compressors	850.6
Electrical Equipments	445.3
Structural supports and misc	684.6
Construction labor	316.2
Buildings	483.0
Engineering and supervision	354.5

Since the gasifier and bioreactor units were modeled as a Gibbs reactor, they cannot be used for a scale up and cost estimation purposes (Rao, 2004). Therefore, these units were not included in the cost analysis.

5.7.2 Ethanol Production Using Molecular Sieves

Sizing and cost analysis of the dehydration process using molecular sieve columns was performed using Aspen Icarus and (Seader, 2009). Table 5.20 shows the total direct cost of this dehydration process.

Sizing of the molecular sieve columns and cost estimation of the desiccant was performed using a user defined unit operation. The price for 330lb of 4Å, 1/8" bead molecular sieve is $950 (eCompressedair, 2009). The total cost of the desiccant was around $628,277. The molecular sieve columns were designed as pressure vessels using equations given in (Seader, 2009). The following equations were used to determine the installed cost of a pressure vessel.

$$C_P = \frac{C_{EI(2008)}}{C_{EI(2006)}} * (F_M C_V + C_{PL}) \qquad (5\text{-}1)$$

Vertical vessels for 4,200 < Weight < 1,000,000 lb

$$C_V = \exp\{7.0132 + 0.18255[\ln(W)] + 0.02297[\ln(W)]^2\} \qquad (5\text{-}2)$$

Vertical vessels for 3 < Diameter (Di) < 21ft and 12 < Length (L) < 40ft

$$C_{PL} = 361.8 D_i^{0.73960} L^{0.70684} \qquad (5\text{-}3)$$

$$Installed\_\cos t = F_{BM} * CP \qquad (5\text{-}4)$$

Where F_M : Material factor (2 for stainless steel (Seader, 2009))

W : Weight of the vessel (lbs)

D_i : Internal diameter (ft)

L : Height of the vessel (ft)

C_P : Purchased cost ($)

C_{EI} : Cost index at a specific time (540 in 2008 and 500 in 2006)

F_{BM} : Bare-Module factor (4.16 for vertical vessels(Seader, 2009))

The weight, diameter and length of the vessel are around 12,160 lb, 24.31 ft, 6.5 in respectively. Using these values, the purchase cost of the vessels at CE value of 500 (in 2006) came out to be $108,206. The cost index for 2008 is 540. The final purchase cost became $116,862. The final installed cost including the desiccant material came out to be around $3,099,800. Table 5.20 shows the direct cost of ethanol production process using molecular sieve columns.

Table 5.20 Cost analysis for ethanol production using molecular sieves separation

Name	Type	Direct Cost $
DIST1-tower	DTW TRAYED	$579,600
DIST1-cond	DHE FIXED T S	$262,300
DIST1-cond acc	DHT HORIZ DRUM	$118,900
DIST1-reflux pump	DCP CENTRIF	$46,300
DIST1-reb	DRB U TUBE	$354,600
PD2	DCP CENTRIF	$53,400
COOLER1	EHE WASTE HEAT	$308,900
FLASH-flash vessel	DVT CYLINDER	$163,100
DIST2-tower	DTW TRAYED	$759,300
DIST2-cond	DHE FIXED T S	$114,200
DIST2-cond acc	DHT HORIZ DRUM	$169,200
DIST2-reflux pump	DCP CENTRIF	$40,200
DIST2-reb	DRB U TUBE	$120,500
HEATER	DHE FLOAT HEAD	$73,600
PD3	DCP CENTRIF	$24,400
PD4	DCP CENTRIF	$40,000
Molecular Sieves		$3,099,800
Total Direct Cost		$6,328,300

5.7.1 Ethanol Production Using Azeotropic Distillation

The sizing and cost analysis of the azeotropic distillation process was carried out without closing the recycle stream. The product ethanol from this process has a composition of 99.6 mole% ethanol. The summarized cost of equipment in the azeotropic distillation process is shown in the following table.

Table 5.21 Cost analysis for ethanol production with azeotropic separation

Name	Type	Direct Cost $
DIST1-tower	DTW TRAYED	$579,600
DIST1-cond	DHE FIXED T S	$262,300
DIST1-cond acc	DHT HORIZ DRUM	$118,900
DIST1-reflux pump	DCP CENTRIF	$46,300
DIST1-reb	DRB U TUBE	$354,600
PD2	DCP CENTRIF	$53,400
COOLER1	EHE WASTE HEAT	$308,900
FLASH-flash vessel	DVT CYLINDER	$163,100
DIST2-tower	DTW TRAYED	$759,300
DIST2-cond	DHE FIXED T S	$114,200
DIST2-cond acc	DHT HORIZ DRUM	$169,200
DIST2-reflux pump	DCP CENTRIF	$40,200
DIST2-reb	DRB U TUBE	$120,500
HEATER	DHE FLOAT HEAD	$73,600
PD3	DCP CENTRIF	$24,400
PD4	DCP CENTRIF	$40,000
DECANTOR	DVT CYLINDER	$103,100
DYHYDRAT-tower	DTW TRAYED	$424,700
DYHYDRAT-reb	DRB U TUBE	$110,200
HX	DHE FLOAT HEAD	$147,500
PD5	DCP CENTRIF	$31,400
PD6	DCP CENTRIF	$27,800
PD7	DCP CENTRIF	$21,200
PD8	DCP CENTRIF	$8,300
RECOVERY-tower	DTW TRAYED	$1,468,300
RECOVERY-cond	DHE FIXED T S	$108,200
RECOVERY-cond acc	DHT HORIZ DRUM	$191,500
RECOVERY-reflux pump	DCP CENTRIF	$45,200
RECOVERY-reb	DRB U TUBE	$120,500
	Total Direct Cost	$6,036,400

As it is shown from the above table, the total direct cost of a dehydration process using molecular sieve columns is slightly higher than the azeotropic process. The cost difference between the two processes was around $190,000.

Chapter 6

Conclusion and Recommendation

6.1 Conclusions

Full scale process models for ethanol production by biomass gasification were developed using Aspen Plus™ simulation software. Different Aspen Plus™ built-in unit operations were integrated to come up with two process models. The simulation was based on the experimental data obtained from an earlier research project conducted at Oklahoma State University (Rao, 2004). An economic comparison between two commonly used dehydration processes (azeotropic and molecular sieves separation) was carried out. In the following sections, conclusions for each process model are provided.

6.1.1 Gasification Process

- The gasification process was modeled using a Gibbs reactor model which predicts the maximum amount that can be produced in a process. The simulation results show higher production of carbon monoxide and hydrogen in the syngas stream. This indicates that there is a potential to increase the experimental hydrogen and carbon monoxide production.

- A temperature sensitivity analysis was carried out to investigate the effect on syngas composition. Higher temperature increases the production of hydrogen, water and carbon monoxide. The production of carbon dioxide and methane decreases as the gasification temperature increases. Therefore, the gasification process should be carried out at high operating temperatures to get higher production of hydrogen and carbon monoxide.
- An air to biomass ratio sensitivity analysis was carried out to identify the effect of the amount of oxygen (in the air stream) on the syngas composition. The increase in air to biomass ratio increases the amount of excess oxygen and hence results in higher carbon dioxide formation due to complete oxidation (combustion). Thus, lower air to biomass ratio must be used for higher production of hydrogen and carbon monoxide.

6.1.2 Fermentation Process

- A Gibbs reactor model was used to model the fermentation process. The results for the base case show that up to 3.69 wt. % of ethanol can be produced in the bioreactor. The higher production of ethanol in the simulation indicates that a higher experimental ethanol production can be achieved at the given operating conditions.
- The amount of water (media flow rate) in the fermentation process affects the production of ethanol. As the media flow rate increases, the percentage ethanol mass fraction increases exponentially. Since a higher ethanol mass fraction product can significantly reduce the energy requirement in the dehydration process, the fermentation process should be carried out at a low media flow rate.

6.1.3 Separation Process Using Flash Drum

- The separation of unreacted gasses using a flash drum is extremely sensitive to the operating conditions. When the flash drum is operated at high temperatures or low pressures, separation of unreacted gasses increases. However, the above operating condition will also result in a higher ethanol loss in the liquid stream. Therefore, the removal of unreacted gases and loss of ethanol must be balanced when selecting the operating conditions.
- A suitable operating condition for removal of unreacted gases is 290-300 K and 1.5 atm which results in less than 5 % ethanol loss.

6.1.4 Separation Process Using Distillation Columns

- The energy consumption of the separation process depends on the number of columns and the product compositions from each column. A separation process using a two-distillation column arrangement can significantly reduce the energy consumption and cost of the process. The optimum distillate concentrations from the first distillation column are between 45 wt% and 50 wt% of ethanol.

6.1.5 Dehydration Process Using Azeotropic Separation or Molecular Sieves

- Production of high purity ethanol using molecular sieves requires less energy than the azeotropic separation process. This can reduce the operating cost of the process significantly which results in a lower price of the final ethanol product.
- The amount of benzene used in the azeotropic process depends on the purity of the feed stream. Less benzene (about 12 mole % benzene) is needed when the feed is at higher ethanol purity (93 wt% ethanol).

6.2 Recommendations and Future Work

Both the gasification and fermentation processes were modeled using the Gibbs reactor model. The Gibbs model is usually used to determine how the process behaves when it is operated at different conditions. However, the Gibbs model predicts only the final product distributions. A kinetic model is required to investigate all the intermediate steps and the product compositions at various locations along the reactor. If the kinetic parameters can be found from literature, kinetic models for gasification and fermentation process can be developed using Aspen Plus™. These models would be helpful for detailed investigation of the two processes.

The current fermentation model does not consider the presence of butanol, acetic acid and other compounds in the product stream. Including these compounds will improve the model prediction.

The current model for a molecular sieve column is only a preliminary design. For a better understanding of the adsorption process, other simulation softwares are needed. One such simulation software that could be used to model molecular sieves is Aspen Adsim™. It is a comprehensive flowsheet simulator for the optimal design, simulation, optimization and analysis of adsorption processes (Aspen, 2003). Future works should focus on preparing a dynamic model for the dehydration process that can be used to identify optimal operating conditions.

A detailed economic analysis to asses the feasibility of the process would be useful. Future works should focus on detailed design of the fermentation and gasification units and also energy integration to improve the economic efficiency of the process.

References:

1. Abrini, J., Naveau, H., and Nyns, E.J. (1994). "Clostridium autoethanogenum, sp. nov., an anaerobic bacterium that produces ethanol from carbon monoxide." Archives of Microbiology 161(4): 345-351.
2. Ahmed, A., Cateni, B. G., Huhnke, R. L., and Lewis, R. S. (2006). "Effects of biomass-generated producer gas constituents on cell growth, product distribution and hydrogenase activity of Clostridium carboxidivorans P7T." Biomass and Bioenergy 30(7): 665-672.
3. Ahmed, A. and Lewis, R. S. (2007). "Fermentation of biomass-generated synthesis gas: Effects of nitric oxide." Biotechnology and Bioengineering 97(5): 1080-1086.
4. AspenTechnology (2003). "Aspen Tech 12.1 User Manuals" Cambridge, Massachusetts.
5. Bettagli, N., Desideri, U., and Fiaschi, D. (1995). "A Biomass Combustion-Gasification Model: Validation and Sensitivity Analysis." Journal of Energy Resources Technology 117(4): 329-336.
6. Bridgwater, A. V. (1995). "The technical and economic feasibility of biomass gasification for power generation." Fuel 74(5): 631-653.
7. Cardona Alzate, C. A. and Sanchez Toro, O. J. (2006). "Energy consumption analysis of integrated flowsheets for production of fuel ethanol from lignocellulosic biomass." Energy 31(Compendex): 2111-2123.

8. Carlson, E. C. (1996). “Don’t Gamble with Physical Properties for Simulations.” Chemical Engineering Progress pp 35-46.
9. Cateni, B. (2007). “Effects of feed composition and gasification parameters on product gas from a pilot scale fluidized bed gasifier.” Diss. Oklahoma State University. Dissertations and Theses at Oklahoma State University - Stillwater, ProQuest. Web. 9 Jul. 2010.
10. Chemical engineering magazine, February 2008
11. Cho, J., and Jeon, J.K. (2006). "Comparison of three- and two-column configurations in ethanol dehydration using azeotropic distillation." Journal of Industrial and Engineering Chemistry 12(2): 206-215.
12. Cho, J. and Jeon, J.K. (2006). "Optimization study on the azeotropic distillation process for isopropyl alcohol dehydration." Korean Journal of Chemical Engineering 23(1): 1-7.
13. Congressional Budget Office (CBO) (2009). "The Impact of Ethanol Use on Food Prices and Greenhouse-Gas Emissions."
14. Corella, J. and Sanz, A. (2005). "Modeling circulating fluidized bed biomass gasifiers. A pseudo-rigorous model for stationary state." Fuel Processing Technology 86(9): 1021-1053.
15. Datar, R. P., Shenkman, R. M., Cateni, B. G., Huhnke, R. L., and Lewis, R. S. (2004). "Fermentation of biomass-generated producer gas to ethanol." Biotechnology and Bioengineering 86(5): 587-594.
16. Dunn, J., Heinzle, E., lngham, J. and lrving, J. (2003). Biological reaction engineering, Second ed., Wiley-VCH, Weinheim.
17. Ecompressedair.com, January 2, 2010

Accessed: http://www.ecompressedair.com/desiccant/molecular-sieve/4a-molecular-sieve-desiccant/18-in-bead-4a-molecular-sieve-desiccant-(330-lb-drum).aspx

18. Environmental Protection Agency (EPA) (1994, 2004, 2008). Report on the Environment.
19. Energy Information Administration (EIA) (2008 and 2009). International energy outlook.
20. Gas processors suppliers association (1998). GPSA engineering data book. 11_{th} edition. Tulsa, Oklahoma, USA.
21. Guffey, F. D. and Wingerson, R. C. (2002). "Fractionation of Lignocellulosic Biomass for Fuel-Grade Ethanol Production." Western Research Institute, Prepared for U.S. Department of Energy, Office of Fossil Energy (No. FC26-98FT40323--12; TRN: US200305%%249).
22. International energy agency (IEA) (2000). World energy outlook
23. Jacques, K. A., Lyons, T. P., and Kelsall, D. R. (2003). The alcohol text book: A reference for the beverage, fuel and industrial alcohol industries., 4^{th} edition. Nottingham university press.
24. Jay, A., Lee, G., Granger, M., and Adam, N. (2007). “Incentives for Near-Term Carbon Dioxide Geological Sequestration: A White Paper prepared for The Gasification Carbon management Work Group”, Carnegie Mellon Electricity Industry Center, Carnegie Mellon University
25. Kalil, S. J., Maugeri, F., and Rodrigues, M. I. (2000). "Response surface analysis and simulation as a tool for bioprocess design and optimization." Process Biochemistry 35(6): 539-550.

26. Klasson, K.T., Ackerson, M.D., Clausen, E.C., and Gaddy, J. L. (1990). "Bioconversion of Synthesis Gas into Liquid or Gaseous Fuels." Proceedings Int'l Symp. on Biol. Proc. of Coal, EPRI and DOE, Orlando.
27. Litwak, D. (1999). "Methodology for the design of economical and environmental friendly processes: An uncertainty approach." Diss. Oklahoma State University. Dissertations and Theses at Oklahoma State University - Stillwater, ProQuest. Web. 9 Jul. 2010.
28. Lei, Z., Wang, H., Zhou, R., and Duan, Z. (2002). "Influence of salt added to solvent on extractive distillation." Chemical Engineering Journal 87(2): 149-156.
29. Llano-Restrepo, M., Aguilar-Arias, J., 2003. Modeling and simulation of saline extractive distillation columns for the production of absolute ethanol. Computers and Chemical Engineering 27 (4),527–549.
30. Lü, P., Kong, X., Wu, C., Yuan, Z., Ma, L., and Chang, J. (2008). "Modeling and simulation of biomass air-steam gasification in a fluidized bed." Frontiers of Chemical Engineering in China 2(2): 209-213.
31. Luyben, W. L. (2006). Distillation Design and Control Using Aspen Simulation. John Wiley and Sons, Inc.
32. Mansaray, K. G., Al-Taweel, A. M., Ghaly, A. E., Hamdullahpur, F., and Ugursal, V. I. (2000). "Mathematical Modeling of a Fluidized Bed Rice Husk Gasifier: Part I-Model Development." Energy Sources, Part A: Recovery, Utilization, and Environmental Effects 22(1): 83 - 98.
33. Maschio, G., Lucchesi, A., and Stoppato, G. (1994). "Production of syngas from biomass." Bioresource Technology 48(2): 119-126.
34. McKendry, P. (2002). "Energy production from biomass (part 3): gasification technologies." Bioresource Technology 83(1): 55-63.

35. Morrison, C. E. (2004). “Production of ethanol from the fermentation of synthesis gas.” M.S. Thesis. Mississippi State Miss.: Mississippi State University, Dave C. Swalm School of Chemical Engineering.
36. Nihtila, M. and Virkkunen, J. (1977), “Practical Identifiability of Growth and Substrate Consumption Models”, Biotechnol. Bioeng., 19, 1831–1850
37. Pascal, F., Dagot, C., Pingaud, H., Corriou, J. P., Pons, M. N., and Engasser, J. M. (1995). "Modeling of an industrial alcohol fermentation and simuiation of the plant by a process simulator." Biotechnology and Bioengineering 46(3): 202-217.
38. Patil, K. N., Huhnke, R. L., and Bellmer, D. D. (2008). “Gasification of switchgrass using a unique downdraft reactor.” American Society of Agricultural and Biological Engineers Annual International Meeting 2008, June 29, 2008 - July 2, 2008, Providence, RI, United states, American Society of Agricultural and Biological Engineers.
39. Patrachari, A. (2008). "Process Simulation, Modeling and Design for Soybean Oil Extraction Using Liquid Propane." M.S. Thesis, Oklahoma State University, Stillwater, OK.
40. Peter, M. (2002), Energy production from biomass: “part 1-overview of biomass and part 2- conversion technologies.” Bioresource Technology 83: 37-46
41. Piccolo, C. and Bezzo, F. (2009). "A techno-economic comparison between two technologies for bioethanol production from lignocellulose." Biomass and Bioenergy 33(3): 478-491.
42. Rao, S. R. (2005). "Biomass to ethanol: Process simulation, validation and sensitivity analysis of a gasifier and a bioreactor." M.S. Thesis, Oklahoma State University, Stillwater, Oklahoma.

43. Renewable Fuels Association (RFA) (2009). "Ethanol Industry outlook." www.ethanolrfa.org
44. Schuster, G., Löffler, G., Weigl, K., and Hofbauer, H. (2001). "Biomass steam gasification - an extensive parametric modeling study." Bioresource Technology 77(1): 71-79.
45. Silva, F. L. H. d., Rodrigues, M. I., and Maugeri, F. (1999). "Dynamic modelling, simulation and optimization of an extractive continuous alcoholic fermentation process." Journal of Chemical Technology and Biotechnology 74(2): 176-182.
46. Seider, W. D., Seader J. D., Lewin D.R., and Widagdo, S. (2009). Product and Process Design Principles: Synthesis, Analysis and Design., 3rd edition, Wiley
47. Wiselogel, A., Tyson, J., and Johnsson, D. (1996). "Biomass feedstock resources and composition." Handbook on bioethanol: production and utilization. Taylor and Francis, Washington, DC, pp 105-118.
48. Yacobucci, B. D. (2006). "Fuel Ethanol: Background and Public Policy Issues." Congressional Research Service Report for US Congress, Library of Congress, RL3329

Appendix A - Simulation Results

Table A.1 Gasification process stream summary

Ethanol process design and economic evaluation				
Stream ID		BIOMASS	AIRFEED	EXHAUST
Temperature	F	77.0	77.0	1499.0
Pressure	psia	36.74	36.74	29.39
Vapor Frac		0.504	1.000	1.000
Mole Flow	lbmol/hr	4597.216	3458.789	6522.672
Mass Flow	lb/hr	58422.503	99788.501	158211.003
Volume Flow	cuft/hr	399708.856	542188.569	4.66462E+6
Enthalpy	MMBtu/hr	501.984	> -0.001	-177.139
Mass Frac				
C		0.407		trace
H2		0.052		0.015
O2		0.440	0.233	trace
N2		0.008	0.767	0.487
H2O		0.093		0.074
CO				0.221
CO2				0.204
CH4				117 PPM
C2H2				trace
C2H4				trace
NO				trace
NO2				trace
N2O				trace
H3N				23 PPM
HNO3				
C2H6O-01				
C6H6				
Mole Flow	lbmol/hr			
C		1979.828		trace
H2		1495.137		1142.321
O2		804.207	726.612	trace
N2		16.549	2732.177	2748.618
H2O		301.496		651.691
CO				1245.913
CO2				732.765
CH4				1.150
C2H2				trace
C2H4				trace
NO				trace
NO2				trace
N2O				trace
H3N				0.215
HNO3				
C2H6O-01				
C6H6				

Table A.2 Fermentation process stream summary

Ethanol process design and economic evaluation				
Stream ID		GASES	H2O	PRODUCT
Temperature	F	98.6	77.0	98.6
Pressure	psia	26.39	36.74	21.39
Vapor Frac		0.932	0.000	0.165
Mole Flow	lbmol/hr	6522.672	19448.740	24384.411
Mass Flow	lb/hr	158210.997	350374.498	508585.495
Volume Flow	cuft/hr	1.37994E+6	311538.930	1.13277E+6
Enthalpy	MMBtu/hr	-258.204	-2388.724	-2698.306
Mass Frac				
C		trace		
H2		0.015		35 PPM
O2		trace		
N2		0.487		0.151
H2O		0.074	1.000	0.710
CO		0.221		58 PPB
CO2		0.204		0.103
CH4		117 PPM		
C2H2		trace		
C2H4		trace		
NO		trace		
NO2		trace		
N2O		trace		
H3N		23 PPM		
HNO3				
C2H6O-01				0.036
C6H6				
Mole Flow	lbmol/hr			
C		trace		
H2		1142.321		8.880
O2		trace		
N2		2748.618		2748.725
H2O		651.691	19448.740	20044.357
CO		1245.913		0.001
CO2		732.765		1185.069
CH4		1.150		
C2H2		trace		
C2H4		trace		
NO		trace		
NO2		trace		
N2O		trace		
H3N		0.215		
HNO3				
C2H6O-01				397.379
C6H6				

Table A.3 Separation process using flash drum stream summary

Ethanol process design and economic evaluation				
Stream ID		PRODUCT	PGAS1	PLIQUID
Temperature	F	98.6	76.7	76.7
Pressure	psia	21.39	19.33	19.33
Vapor Frac		0.165	1.000	0.000
Mole Flow	lbmol/hr	24384.411	3909.598	20474.812
Mass Flow	lb/hr	508585.495	125738.592	382846.903
Volume Flow	cuft/hr	1.13277E+6	1.16454E+6	6221.114
Enthalpy	MMBtu/hr	-2698.306	-191.241	-2517.320
Mass Frac				
C				
H2		35 PPM	142 PPM	24 PPB
O2				
N2		0.151	0.608	0.001
H2O		0.710	0.013	0.939
CO		58 PPB	235 PPB	trace
CO2		0.103	0.373	0.014
CH4				
C2H2				
C2H4				
NO				
NO2				
N2O				
H3N				
HNO3				
C2H6O-01		0.036	0.006	0.046
C6H6				
Mole Flow	lbmol/hr			
C				
H2		8.880	8.875	0.004
O2				
N2		2748.725	2728.588	20.137
H2O		20044.357	89.950	19954.407
CO		0.001	0.001	trace
CO2		1185.069	1064.574	120.495
CH4				
C2H2				
C2H4				
NO				
NO2				
N2O				
H3N				
HNO3				
C2H6O-01		397.379	17.610	379.769
C6H6				

Table A.4 First distillation stream summary

Ethanol process design and economic evaluation					
Stream ID		F1	B1	D1	V1
Temperature	F	76.7	228.4	49.5	49.5
Pressure	psia	20.57	20.17	16.17	16.17
Vapor Frac		0.000	0.000	0.000	1.000
Mole Flow	lbmol/hr	20474.812	19681.148	654.773	138.891
Mass Flow	lb/hr	382846.903	354573.287	22626.177	5647.439
Volume Flow	cuft/hr	6221.133	6251.492	421.183	46947.748
Enthalpy	MMBtu/hr	-2517.318	-2363.530	-80.463	-19.058
Mass Frac					
C					
H2		24 PPB	trace	trace	2 PPM
O2					
N2		0.001	trace	225 PPM	0.099
H2O		0.939	1.000	0.213	0.020
CO		trace	trace	trace	41 PPB
CO2		0.014	trace	0.035	0.799
CH4					
C2H2					
C2H4					
NO					
NO2					
N2O					
H3N					
HNO3					
C2H6O-01		0.046	55 PPM	0.752	0.081
C6H6					
Mole Flow	lbmol/hr				
C					
H2		0.004	trace	trace	0.004
O2					
N2		20.137	trace	0.182	19.955
H2O		19954.407	19680.724	267.286	6.396
CO		trace	trace	trace	trace
CO2		120.495	trace	17.927	102.568
CH4					
C2H2					
C2H4					
NO					
NO2					
N2O					
H3N					
HNO3					
C2H6O-01		379.769	0.424	369.378	9.968
C6H6					

Table A.5 Second distillation stream summary

Ethanol process design and economic evaluation					
Stream ID		F2	D2	B2	V2
Temperature	F	49.4	137.4	230.5	137.4
Pressure	psia	20.57	16.17	21.37	16.17
Vapor Frac		0.000	0.000	0.000	1.000
Mole Flow	lbmol/hr	654.773	425.867	201.723	27.183
Mass Flow	lb/hr	22626.177	17714.746	3724.660	1186.772
Volume Flow	cuft/hr	10488.456	6821.734	3231.292	10774.356
Enthalpy	MMBtu/hr	-80.453	-50.470	-24.199	-3.775
Mass Frac					
C					
H2		trace	trace	trace	4 PPB
O2					
N2		225 PPM	4 PPM	trace	0.004
H2O		0.213	0.069	0.960	0.016
CO		trace	trace	trace	2 PPB
CO2		0.035	0.006	trace	0.578
CH4					
C2H2					
C2H4					
NO					
NO2					
N2O					
H3N					
HNO3					
C2H6O-01		0.752	0.925	0.040	0.401
C6H6					
Mole Flow	lbmol/hr				
C					
H2		trace	trace	trace	trace
O2					
N2		0.182	0.003	trace	0.179
H2O		267.286	67.716	198.495	1.076
CO		trace	trace	trace	trace
CO2		17.927	2.333	trace	15.594
CH4					
C2H2					
C2H4					
NO					
NO2					
N2O					
H3N					
HNO3					
C2H6O-01		369.378	355.816	3.228	10.334
C6H6					

Table A.6 Azeotropic separation process stream summary

Ethanol process design and economic evaluation							
Stream ID		FV1	RECYCLE	REFLUX	D2	B2	MAKEUP
Temperature	K	353.9	345.0	324.5	358.7	372.8	340.0
Pressure	atm	2.20	2.20	2.19	2.00	2.20	2.25
Vapor Frac		0.000	0.000	0.000	1.000	0.000	0.000
Mole Flow	kmol/hr	192.266	187.200	267.158	485.524	161.100	0.900
Mass Flow	kg/hr	8000.010	8649.853	19197.916	28414.589	7433.191	70.302
Volume Flow	l/min	179.576	183.303	4452.641	119090.860	175.562	15.000
Enthalpy	MMBtu/hr	-49.499	-38.624	-1.713	-31.284	-40.582	0.047
Mass Frac							
C							
H2							
O2							
N2							
H2O		0.069	0.073	0.004	0.044	553 PPM	
CO							
CO2							
CH4							
C2H2							
C2H4							
NO							
NO2							
N2O							
H3N							
HNO3							
C2H6O-01		0.931	0.643	0.107	0.270	0.994	
C6H6			0.284	0.890	0.686	0.006	1.000
Mole Flow	kmol/hr						
C							
H2							
O2							
N2							
H2O		30.567	35.006	4.135	69.480	0.228	
CO							
CO2							
CH4							
C2H2							
C2H4							
NO							
NO2							
N2O							
H3N							
HNO3							
C2H6O-01		161.700	120.744	44.384	166.513	160.314	
C6H6			31.450	218.639	249.531	0.558	0.900

Table A.6 Dehydration process using molecular sieves stream summary

Ethanol process design and economic evaluation				
Stream ID		FEEDMS	WATER	ETHA
Temperature	K	363.0	363.0	363.0
Pressure	atm	1.16	1.16	1.16
Vapor Frac		1.000	0.000	0.000
Mole Flow	kmol/hr	186.200	23.129	163.071
Mass Flow	kg/hr	7931.805	440.086	7491.720
Volume Flow	l/min	79702.832		
Enthalpy	MMBtu/hr	-41.080	0.000	0.000
Mass Frac				
C				
H2		trace	trace	trace
O2				
N2		6 PPM	51 PPM	3 PPM
H2O		0.052	0.910	0.002
CO		trace	trace	trace
CO2		0.008	0.073	0.004
CH4				
C2H2				
C2H4				
NO				
NO2				
N2O				
H3N				
HNO3				
C2H6O-01		0.940	0.017	0.994
C6H6				
Mole Flow	kmol/hr			
C				
H2		trace	trace	trace
O2				
N2		0.002	0.001	0.001
H2O		22.929	22.241	0.688
CO		trace	trace	trace
CO2		1.451	0.726	0.726
CH4				
C2H2				
C2H4				
NO				
NO2				
N2O				
H3N				
HNO3				
C2H6O-01		161.819	0.162	161.657
C6H6				

Appendix B -Sensitivity Analysis Results

Table B.1 Effect of temperature on gasification process

	Mole Flow (Kmol/hr)						
	Gasification Temperature (K)	**CO_2**	**CO**	**H_2**	**N_2**	**CH_4**	**H_2O**
1	800.00	0.37	0.13	0.21	0.83	0.09	0.14
2	844.44	0.33	0.21	0.29	0.83	0.06	0.14
3	888.89	0.29	0.28	0.35	0.83	0.02	0.15
4	933.33	0.27	0.32	0.37	0.83	0.01	0.16
5	977.78	0.25	0.35	0.37	0.83	0.00	0.17
6	1022.22	0.24	0.36	0.36	0.83	0.00	0.18
7	1066.67	0.23	0.37	0.35	0.83	0.00	0.19
8	1111.11	0.22	0.38	0.34	0.83	0.00	0.20
9	1155.56	0.21	0.39	0.33	0.83	0.00	0.21
10	1200.00	0.20	0.40	0.32	0.83	0.00	0.22

Table B.2 Effect of air/biomass ratio on gasification process

	Mass Flow (Kg/hr)						
	Air/ratio Ratio	**CO_2**	**CO**	**H_2**	**N_2**	**CH_4**	**H_2O**
1	0.57	2.97	14.80	0.97	7.81	0.00	1.07
2	1.20	6.69	12.48	0.82	16.33	0.00	2.43
3	1.83	10.43	10.10	0.67	24.85	0.00	3.80
4	2.46	14.17	7.73	0.51	33.38	0.00	5.19
5	3.09	17.89	5.36	0.36	41.90	0.00	6.58
6	3.72	21.60	3.00	0.20	50.42	0.00	7.98
7	4.35	25.29	0.65	0.04	58.94	0.00	9.38
8	4.98	26.31	0.00	0.00	67.47	0.00	9.77
9	5.61	26.31	0.00	0.00	75.99	0.00	9.77
10	6.24	26.31	0.00	0.00	84.51	0.00	9.77

Table B.3 Effect of media flow rate on fermentation process

	Mass Fraction					
	Media Flow Kg/sec	**Ethanol**	**CO**	**CO_2**	**H_2**	**N_2**
1	1.00E-06	0.0445	2.45E-07	0.1939	0.0031	0.4900
2	2.00E-06	0.0369	1.71E-07	0.1456	0.0022	0.3682
3	**3.00E-06**	**0.0315**	**1.30E-07**	**0.1166**	**0.0017**	**0.2948**
4	4.00E-06	0.0275	1.04E-07	0.0972	0.0013	0.2459
5	5.00E-06	0.0244	8.66E-08	0.0834	0.0011	0.2109
6	6.00E-06	0.0219	7.37E-08	0.0730	0.0010	0.1846
7	7.00E-06	0.0199	6.39E-08	0.0649	0.0008	0.1641
8	8.00E-06	0.0182	5.62E-08	0.0584	0.0007	0.1477
9	**9.00E-06**	**0.0168**	**5.01E-08**	**0.0531**	**0.0007**	**0.1343**
10	1.00E-05	0.0156	4.50E-08	0.0487	0.0006	0.1232

Table B.4 Effect of media flow rate on fermentation process

P(atm)	Temperature(K)	% Ethanol Loss	% N_2 Removal	% CO_2 Removal	% H_2 Removal
1.00	290.00	3.54	99.40	90.59	99.96
1.00	296.11	5.24	99.44	91.87	99.96
1.00	302.22	7.59	99.48	92.99	99.96
1.00	308.33	10.79	99.52	93.98	99.96
1.00	314.44	15.03	99.56	94.85	99.97
1.00	320.56	20.51	99.60	95.64	99.97
1.00	326.67	27.40	99.64	96.35	99.97
1.00	332.78	35.79	99.68	97.00	99.97
1.00	338.89	45.64	99.73	97.60	99.97
1.00	345.00	56.71	99.78	98.16	99.98
1.32	290.00	2.65	99.20	87.78	99.95
1.32	296.11	3.94	99.25	89.38	99.95
1.32	302.22	5.73	99.30	90.78	99.95
1.32	308.33	8.17	99.35	92.01	99.95
1.32	314.44	11.42	99.40	93.10	99.95
1.32	320.56	15.67	99.44	94.07	99.95
1.32	326.67	21.10	99.49	94.95	99.96
1.32	332.78	27.84	99.54	95.75	99.96
1.32	338.89	35.96	99.60	96.48	99.96
1.32	345.00	45.42	99.65	97.16	99.97
2.00	290.00	1.69	98.75	82.06	99.92
2.00	296.11	2.52	98.83	84.26	99.92
2.00	302.22	3.68	98.90	86.20	99.92
2.00	308.33	5.28	98.97	87.92	99.92
2.00	314.44	7.42	99.04	89.43	99.92
2.00	320.56	10.25	99.11	90.78	99.93
2.00	326.67	13.92	99.17	91.98	99.93
2.00	332.78	18.57	99.24	93.07	99.93
2.00	338.89	24.33	99.31	94.07	99.94
2.00	345.00	31.29	99.38	94.99	99.94
3.00	290.00	1.08	98.06	74.57	99.87
3.00	296.11	1.62	98.19	77.46	99.88
3.00	302.22	2.37	98.30	80.04	99.88
3.00	308.33	3.41	98.41	82.34	99.88
3.00	314.44	4.83	98.50	84.38	99.88
3.00	320.56	6.70	98.60	86.20	99.88
3.00	326.67	9.16	98.69	87.84	99.89
3.00	332.78	12.31	98.78	89.31	99.89
3.00	338.89	16.28	98.87	90.65	99.89
3.00	345.00	21.18	98.96	91.88	99.90

Table B.5 Energy consumption and cost comparison of different Column arrangements

Different Column Arrangements	Heat duty(Btu/hr) in millions		Cost ($) in millions
	Reboiler	Condenser	
One	178.72	128.67	2.13
Two(0.45)	95.60	45.51	1.31
Two(0.5)	101.48	51.38	1.59
Two(0.6)	101.48	65.97	1.64
Two(0.7)	133.95	83.80	1.59
Three	102.42	52.30	1.67

Table B.6 Block summary of a separation process using one distillation column

Distillation Column Parameters	
Minimum reflux ratio:	11.307
Actual reflux ratio:	16.961
Minimum number of stages:	32.312
Number of actual stages:	49.211
Feed stage:	48.454
Number of actual stages above feed:	47.454
Reboiler heating required (Btu/hr):	178722364
Condenser cooling required (Btu/hr):	128674721
Distillate temperature ^{o}F:	177.161
Bottom temperature ^{o}F:	232.512
Distillate to feed fraction:	0.021

Table B.7 Stream summary of separation process using one distillation column

Mole Flow (lbmol/hr)	**Feed**	**Distillate**	**Bottoms**
ETHANOL	379.56	356.79	22.77
WATER	19826.17	68.60	19757.58
Mass Frac			
ETHANOL	0.05	0.93	0.00
WATER	0.95	0.07	1.00
Total Flow lbmol/hr	20205.74	425.39	19780.35
Total Flow lb/hr	374660	17672.73	356987
Total Flow cuft/hr	6176.83	381.12	6316.27
Temperature F	98.36	177.16	232.51
Pressure psia	20.57	16.17	22.04

Table B.8 Block (Column 1) summary of separation process using 2 distillation columns

First Distillation Column Parameters	
Minimum reflux ratio:	2.875
Actual reflux ratio:	4.313
Minimum number of stages:	4.497
Number of actual stages:	7.807
Feed stage:	5.641
Number of actual stages above feed:	4.641
Reboiler heating required (Btu/hr):	122752272
Condenser cooling required (Btu/hr):	72819192
Distillate temperature ^{o}F:	180.297
Bottom temperature ^{o}F:	233.114
Distillate to feed fraction:	0.039

Table B.9 Stream summary of the first distillation column

Mole Flow (lbmol/hr)	Feed	Distillate	Bottoms
ETHANOL	379.56	375.77	3.80
WATER	19826.17	412.38	19413.79
Mass Frac			
ETHANOL	0.05	0.70	0.00
WATER	0.95	0.30	1.00
Total Flow lbmol/hr	20205.74	788.15	19417.58
Total Flow lb/hr	374660	24740.43	349920
Total Flow cuft/hr	6176.83	506.40	6189.29
Temperature F	98.36	180.30	233.11
Pressure psia	20.57	16.17	22.04

Table B.10 Block(Column II) summary of separation process using 2 distillation columns

First Distillation Column Parameters	
Minimum reflux ratio:	0.355
Actual reflux ratio:	0.532
Minimum number of stages:	22.681
Number of actual stages:	44.553
Feed stage:	37.488
Number of actual stages above feed:	36.488
Reboiler heating required (Btu/hr):	11192933.1
Condenser cooling required (Btu/hr):	10981180.4
Distillate temperature ^{o}F:	177.161
Bottom temperature ^{o}F:	214.056
Distillate to feed fraction:	0.540

Table B.11 Stream summary of the second distillation column

Mole Flow (lbmol/hr)	Feed	Distillate	Bottoms
ETHANOL	375.77	356.98	18.79
WATER	412.38	68.74	343.64
Mass Frac			
ETHANOL	0.48	0.84	0.05
WATER	0.52	0.16	0.95
Total Flow lbmol/hr	0.70	0.93	0.12
Total Flow lb/hr	0.30	0.07	0.88
Total Flow cuft/hr	788.15	425.72	362.43
Temperature F	24740.43	17684.10	7056.33
Pressure psia	506.42	381.36	127.58

Appendix C - Input Files of the Gasifier, Bioreactor, Flash drum and Distillation Columns.

TITLE – 'Ethanol production by biomass gasification'

DATABANKS 'APV70 PURE22' / 'APV70 AQUEOUS' / 'APV70 SOLIDS' / 'APV70 INORGANIC' / NOASPENPCD

PROP-SOURCES 'APV70 PURE22' / 'APV70 AQUEOUS' / 'APV70 SOLIDS'/'APV70 INORGANIC'

COMPONENTS
C, H_2, O_2, N_2, H_2O, CO, CO_2,CH_4, C_2H_2, C_2H_4, NO, NO_2, N_2O, H_3N, HNO_3, C_2H_6O, C_6H_6

FLOWSHEET BIOREACT
BLOCK BIOREA IN=GASES H2O OUT=PRODUCT
BLOCK DIST1 IN=F1 OUT=V1 D1 B1
BLOCK PD2 IN=PLIQUID OUT=F1

FLOWSHEET COOLER
BLOCK COOLER1 IN=EXHAUST OUT=GASES

FLOWSHEET FLASHD
BLOCK FLASH IN=PRODUCT OUT=PGAS1 PLIQUID

FLOWSHEET GASI
BLOCK GASIFIER IN=BIOMASS AIRFEED OUT=EXHAUST
BLOCK PD3 IN=D1 OUT=F2
BLOCK DIST2 IN=F2 OUT=V2 D2 B2
BLOCK PD4 IN=D2 OUT=D2H
BLOCK HEATER IN=D2H OUT=FEEDMS
BLOCK VV1 IN=B1 OUT=B1P
BLOCK VV2 IN=B2 OUT=B2P
BLOCK VW IN=MEDIA OUT=H2O

PROPERTIES NRTL
PROPERTIES SOLIDS GASI FREE-WATER=STEAM-TA SOLU-WATER=3&
TRUE-COMPS=YES / NRTL BIOREACT FREE-WATER=STEAM-TA &
SOLU-WATER=3 TRUE-COMPS=YES / NRTL COOLER &
FREE-WATER=STEAM-TA SOLU-WATER=3 TRUE-COMPS=YES / NRTL &
FLASHD FREE-WATER=STEAM-TA SOLU-WATER=3 TRUE-COMPS=YES

PROP-DATA NRTL-1
IN-UNITS ENG
PROP-LIST NRTL
BPVAL H2O H3N -6.268400000 2745.817718 .3000000000 0.0 0.0 0.0 50.00000360 196.7000024
BPVAL H3N H2O 9.612100000 -5819.068573 .3000000000 0.0 0.0 0.0 50.00000360 196.7000024
BPVAL H2O C2H6O 3.457800000 -1054.945612 .3000000000 0.0 0.0 0.0 76.98200338 212.0000023
BPVAL C2H6O H2O -.8009000000 443.1239965 .3000000000 0.0 0.0 0.0 76.98200338 212.0000023
BPVAL H2O C6H6 151.8580629 -10717.75269 .2000000000 0.0 -20.02540000 0.0 33.44000373 170.6000026
BPVAL C6H6 H2O 49.63587171 1064.461671 .2000000000 0.0 -7.562900000 0.0 33.44000373 170.6000026
BPVAL C2H6O C6H6 .5686000000 -98.64791921 .3000000000 0.0 0.0 0.0 68.00000346 176.1800026
BPVAL C6H6 C2H6O -.9155000000 1587.651827 .3000000000 0.0 0.0 0.0 68.00000346 176.1800026

STREAM AIRFEED
IN-UNITS ENG
SUBSTREAM MIXED TEMP=25. <C> PRES=3. <atm> MASS-FLOW=45263.3 <kg/hr>
MASS-FRAC O2 0.233 / N2 0.767

STREAM BIOMASS
IN-UNITS ENG
SUBSTREAM MIXED TEMP=25. <C> PRES=3. <atm> MASS-FLOW=26500. <kg/hr>
MASS-FRAC C 0.40703 / H2 0.05159 / O2 0.440475 / N2 0.007935 / H2O 0.09297

STREAM MEDIA
SUBSTREAM MIXED TEMP=25. <C> PRES=2.5 <atm> MOLE-FLOW=8821.8 <kmol/hr>
MASS-FRAC H2O 1.

BLOCK COOLER1 HEATER
IN-UNITS ENG
PARAM TEMP=37. <C> PRES=-3. <psi>

BLOCK HEATER HEATER
PARAM TEMP=363. PRES=-5. <psi>

BLOCK FLASH FLASH2
PARAM TEMP=298. PRES=1.315 <atm>

BLOCK DIST1 RADFRAC
PARAM NSTAGE=12 EFF=MURPHREE
COL-CONFIG CONDENSER=PARTIAL-V-L
FEEDS F1 7
PRODUCTS B1 12 L / D1 1 L / V1 1 V
P-SPEC 1 1.1 <atm>
COL-SPECS DP-STAGE=0.1 <psi> MOLE-RDV=0.175 &
MOLE-D=360. <kmol/hr> MOLE-RR=6. DP-COND=3. <psi>
STAGE-EFF 1 0.9 / 2 0.65 / 11 0.65 / 12 0.9

BLOCK DIST2 RADFRAC
PARAM NSTAGE=24 EFF=MURPHREE
COL-CONFIG CONDENSER=PARTIAL-V-L
FEEDS F2 16
PRODUCTS D2 1 L / B2 24 L / V2 1 V
P-SPEC 1 1.1 <atm>
COL-SPECS DP-STAGE=0.1 <psi> MOLE-RDV=0.06 MOLE-D=205.5 <kmol/hr> MOLE-RR=1.45 DP-COND=3. <psi>
STAGE-EFF 1 0.9 / 2 0.65 / 23 0.65 / 24 0.9

BLOCK BIOREA RGIBBS
PARAM TEMP=37. <C> PRES=-5. <psi> NPHASE=2
PROD CO / CO2 / H2 / N2 / H2O / C2H6O

BLOCK GASIFIER RGIBBS
IN-UNITS ENG
PARAM TEMP=815. <C> PRES=2. <atm>
PROD C/H2/O2/N2/H2O/CO/CO2/CH4 /C2H2 / C2H4 / NO / NO2 / N2O / H3N / HNO3

BLOCK PD2 PUMP
PARAM PRES=1.4 <atm>

BLOCK PD3 PUMP
PARAM PRES=1.4 <atm>

BLOCK PD4 PUMP
PARAM PRES=1.5 <atm>

BLOCK VV1 VALVE
PARAM P-DROP=0.

BLOCK VV2 VALVE
PARAM P-DROP=0.

BLOCK VW VALVE
PARAM P-DROP=0. <psi>

Input Summary of Azeotropic Separation Process

TITLE – 'Ethanol dehydration using azeotropic separation process"

DATABANKS 'APV70 PURE22' / 'APV70 AQUEOUS' / 'APV70 SOLIDS' /'APV70 INORGANIC' / NOASPENPCD

PROP-SOURCES 'APV70 PURE22' / 'APV70 AQUEOUS' / 'APV70 SOLIDS'/ 'APV70 INORGANIC'

COMPONENTS
C, H_2, O_2, N_2, H_2O, CO, CO_2,CH_4, C_2H_2, C_2H_4, NO, NO_2, N_2O, H_3N, HNO_3, C_2H_6O, C_6H_6

FLOWSHEET BIOREACT
BLOCK V1 IN=FV1 OUT=F2
BLOCK V2 IN=RECYCLE OUT=RF
BLOCK DYHYDRAT IN=F2 RF REFLUX2 OUT=D2 B2
BLOCK V3 IN=D2 OUT=D2C
BLOCK V4 IN=REFLUX OUT=REFLUX2
BLOCK HX IN=D2C OUT=D2D
BLOCK M1 IN=ORG BENZ OUT=REFL
BLOCK PD3 IN=ORGANIC OUT=ORG
BLOCK DECANTOR IN=D2D OUT=AQUEOUS ORGANIC

FLOWSHEET GASI
BLOCK PD4 IN=AQUEOUS OUT=FV2
BLOCK V6 IN=FV2 OUT=F3
BLOCK RECOVERY IN=F3 OUT=D3 B3
BLOCK PD6 IN=B3 OUT=BV3
BLOCK PD5 IN=D3 OUT=D3RECYCL
BLOCK VB2 IN=B2 OUT=B2O
BLOCK V5 IN=MAKEUP OUT=BENZ
BLOCK VR1 IN=REFL OUT=REFLUX
BLOCK VB3 IN=BV3 OUT=BWATER

PROPERTIES NRTL
PROPERTIES SOLIDS GASI FREE-WATER=STEAM-TA SOLU-WATER=3 &
TRUE-COMPS=YES / NRTL BIOREACT FREE-WATER=STEAM-TA &
SOLU-WATER=3 TRUE-COMPS=YES

PROP-DATA NRTL-1

IN-UNITS ENG
PROP-LIST NRTL
BPVAL H2O H3N -6.268400000 2745.817718 .3000000000 0.0 0.0 0.0 50.00000360 196.7000024
BPVAL H3N H2O 9.612100000 -5819.068573 .3000000000 0.0 0.0 0.0 50.00000360 196.7000024
BPVAL H2O C2H6O3.457800000 -1054.945612 .3000000000 0.0 0.0 0.0 76.98200338 212.0000023
BPVAL C2H6O H2O -.8009000000 443.1239965 .3000000000 0.0 0.0 0.0 76.98200338 212.0000023
BPVAL H2O C6H6 151.8580629 -10717.75269 .2000000000 0.0 -20.02540000 0.0 33.44000373 170.6000026
BPVAL C6H6 H2O 49.63587171 1064.461671 .2000000000 0.0 -7.562900000 0.0 33.44000373 170.6000026
BPVAL C2H6O C6H6 .5686000000 -98.64791921 .3000000000 0.0 0.0 0.0 68.00000346 176.1800026
BPVAL C6H6 C2H6O -.9155000000 1587.651827 .3000000000 0.0 0.0 0.0 68.00000346 176.1800026

STREAM FV1
SUBSTREAM MIXED TEMP=353.871692 PRES=2.2 <atm> MOLE-FLOW=192.266247 <kmol/hr>
MOLE-FLOW H2O 30.5667 <kmol/hr> / C2H6O 161.6995 <kmol/hr>

STREAM MAKEUP
SUBSTREAM MIXED TEMP=340. PRES=2.25 <atm> MOLE-FLOW=0.00025
MOLE-FRAC C6H6 1.

STREAM RECYCLE
SUBSTREAM MIXED TEMP=345. PRES=2.2 <atm> MOLE-FLOW=0.052
MOLE-FRAC H2O 0.187 / C2H6O 0.645 / C6H6 0.168

STREAM REFLUX
SUBSTREAM MIXED TEMP=345. PRES=2.2 <atm> MOLE-FLOW=0.0787
MOLE-FRAC H2O 0.015 / C2H6O 0.166 / C6H6 0.819

BLOCK M1 MIXER
PARAM PRES=2.2 <atm>

BLOCK HX HEATER
PARAM TEMP=313. PRES=-0.1 <atm> NPHASE=2
BLOCK-OPTION FREE-WATER=NO

BLOCK DECANTOR DECANTER
PARAM PRES=1.5 <atm> DUTY=0. L2-COMPS=C6H6

BLOCK DYHYDRAT RADFRAC
PARAM NSTAGE=31 ALGORITHM=NEWTON INIT-OPTION=AZEOTROPIC MAXOL=200
COL-CONFIG CONDENSER=NONE
FEEDS F2 15 / RF 10 / REFLUX2 1
PRODUCTS D2 1 V / B2 31 L
P-SPEC 1 2. <atm>
COL-SPECS DP-STAGE=0.1 <psi> MOLE-B=161.1 <kmol/hr>
TRAY-SIZE 1 2 30 SIEVE

BLOCK RECOVERY RADFRAC
PARAM NSTAGE=21
COL-CONFIG CONDENSER=TOTAL
FEEDS F3 11
PRODUCTS B3 21 L / D3 1 L
P-SPEC 1 1.1 <atm>
COL-SPECS DP-STAGE=0.1 <psi> MOLE-B=29.5 <kmol/hr> MOLE-RR=2. DP-COND=3. <psi>
TRAY-SIZE 1 2 20 SIEVE

BLOCK PD5 PUMP

PARAM PRES=2.2 <atm>

BLOCK PD6 PUMP
PARAM DELP=0.5 <atm>

BLOCK PD7 PUMP
PARAM PRES=1.5 <atm>

BLOCK PD8 PUMP
PARAM PRES=1.5 <atm>

BLOCK V1 VALVE
PARAM P-OUT=2.09526435 <atm>

BLOCK V2 VALVE
PARAM P-OUT=2.06124137 <atm>

BLOCK V3 VALVE
PARAM P-OUT=1.9 <atm>

BLOCK V4 VALVE
PARAM P-OUT=2. <atm>

BLOCK V5 VALVE
PARAM P-OUT=2.2 <atm>

BLOCK V6 VALVE
PARAM P-OUT=1.36537926 <atm>

BLOCK VB2 VALVE
PARAM P-OUT=2. <atm>

BLOCK VB3 VALVE
PARAM P-OUT=1.4 <atm>

BLOCK VR1 VALVE
PARAM P-OUT=2.19 <atm>

APPENDIX D - Cost Estimation and Sizing

1. Gasifier and Bioreactor

Name	Bioreactor	Gasifier
Liquid volume (gallons)	549952.76	118028.32
Vessel diameter (ft)	30	18
Vessel tangent to tangent height (ft)	104	62
Design gauge pressure (psig)	35.30	35.30
Design temperature (°F)	250	1549
Direct cost ($)	N/A	N/A

2. Flash Drum

Name	FLASH-flash vessel
Liquid volume (gallons)	6189.91
Vessel diameter (ft)	7.00
Vessel tangent to tangent height (ft)	21.50
Design gauge pressure (psig)	35.30
Design temperature (°F)	250
Operating temperature (°F)	98.60
Direct cost ($)	$163,100

3. Distillation I and II Tower

Name	DIST1-tower	DIST2-tower
Tray type	SIEVE	SIEVE
Vessel diameter (ft)	14.50	13.50
Vessel tangent to tangent height (ft)	42	76
Design gauge pressure (psig)	35.30	35.30
Design temperature (°F)	278.44	280.54
Operating temperature (°F)	228.44	230.54
Number of trays	15	32
Tray spacing (in)	24	24
Direct cost ($)	$579,600	$759,300

4. Distillation I and II Condenser

Name	DIST1-cond	DIST2-cond
Heat transfer area (SF)	9895.45	1824.90
Tube design gauge pressure (psig)	35.30	60.30
Tube design temperature (°F)	250.00	250.00
Tube outside diameter (in)	1	1
Shell design gauge pressure (psig)	35.30	35.30
Shell design temperature (°F)	250	250
Tube length extended (ft)	20	20
Tube pitch (in)	1.25	1.25
Number of tube passes	1	1
Number of shell passes	1	1
Direct cost ($)	$262,300	$114,200

Name	DIST1-cond acc	DIST2-cond acc
Liquid volume (gallons)	3021.51	13801.70
Vessel diameter (ft)	5.50	9
Vessel tangent to tangent length (ft)	17	29
Design gauge pressure (psig)	35.30	35.30
Design temperature (°F)	70	250
Operating temperature (°F)	49.51	137.40
Direct cost ($)	$118,900	$169,200

5. Distillation I and II Reboiler

Name	Dist I -reb	Dist II -reb
Heat transfer area (sf)	8554.58	1164.34
Tube design gauge pressure (psig)	110	110
Tube design temperature (°F)	377	377
Tube outside diameter (in)	1	1
Shell design gauge pressure (psig)	68.60	68.60
Shell design temperature (°F)	278	280
Tube length extended (ft)	20	20
Tube pitch (in)	1.25	1.25
Tube pitch symbol	Triangular	Triangular
Number of tube passes	2	2
Duty (mmbtu/hr)	164.12	21.97
TEMA type	BKU	BKU
Direct cost ($)	$354,600	$120,50

6. Ethanol Concentrator Pumps

Name	Dist I-reflux pump	Dist II -reflux pump
Liquid flow rate (gpm)	477.85	2378.69
Fluid head (ft)		
Fluid specific gravity	0.86	0.04
Design gauge pressure (psig)	35.30	35.30
Design temperature (°F)	70	250
Fluid viscosity (cp)	1.43	0.60
Pump efficiency	70	70
Direct cost ($)	$46,300	$40,200

Name	PD2	PD3	PD4
Liquid flow rate (gpm)	853.18	57.76	935.55
Fluid head (ft)	2.93	11.83	326.44
Fluid specific gravity	0.99	0.86	0.04
Design gauge pressure (psig)	35.30	35.30	35.30
Design temperature (°F)	250	70	250
Fluid viscosity (cp)	0.91	1.43	0.60
Pump efficiency	75.08	78.97	75.82
Direct cost ($)	$53,400	$24,400	$40,000

7. Dehydration and Recovery Towers

Name	DYHYDRAT-tower	RECOVERY-tower
Tray type	SIEVE	SIEVE
Vessel diameter (ft)	5.5	22.5
Vessel tangent to tangent height (ft)	98	68
Design gauge pressure (psig)	35.30	35.30
Design temperature (°F)	261.33	280.73
Operating temperature (°F)	211.33	230.73
Number of trays	43	28
Tray spacing (in)	24	24
Molecular weight Overhead prod	58.52	46.13
Direct cost ($)	$424,700	$1,468,300

7. Dehydration and Recovery Reboilers

Name	DYHYDRAT-reb	RECOVERY-reb
Heat transfer area (SF)	1148.26	1163.74
Tube design gauge pressure (psig)	110	110
Tube design temperature (°F)	377	377
Tube outside diameter (in)	1	1
Shell design gauge pressure (psig)	68.6	68.6
Shell design temperature (°F)	261	280
Tube length extended (ft)	20	20
Tube pitch (in)	1.25	1.25
Tube pitch symbol	TRIANGULAR	TRIANGULAR
Number of tube passes	2	2
Duty [MMBTU/H]	17.98	21.81
TEMA type	BKU	BKU
Direct cost ($)	$110,200	$120,500

7. Recovery Tower Condenser

Name	RECOVERY-cond
Heat transfer area (SF)	1385.81
Tube design gauge pressure (psig)	60.3
Tube design temperature (°F)	250
Tube outside diameter (in)	1
Shell design gauge pressure (psig)	35.3
Shell design temperature (°F)	250
Tube length extended (ft)	20
Tube pitch (in)	1.25
Number of tube passes	1
Number of shell passes	1
Direct cost ($)	$108,200

Name	RECOVERY-cond acc
Liquid volume (gallons)	16173.22
Vessel diameter (ft)	9.5
Vessel tangent to tangent length (ft)	30.5
Design gauge pressure (psig)	35.304
Design temperature (°F)	250
Operating temperature (°F)	183.48
Direct cost ($)	$191,500

7. Dehydration and Recovery Unit Pumps

Name	PD5	PD6	PD7	PD8	RECOVERY-reflux pump
Liquid flow rate (gpm)	108.89	54.23	919.10	142.87	2757.29
Fluid head (ft)	27.93	20.46	294.38	124.88	
Fluid specific gravity	0.85	0.83	0.05	0.018	0.05
Design gauge pressure (psig)	35.30	35.30	35.30	35.30	35.30
Design temperature (°F)	250	250	250	281.01	250
Fluid viscosity (cp)	0.46	0.75		0.25	
Pump efficiency	53.41	76.79	75.68	56.86	70
Direct cost ($)	$31,400	$27,800	$21,200	$8,300	$45,200

7. Heat exchanger

Name	HX
Heat transfer area [SF]	2640.69
Tube design gauge pressure (psig)	60.3
Tube design temperature (°F)	250
Tube outside diameter (in)	1
Shell design gauge pressure (psig)	35.3
Shell design temperature (°F)	250
Tube length extended (ft)	20
Tube pitch (in)	1.25
Number of tube passes	2
Number of shell passes	1
Direct cost ($)	$147,500

7. Decantor

Name	DECANTOR
Item Reference Number	1
Liquid volume (gallons)	1128.11
Vessel diameter (ft)	4
Vessel tangent to tangent height (ft)	12
Design gauge pressure (psig)	35.30
Design temperature (°F)	250
Operating temperature (°F)	112.04
Direct cost ($)	$103,100

APPENDIX E - VBA Program Code for Molecular sieve

The design for a molecular sieve was carried out by developing a user defined unit operation. The following program code for the new unit was written in VBA (Visual Basic for Application) using Excel.

```
Option Explicit
'Variables used for calculating bed diameter
    Dim B As Double, C As Double, Pi_value As Double
    Dim Mass_Flow As Double, Vol_Flow As Double, Viscosity As Double
    Dim Density As Double, Max_P_Drop As Double
    Dim V_max As Double, V_adj  As Double, D_Min As Double, D_Selected As Double,
    Adj_P_Drop As Double

'Variables used for calculating desiccant mass
    Dim Water_Flow_Rate As Double, Adsorption_Period As Double
    Dim Regen_Period As Double, Inlet_Tem As Double
    Dim Price As Double, Num_Of_Sieves As Double, Relative_Sat As Double
    Dim Css As Double, CT As Double, Des_Mass  As Double

'Variables used for calculating bed height
    Dim Bulk_Den As Double, Z As Double
    Dim L_Sat_Zone As Double, L_Mass_Tra_Zone As Double, Tot_Price As Double
    Dim Tot_Height As Double, Tot_P_Drop As Double, Tot_Sieve_w As Double

'Variables used for calculating the vessel tickness and total heat
    Dim Design_P As Double, Design_T As Double, Heating, Tensile_Str As Double
    Dim Tickness As Double, Wei_of_Steel As Double, Qtr_reg_load As Double, T As Double
    Dim Qw As Double, Qsi As Double, Qst As Double, Q_heat_loss As Double

'Variables used for calculating the flow rate of regeneration gas
    Dim CP As Double, Heat_time As Double, Gas_Den As Double
    Dim Reg_Mass As Double, Reg_Vol_Rate As Double



Sub Bed_Diameter()
'Sub program to calculate the bed diameter
    Pi_value = Application.WorksheetFunction.Pi
    B = MSD.Cells(4, 3).Value             'B coefficient of the ergun equation
    C = MSD.Cells(4, 4).Value             'C coefficient of the ergun equation
    Viscosity = MSD.Cells(17, 8).Value  'Viscosity of the mixture
    Density = MSD.Cells(18, 8).Value    'Density of the mixture
    Max_P_Drop = MSD.Cells(19, 8).Value 'Maximum allowable pressure drop
    Mass_Flow = MSD.Cells(20, 8).Value  'Mass flow rate of the mixture

    'Maximum velocity and the minimum diameter needed
    V_max = (Max_P_Drop / (C * Density) + ((B / C) * (Viscosity / Density) / 2) ^ 2) ^ 0.5 - ((B
    / C) * (Viscosity / Density) / 2)
```

```
    Vol_Flow = Mass_Flow / (60 * Density)
    D_Min = (4 * Vol_Flow / (Pi_value * V_max)) ^ 0.5

    'Rounding the min. diameter the nearest integer
    If (Round(D_Min) - D_Min) < 0 Then
       D_Selected = Round(D_Min) + 0.5
    Else:    D_Selected = Round(D_Min)
    End If

    'Calculating the adjusted velocity and pressure drop
    V_adj = V_max * (D_Min / D_Selected) ^ 2
    Adj_P_Drop = Max_P_Drop * (V_adj / V_max) ^ 2

    'Output
    MSD.Cells(5, 13).Value = V_max
    MSD.Cells(6, 13).Value = D_Min
    MSD.Cells(9, 13).Value = D_Selected
    MSD.Cells(10, 13).Value = V_adj
    MSD.Cells(11, 13).Value = Adj_P_Drop
```

End Sub

Sub Desiccant_Mass()
‘Desiccant mass calculator

```
    'Input parameter to calculate desiccant mass
    Water_Flow_Rate = MSD.Cells(30, 8).Value
    Relative_Sat = MSD.Cells(31, 8).Value
    Adsorption_Period = MSD.Cells(32, 8).Value
    Regen_Period = MSD.Cells(33, 8).Value
    Inlet_Tem = MSD.Cells(34, 8).Value
    Price = MSD.Cells(35, 8).Value
    Num_Of_Sieves = MSD.Cells(36, 8).Value

    'Temperature correctional factor
    If Inlet_Tem < 75 Then
       Css = 1
    ElseIf Inlet_Tem > 190 Then
       Css = 0.7
    Else
       Css = -0.0026 * Inlet_Tem + 1.1974
    End If

    'Relative humidity correctional factor
    If Relative_Sat < 15 Then
       CT = 0.86
    ElseIf Relative_Sat > 82 Then
       CT = 1
    Else
       CT = 0.084 * Log(Relative_Sat) / Log(10) + 0.6306
```

```
    End If

    Des_Mass = (Water_Flow_Rate * Adsorption_Period) / (0.13 * Css * CT)

    'Output
    MSD.Cells(26, 13).Value = CT
    MSD.Cells(27, 13).Value = Css
    MSD.Cells(28, 13).Value = Des_Mass

End Sub


Sub Bed_Height()
'Bed height calculation
    Bulk_Den = MSD.Cells(43, 8).Value
    Z = 1.7

    L_Sat_Zone = (Des_Mass * 4) / (Pi_value * D_Selected ^ 2 * Bulk_Den)
    L_Mass_Tra_Zone = (V_adj / 35) ^ 0.3 * Z
    Tot_Height = L_Sat_Zone + L_Mass_Tra_Zone
    Tot_P_Drop = Tot_Height * Adj_P_Drop

    Tot_Sieve_w = (Tot_Height / L_Sat_Zone) * Des_Mass
    Tot_Price = Price * Num_Of_Sieves * Tot_Sieve_w

    'Output
    MSD.Cells(42, 13).Value = Z
    MSD.Cells(43, 13).Value = L_Sat_Zone
    MSD.Cells(44, 13).Value = L_Mass_Tra_Zone
    MSD.Cells(45, 13).Value = Tot_Height
    MSD.Cells(46, 13).Value = Tot_P_Drop
    MSD.Cells(47, 13).Value = Tot_Sieve_w
    MSD.Cells(48, 13).Value = Tot_Price

End Sub


Sub Vessel_Tickness_and_Tot_Heat()
'Vessel thickness calculation
    'Input parameters
    Design_P = MSD.Cells(75, 8).Value
    Design_T = MSD.Cells(76, 8).Value
    Heating_T = MSD.Cells(77, 8).Value
    Tensile_Str = MSD.Cells(78, 8).Value

    Tickness = (12 * D_Selected * Design_P) / (2 * Tensile_Str - 1.2 * Design_P)
    Wei_of_Steel = 155 * (Tickness + 0.125) * (L_Sat_Zone + L_Mass_Tra_Zone + 0.75 *
    D_Selected + 3) * D_Selected
```

```
    Qw = 1800 * Water_Flow_Rate
    Qsi = Tot_Sieve_w * 0.24 * (Heating_T - Design_T)
    Qst = Wei_of_Steel * 0.12 * (Heating_T - Design_T)
    Q_heat_loss = (Qw + Qsi + Qst) * 0.1
    Qtr_reg_load = 2.5 * (Qw + Qsi + Qst + Q_heat_loss)

    'Output
    MSD.Cells(58, 13).Value = Tickness
    MSD.Cells(59, 13).Value = Wei_of_Steel
    MSD.Cells(60, 13).Value = Qw
    MSD.Cells(61, 13).Value = Qsi
    MSD.Cells(62, 13).Value = Qst
    MSD.Cells(63, 13).Value = Q_heat_loss
    MSD.Cells(64, 13).Value = Qtr_reg_load

End Sub



Sub Regeneration_Flow_rate()
'Regeneration mass flow rate calculation
    CP = MSD.Cells(87, 8).Value
    Heat_time = MSD.Cells(88, 8).Value
    Gas_Den = MSD.Cells(89, 8).Value

    Reg_Mass = Qtr_reg_load / ((CP * (Heating_T - Design_T) * Heat_time))
    Reg_Vol_Rate = Reg_Mass * Gas_Den
    'Output
    MSD.Cells(84, 13).Value = Reg_Mass
    MSD.Cells(85, 13).Value = Reg_Vol_Rate

End Sub

Sub Step1()
      Call Bed_Diameter
End Sub

Sub Step2()
     Call Bed_Diameter
     Call Desiccant_Mass
End Sub

Sub Step3()
    Call Bed_Diameter
    Call Desiccant_Mass
    Call Bed_Height
End Sub

Sub Step4()
    Call Bed_Diameter
```

```
    Call Desiccant_Mass
    Call Bed_Height
    Call Vessel_Tickness_and_Tot_Heat
End Sub

Sub Step5()
    Call Bed_Diameter
    Call Desiccant_Mass
    Call Bed_Height
    Call Vessel_Tickness_and_Tot_Heat
    Call Regeneration_Flow_rate
End Sub

Sub CtVsRS()
    frmCtVsRS.Show
End Sub

Sub CtVsT()
    frmCtVsT.Show
End Sub

Sub Help()
    frmHelp.Show
End Sub
```

VITA

Solomon Gebreyohannes

Candidate for the Degree of

Master of Science

Thesis: PROCESS DESIGN AND ECONOMIC EVALUATION OF AN ETHANOL PRODUCTION PROCESS BY BIOMASS GASIFICATION

Major Field: Chemical Engineering

Biographical:

Education:

- Completed the requirements for Master of Science in Chemical Engineering at Oklahoma State University, Stillwater, Oklahoma - December 2010
- Bachelor of Science in Chemical Engineering, Bahir Dar University, Bahir Dar, Amhara, Ethiopia - June 2007

Experience:

- Research Assistant to Dr. A. Johannes, OSU, August 2008 - August 2010
- Graduate Assistant, Bahir Dar University, Bahir Dar, Amhara, Ethiopia June 2007 - June 2008

Professional Memberships:

- Golden Key International Honour Society
- American Institute of Chemical Engineers (AICHE), OSU chapter

Name: Solomon Gebreyohannes Date of Degree: December, 2010

Institution: Oklahoma State University Location: Stillwater, Oklahoma

Title of Study: PROCESS DESIGN AND ECONOMIC EVALUATION OF AN ETHANOL PRODUCTION PROCESS BY BIOMASS GASIFICATION

Pages in Study: 122 Candidate for the Degree of Master of Science

Major Field: Chemical Engineering

Scope and Method of Study:

A large number of studies are being conducted on finding eco-friendly substitutes for petroleum-based fuels. Utilizing biomass as an energy source can significantly reduce dependency on petroleum, and the emission of greenhouse gases. Ethanol can be produced by gasification of biomass and then subsequent fermentation of the syngas.

The objective of this research is to develop full scale steady-state process models for ethanol production from syngas using a computer aided simulation (ASPEN^{TM} Plus software). Simulation results were compared with experimental data obtained from an earlier research project conducted at Oklahoma State University. Sensitivity analyses were performed on major units in the process model to determine the minimum ethanol production cost. An economic comparison was also carried out on two commonly used chemical separation processes (Azeotropic distillation and molecular sieve).

Findings and Conclusions:

The two processes were successfully modeled. These process models show that 99.5 wt% ethanol can be produced using either azeotropic or molecular sieve separation. The simulation results indicate that there is a potential to increase the experimental H_2 and CO_2 production in the gasifier and higher experimental conversion to ethanol is possible in the syngas fermentation process.

The production of high purity ethanol using molecular sieves requires less energy than the azeotropic separation process. This can reduce the operating cost of the process significantly which results in a lower price of the final ethanol product.

ADVISER'S APPROVAL: Dr. A. Johannes